TÉCNICO LISBOA

Development of a non-invasive method for the *in vitro* monitoring of 3D cell cultures

Maria Margarida dos Santos Queluz Rodrigues

Thesis to obtain the Master of Science Degree in

Biological Engineering

Supervisors: Prof. Cornelia Kasper

Prof. Cláudia Alexandra Martins Lobato da Silva

Examination Committee

Chairperson: Prof. Gabriel António Amaro Monteiro

Supervisor: Prof. Cláudia Alexandra Martins Lobato da Silva

Member of Committee: Dr. Ana Margarida Pires Fernandes-Platzgummer

November 2019

I declare that this document is an original work of my own authorship and that it fulfils all the requirements of the Code of Conduct and Good Practices of the *Universidade de Lisboa*.

“Para ser grande, sê inteiro: nada

Teu exagera ou exclui.

Sê todo em cada coisa. Põe quanto és

No mínimo que fazes.

Assim em cada lago a lua toda

Brilha, porque alta vive.”

Ricardo Reis

Preface

The work presented in this thesis was performed at the Department of Biotechnology of the University of Natural Resources and Life Sciences (Vienna, Austria), during the period of March-August 2019, under the supervision of Prof. Cornelia Kasper and Dr. Sebastian Kress, and within the frame of the Erasmus programme. The thesis was co-supervised at Instituto Superior Técnico by Prof. Cláudia Alexandra Martins Lobato da Silva.

Acknowledgements

First, I would like to express my gratitude to Professor Cornelia Kasper for welcoming me in her research group and giving me the opportunity to develop my master thesis at the University of Natural Resources and Life Sciences, in Vienna.

A special thanks goes to Doctor Sebastian Kress for giving me the chance to work in this interesting topic and for all the support, trust and availability during my internship.

I would also like to express my thanks to all the Kasper group members, Doctor Dominik Egger, Anne Lauermann, the PhD student Ciara Almeria, the MSc student Nicholas Kehrer, and the BSc students Michelle Roy and Anita Kóvacs, for helping me to develop my skills and performance in the laboratory, but especially, for their friendship and for providing the best working environment and conditions.

I want to thank Professor Cláudia Martins Lobato da Silva for being supervisor of this work and for always being available to help and give advice for improvement.

I would like to acknowledge my friends. To my favourite Chinese girls, Fifijin and Ana Li; my lovely friends Jo, Leo and Melita; my dearest badminton friend Nunu; and my IST groups “Niggaz” and “Sugar Mamas”, a huge thanks for always having my back and cheering me up whenever I needed during my college studies and thesis development. I would also like to thank Vienna Racket Club for letting me be part of their badminton family and always be so cheerful and nice during my stay abroad.

Finally, my deepest gratitude goes to my family, because without them this work would never see the light of the day. To my grandmother, for all the prayers towards my happiness and success. To my aunt and to Nelinho, for the everyday calls during my stay in Vienna that boosted my confidence and willingness to do better the next day. To my sister, the most stubborn, but the kindest of souls after the morning coffee. And to my parents, the foundations of my life, for enabling my education and granting me the opportunity of studying and living abroad, for not accepting me to give less than the best, for always being right, and most importantly, for their endless support and love.

Abstract

Mesenchymal stromal cells (MSC) show great promise in regenerative medicine due to their noticeable properties, such as immunomodulatory capacity and multi-differentiation potential. MSC are isolated from tissues and expanded *in vitro* to achieve relevant quantities for cell-based therapies, and can be further seeded to three-dimensional (3D) platforms and differentiated for tissue engineering purposes.

Current methodologies to examine 3D-cultures are based on endpoint analysis, which requires cell samples to be sacrificed, influences the growing conditions and enhances the risk of contamination due to regular handling.

In this work, a mini-perfusion bioreactor system was used to dynamically cultivate adipose-derived MSC (adMSC) in 3D platforms. A catheter was inserted within the cell construct to non-invasively acquire medium samples in a continuous operation, thus enabling for the monitoring of the cultivation by biological parameter analysis and preventing the usage of endpoint methodologies.

Prior to the cultivation inside the reactor, the cytotoxicity of the reactor material was assessed, and the cell seeding to collagen membranes and alginate hydrogels was optimized. Additionally, the diffusional capacity and the adMSC trilineage differentiation within these scaffolds were characterized.

Cells remained viable for up to 7 days when cultivated under perfusion inside the mini-bioreactor, as demonstrated via calcein-AM/PI staining. Glucose/lactate monitoring within the cell-constructs was possible due to sampling acquired through the catheter, which enabled to predict the cell behaviour during cultivation in a non-invasive manner.

These findings support the potential of using this novel concept of coupling a catheter to the mini-perfusion reactor, towards the creation of an optimized 3D-culture monitoring system.

Keywords

Mesenchymal stromal cells (MSC)
Regenerative medicine
Dynamic cultivation
Perfusion bioreactor
Three-dimensional (3D) cell cultivation
3D cell cultivation monitoring

Resumo

As células estromais mesenquimais (MSC) têm um elevado potencial de utilização na medicina regenerativa, justificado por um conjunto de propriedades notáveis, como a capacidade imunomodulatória e de multi-diferenciação. As MSC são isoladas a partir de tecidos e expandidas *in vitro* de modo a se alcançarem quantidades relevantes para terapias celulares, podendo ser posteriormente cultivadas em plataformas tridimensionais (3D) e diferenciadas para fins de engenharia de tecidos.

Atualmente, as metodologias para examinar culturas 3D são baseadas em análises “endpoint”, que sacrificam as amostras celulares, influenciam as condições de crescimento e aumentam o risco de contaminação devido ao manuseamento regular.

No presente trabalho, foi utilizado um mini-reator de perfusão com o objetivo de cultivar dinamicamente, em plataformas 3D, MSC provenientes do tecido adiposo (adMSC). Para esse efeito, foi inserido um catéter dentro das construções celulares para se obterem amostras de forma não invasiva e contínua, permitindo a monitorização da cultura via análise de parâmetros biológicos e prevenindo o uso de metodologias “endpoint”.

Previamente à cultura no interior do reator, avaliou-se a citotoxicidade do seu material de construção, e otimizou-se o método de cultura celular em membranas de colágeno e hidrogéis de alginato. Adicionalmente, caracterizou-se a capacidade difusional e a diferenciação de adMSC nessas plataformas.

Através de “calcein-AM/PI staining”, demonstrou-se que as células permaneceram viáveis por até 7 dias de cultura sob perfusão dentro do mini-biorreator. A monitorização de glucose/lactato nas construções celulares foi possível devido à obtenção de amostras através do catéter, o que permitiu prever de forma não invasiva o comportamento celular durante a cultura.

Estes resultados suportam o potencial desta nova configuração de acoplamento de um catéter ao reator de mini-perfusão, com vista à criação de um sistema otimizado de monitorização de culturas 3D.

Palavras-chave

Células estromais mesenquimais (MSC)
Medicina regenerativa
Bioreactor de perfusão
Cultura dinâmica
Cultura celular tri-dimensional (3D)
Monitorização de culturas celulares 3D

Table of Contents

List of Figures

List of Tables

List of Abbreviations

2D	Two-dimensional
3D	Three-dimensional
(-)-Ctrl	Negative control
α-MEM	Alpha-modified Eagle medium
adMSC	Adipose-derived mesenchymal stromal cells
AG	Alginate gel
AT	Adipose tissue
BM	Bone marrow
C	Clear resin
CBS	Cord blood serum
Ctrl	Control
C(+)UVc	Clear resin cured/hardened with UV after 3D-printing
C-UV$n\times$	Clear resin n times sterilized via UV-light
DAPI	4′,6-diamidino-2-phenylindole
ddH_2O	Double-distilled water
DMEM	Dulbecco's modified Eagle medium
DMSO	Dimethyl sulfoxide
ECM	Extracellular matrix
EDTA	Ethylenediaminetetraacetic acid
ESC	Embryonic stromal cells
EtOH	Ethanol
FBR	Fluidized/fixed-bed reactor
HF	Hollow fiber
HIF	Hypoxia inducible factor
hMSC	Human mesenchymal stromal cell
hPL	Human platelet lysate
iPSC	Induced pluripotent stromal cell
ISCT	International Society for Cellular Therapy
FBS	Fetal bovine serum
HT	High Temp resin
HT-P	High Temp resin with parylene-coating
HT-P$n\times$	High Temp resin with parylene-coating n times autoclave-sterilized
HT-γ	High Temp times sterilized via γ-irradiation
LDH	Lactate dehydrogenase

MD	MatriDerm®
MS	MatriStypt®
MSC	Mesenchymal stromal cell
MTT	3-(4,5-dimethylthiazol-2-yl)-2,5-diphenyltetrazolium bromide
OCR	Oxygen consumption rate
OXPHOS	Mitochondrial oxidative phosphorylation
PBS	Phosphate buffer saline
PD	Petri Dish
PDH	Pyruvate dehydrogenase
PFA	Paraformaldehyde
PI	Propidium iodide
PPR	Parallel-plate reactor
ROS	Reactive oxygen species
rpm	Revolutions per minute
RWV	Rotary wall vessel
SDS	Sodium dodecyl sulphate
STR	Stirred tank reactor
TCA	Tricarboxylic acid
TGF-β	Transforming growth factor beta
UC	Umbilical cord
UCB	Umbilical cord blood
UV	Ultraviolet
WJ	Wharton’s jelly
WP	Well-plate
WR	Wave reactor

Chapter 1

Introduction

This chapter gives a brief overview of the current State-of-the-Art concerning the scope of the work. At the end of the chapter, the aim of studies is provided.

1.1 Mesenchymal stromal cells

Mesenchymal stromal cells (MSC) are adult multipotent stem cells capable of self-renewal and able to differentiate into specialized cell types. They exhibit a great potential to be used in cell-based therapies and tissue engineering due to their role in the regulation of immune [1] and inflammatory responses [2] and tissue regeneration mechanisms [3]. These are due to their ability in secreting growth factors, cytokines and other signalling molecules to the medium [4], and their capacity to migrate to injury sites [5]. MSC are also attractive to other biomedical fields such as drug screening or disease modelling.

Human MSC (hMSC) were first discovered within the bone marrow (BM) [6], but other sources have been identified since then, including perinatal tissue (*e.g.* Wharton's jelly, WJ; umbilical cord, UC; umbilical cord blood, UCB) [7], adipose tissue (AT) [8], endometrium [9], menstrual blood [10], lung [11], dental pulp [12] and synovial tissue/fluid [13].

BM is a frequently used source of MSC for both experimental and clinical applications, and most of the knowledge concerning these cells comes from BM studies. MSC from BM were concluded to decrease with age, and their isolation is considered invasive and painful [14]. In turn, although invasive, the collection of AT is painless; MSC from AT were found to exhibit a good proliferative capacity [15]. Perinatal tissues (*e.g.* UC, UCB, WJ) have also been studied as sources of MSC. These tissues are the most promising sources in terms of youthfulness [16], while being a non-invasive and painless source of MSC to mother and child.

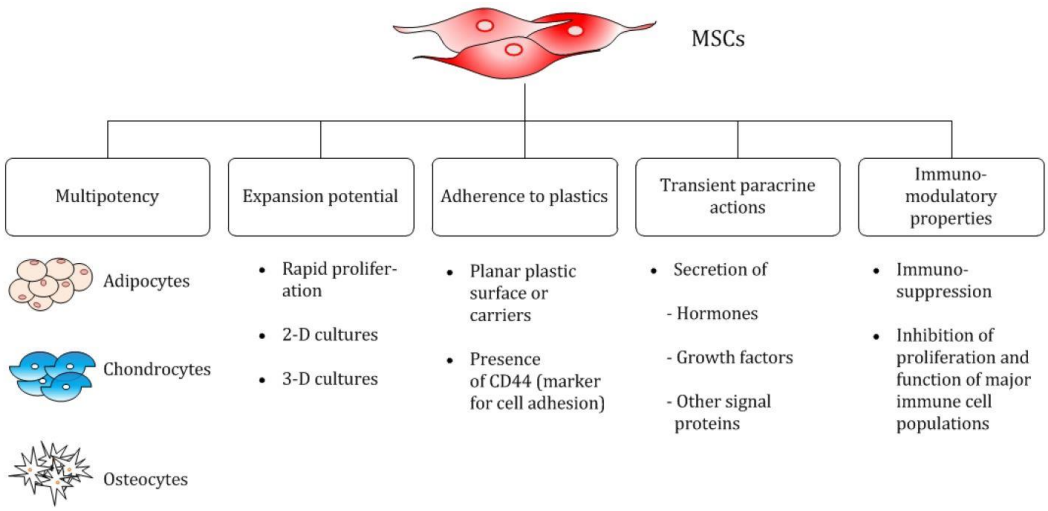

Figure 1-1 Main properties of MSC. MSC show great promise in regenerative medicine due to their multipotency, paracrine secretion of growth factors and cytokines and immunomodulatory capacity (adapted from [17]).

Despite the source heterogeneity of hMSC, a minimal set of criteria must be met to characterize these cells when working in laboratory or clinical studies. According to the Mesenchymal and Tissue Stem Cell Committee of the International Society for Cellular Therapy (ISCT), MSC must be plastic-adherent, capable of trilineage differentiation (adipogenic, chondrogenic, osteogenic) and express specific surface markers ($CD105^+$, $CD73^+$, $CD90^+$, $CD45^-$, $CD14^-$, $CD19^-$ and $HLADR^-$) [18].

Compared with embryonic and induced pluripotent stem cells (ESC and iPSC, respectively), which are pluripotent cells that can give rise to all cell types derived from the three primary germ layers (ecto-, meso-, and endoderm), the differentiation potential and self-renewal ability of MSC is more limited, as the latter are multipotent (more mature in the differentiation process). MSC give rise to cells derived mainly from the mesoderm (adipocytes, osteoblasts and chondrocytes), although MSC differentiation into neurons [19], cardiomyocytes [20] and epithelial cells [21], which are not originated from the mesoderm, have been reported. Nonetheless, the possibility of teratoma formation [22] and immunological rejection have been reported when using ESC and iPSC based therapies [23], rising awareness and concern in using these cells for therapeutic purposes. Moreover, as embryos are the source of ESC, the usage of these cells is controversial. In turn, as MSC are more mature, they bypass the risk of developing teratomas associated to transplantation with prenatal stem cells (*e.g.* ESC), while avoiding ethical issues. Furthermore, MSC offer the possibility of immune evasiveness [24] after allogeneic transplantations, making them attractive for stem cell based therapies.

Inflammatory signals induce the production and secretion of growth factors and cytokines by MSC. As aforementioned, these biomolecules aid in tissue regeneration by promoting angiogenesis, rehabilitation of the extracellular matrix (ECM) and differentiation of tissue progenitor cells. Additionally, MSC sense chemokines through specific receptors, and have the ability to migrate towards inflammatory signals and regulate immune and resident progenitor populations in the inflammation microenvironment of tissues [2, 25]. These properties, combined with the capacity of differentiation into specific cell types, fairly easy isolation, good proliferative potential and free from teratoma formation, make MSC a promising tool as a regenerative therapy to address medical conditions associated with chronic tissue damage, including cardiovascular diseases, spinal cord injuries and ischemic stroke, and specially immune disorders and inflammation that are not treatable by conventional methods, such as graft-versus-host disease (GvHD) [26], multiple sclerosis and diabetic nephropathy.

Although MSC are promising for therapeutic purposes, the donor variability, the high number of cells needed for therapeutic purposes, differing protocols for MSC manipulation, and lack of reproducible results are major hurdles that need to be circumvented in order for MSC based therapies to be considered safe by the scientific community. Standardized protocols for cell isolation, culture, expansion and differentiation, as well as tight quality controls are determinant to achieve an effective and reproducible MSC based therapy.

1.2 Isolation of mesenchymal stromal cells

MSC population propagated *in vitro* is influenced by the way these cells are harvested from the donor tissue. Isolation protocols have an impact on the isolated cells morphology [27] and may also induce epigenetic and genetic changes, which may affect their plasticity and utility [28]. Taking advantage of their plastic-adherent capacity, the most commonly used isolation procedures are density

gradient separation (for MSC deriving from suspensions, such as peripheral blood, UCB and BM), and enzymatic and explant methods (when MSC are extracted from tissues).

Ficoll-paque is commonly used when performing the density gradient separation. This separation media allows the separation of mononuclear cells within bone marrow and blood samples. First, the cell suspension is added on top of the Ficoll-paque media inside a centrifugal tube, which is then centrifuged; the differential migration of cells during centrifugation creates several layers containing different cell types. The layer corresponding to the desired mononuclear cells is then collected and washed. Subsequently, the cells are cultivated in plastic culture vessels for 24-48 hours to allow cell adhesion. After that period, the media is removed and the plates are washed with PBS to remove non-adherent cells. Finally, medium is replaced for further expansion of MSC [15, 29].

In the explant method, the tissue is first rinsed to remove blood cells and then mechanically fragmented into small segments up to a few millimeters in length, the optimal size to enhance the diffusion of oxygen and nutrients towards the cells, while preventing their mechanical destruction. Then, the tissue pieces are cultured in plastic culture vessels with growth medium, and MSC grow out from those pieces onto the culture dish surface. After a few days, the tissue fragments are removed [30] and MSC are further expanded.

In the enzymatic digestion method, the tissue is also rinsed and chopped into small pieces. The second step comprises the incubation of the tissue pieces in an enzymatic solution that degrades the ECM, releasing single cells or small cell aggregates which are then resuspended and transferred to culture dishes containing growth medium to further expand MSC [30].

In the scope of this work, in which MSC derived from adipose tissue are used, a further discussion tackling the explant and enzymatic methods is relevant. It was reported that the extraction of MSC from UC, AT and WJ via explant method results in a higher yield [15, 16] and increases the cell viability [16], while preventing possible cell damage induced by enzymes used to isolate cells from the ECM. Explant method is a simple and cost-effective way to harvest MSC when compared to the enzymatic digestion, since it does not need incubation with enzymes and depends on the MSC capacity to migrate from the tissue and adhere to the surface of the culture vessels [15, 16]. In another study, although the cell yield was lower in a given timeframe, the explant method appeared to be more robust to extract MSC from UC comparatively to the digestion method [31]. The general lower yield obtained with the enzymatic protocols may be related with the often poorly defined enzyme solutions and the broad range of incubation times, dependent on the purity and source of the enzymes. Moreover, this method enhances the risk of degradation of cellular external lamina, preventing MSC from adhering to the surface of culture vessels after enzymatic digestion [31].

Nevertheless, it is arduous to compare directly different studies due to several biasing factors including donor variability, medium composition and protocol variation.

1.3 Expansion of mesenchymal stromal cells

1.3.1 Three-dimensional cell culture

Two-dimensional (2D) culture systems, such as well-plates and T-flasks, have been the protocol of choice to study adherent cultures due to their simplicity and easy handling. These are static culture devices consisting of a single unstirred compartment where nutrients diffuse to cells and gas exchange occurs at the media/gas interface [32]. This type of monolayer method is limited though, since cells do not exist in an isolated 2D microenvironment *in vivo* but are rather surrounded by different cell types and three-dimensional (3D) structures (*i.e*. ECM), which regulate the distribution of several chemicals, such as signalling molecules, nutrients, metabolites and oxygen. Hence, 2D culture overlooks important cues to the cell fate including mechanical, cell-cell and cell-ECM interactions [33]. Abnormal cell function [34], dedifferentiation [34, 35] and alteration on cell morphology [35, 36] have been reported when cells were cultivated in planar surfaces.

In turn, 3D cell cultures provide physiologically relevant cues that better mimic the *in vivo* microenvironment, namely 3D allows cells to exhibit a morphology and migration mode similar to that found *in vivo*, which determines their biological activity [37] and enhance the degree of cell interaction with their immediate surroundings, greatly affecting their cellular function [38, 39]. Furthermore, compared to 2D, 3D cell culture has the advantage of allowing for a higher surface to volume ratio.

Three-dimensional formats for the cultivation of MSC can have one of two formats: scaffold-free platforms, such as aggregates, and scaffold-based approaches, including porous microcarriers, scaffolds and hydrogels (Figure 1-2).

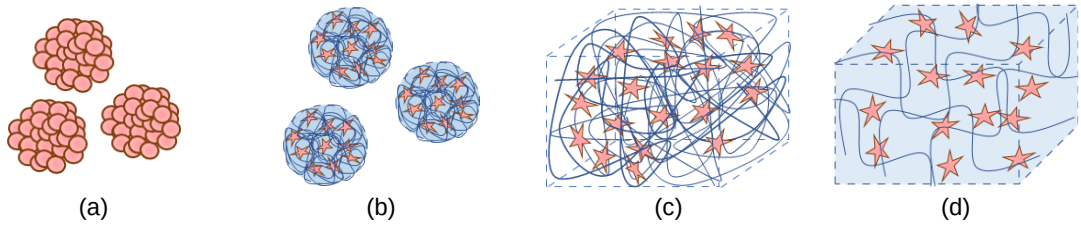

Figure 1-2 Three-dimensional platforms for the cultivation of MSC (in orange) can be scaffold-free in (a) aggregates, or scaffold-based in (b) macroporous microcarriers, (c) porous/fibrous scaffolds; or (d) hydrogels.

Aggregates

As MSC are anchorage dependent cells, when not in presence of a physical surface they have the need to attach to one another, forming the so-called cell spheroids or aggregates. The attachment of cells involves three steps: the first contact is mediated by cadherin-cadherin and integrin-ECM interactions, followed by a period of delay for reorganization and pause in compaction, and finally a strong interaction between cadherins drives the transition from loose to compact spheroids [40].

In comparison to 2D culture, aggregate cultivation of MSC was shown to enhance several biological properties, resulting in increased cell viability, proliferation, differentiation and improvement of their

therapeutic potential [41]. Some studies have reported cultivation of MSC aggregates in dynamic systems, including rotating wall vessel and stirred tank bioreactors [40, 42]. The advantages of this cultivation method are the capability to address the architecture of tissues/organs, generate aggregates with cell heterogeneity and achieve high cell yields under controlled conditions [43]. However, the spheroids tend to have uncontrolled diameters when operated within a bioreactor, and large diameters can develop necrotic cores due to limitations in mass transfer of nutrients. Furthermore, at the end of the expansion stage, the aggregates must be disassociated to harvest single cells, presenting a limitation of this culture method as the disassociation can be damaging to adhesion proteins on the cell membranes [44].

Microcarriers

Microcarriers are produced from natural or synthetic materials and are commonly used to grow anchorage dependent cells in suspension culture. They can have two distinct conformations: i) non-porous/microporous beads, in which cells grow on the surface; and ii) macroporous beads, in which cells are able to migrate and grow inside the bead, enabling for a 3D culture. Their diameter are typically in the ranges of 100-400 µm, providing a larger surface area for cell growth compared to planar cultures and allowing for higher cell yields to be achieved. Moreover, the surface and mechanical properties of the microcarriers can be enhanced with different coating materials (*e.g.* ECM proteins, surface proteins) that better suits the cell type being grown. The microcarriers are suspended within the bioreactor, but if hydrodynamic forces in the suspension culture are not controlled, the microcarriers can strike each other causing damage to the attached cells on the exterior surface; these forces must be understood, particularly when expanding sensible cell types, as MSC [44]. Moreover, the harvest of cells can be challenging, especially for those grown in macroporous beads. Enzymes are used to remove cells from the microcarriers, which can damage adhesion proteins and affect the therapeutic capacity of the MSC. To circumvent this limitation, degradable microcarriers have been recently developed [45]. Most studies on MSC culture in microcarriers have focused on cell expansion and differentiation although recently, with the development of biodegradable substances, efforts are being held to test the feasibility of using microcarriers for clinical applications in the field of regenerative medicine [46].

Porous and fibrous scaffolds

Porous and fibrous scaffolds are 3D constructs with interconnected pores that have been used in scaffold-based tissue engineering and regenerative medicine; these can also be used to expand anchorage dependent therapeutic cells within bioreactors. The bulk material for the scaffold fabrication includes metals, glasses, polymers and ceramics, in which natural polymers (*e.g.* chitosan and collagen) are the most common due to the possibility to control their biocompatibility, chemical and structural properties. The pores in the scaffold have several sizes and shapes that enable the diffusion of nutrients and removal of metabolites during cell expansion. They can be customized to meet the desired specifications and their surface properties can be modified to enhance cell adhesion. Furthermore, compared to planar cultures, high cell densities can be achieved by providing a higher surface area for attachment, improving the efficiency of the cultivation. Limited research has been developed using this

method for cell expansion and harvesting [44], with most of the available literature focusing on scaffolds for bone or cartilage related differentiation, and therapeutic purposes.

Examples of porous matrices are MatriStypt® and MatriDerm®, composed of naturally crosslinked collagen and collagen-elastin, respectively, two of the main fibrous ECM proteins [47]. Their matrix structure allows for cell migration, cell communication and transport of oxygen and nutrients.

Hydrogels

Cells are entrapped inside cross linked polymer chains prepared from natural or synthetic polymers that closely resemble the naturally hydrated ECM of natural soft tissue [48]. Although the control over the gelation kinetics and mechanical properties is limited, natural hydrogels of non-animal origin, such as the brown algae derived alginate, are preferable due to their biocompatibility and mild gelation conditions [49].

Over the last years, alginate has exhibited a great applicability as a platform for cell immobilization due to its ability to form hydrogels at physiological conditions, mild dissolution for cell retrieval, transparency for microscopic analysis and pore network that allows diffusion of nutrients and metabolites [50]. Alginate has a limited inherent cell adhesion and cellular interaction, which is an advantage for cell embedment applications, but may be a drawback for tissue engineering purposes. Nevertheless, alginates can be modified by the addition of biomolecules that allow for cell attachment.

The ionic gelation of alginate hydrogels is formed in the presence of divalent cations (*e.g.* Ca^{2+}) and can therefore be dissolved using chelating agents for these type of cations, such as ethylenediaminetetraacetic acid (EDTA); this allows a mild release of the embedded cells that can further be separated via centrifugation, filtration, flow cytometry or similar separation techniques. For a three dimensional assemble, cells are suspended in the hydrogel precursor solution prior to the gel cross linkage [50]. For bead formation, drops of the cell-alginate suspension are added to a solution containing gelling ions (*e.g.* $CaCl_2$) that allows chemical/physical cross-linkage of the alginate, and thus cell encapsulation; the bead size is determined by the technique used (*e.g.* extrusion through a needle, coaxial flow, electrostatic generator, *etc.*), alginate solution viscosity (normally 1-2% (w/v)) and rate of alginate flow [50]. For a scaffold-like conformation, the hydrogel is casted inside a mould with the desired size and shape, by adding the cell-alginate suspension to that mould followed by the ionic solution that polymerizes the gel.

When expanded inside dynamic bioreactors, the entrapped cells are protected from the fluid shear stress that cells are subject to. For therapeutic purposes, hydrogels have the potential to be used as an integrated approach since cells can be directly delivered to the defect site using that platform as vehicle. Additionally, the embedded cells are protected from the immune system of the patient, improving the chances of engraftment at the defect site. This form of 3D culture has been mostly implemented in tissue engineering studies rather than MSC expansion [44].

1.3.2 Dynamic culture

To take advantage on the therapeutic properties of MSC in cell base therapies or regenerative medicine, the usage of scalable systems with optimized cultivation conditions is of utmost importance in order to generate a large number of clinical grade MSC.

Cultivation in bioreactors is the most cost-effective approach for cell expansion. In addition to allowing reproducible cell growth, reducing variability and possibly being scalable, bioreactors reduce the time and labour work, footprint and risk of contamination associated to the several cell passages needed when cultivating MSC in planar surfaces.

In static cultivations, the gas exchange occurs in the liquid-gas interphase and mass gradients may arise during cultivations, leading to medium heterogeneity that can influence the quality and yield of the cells [17]. Bioreactors that accommodate dynamic culture conditions play an important role in growing cells *in vitro* that more closely resemble the physiological environment, since cells can be subjected to mechanical cues, the transport of mass and energy are enhanced, and 3D platforms for cell culture can be integrated within these systems. Regarding the power input, dynamic bioreactors suitable for MSC culture can be mechanically or hydraulically driven (Figure 1-3) [17].

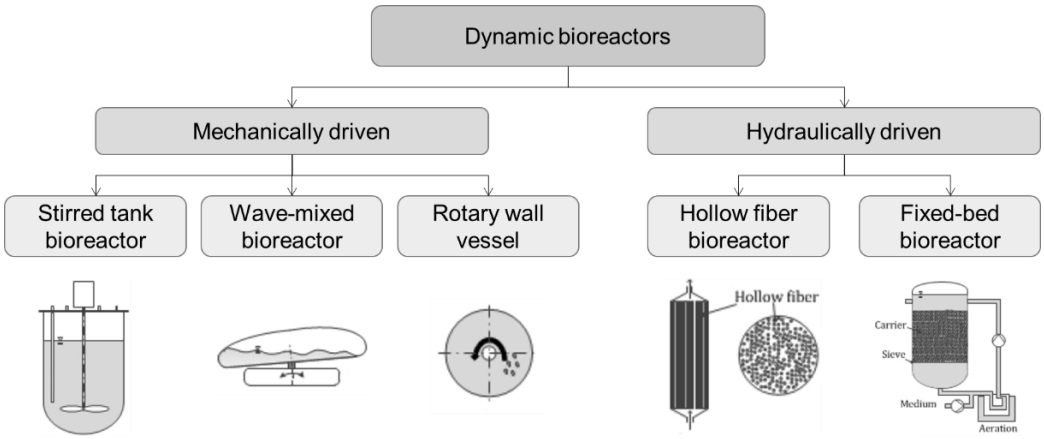

Figure 1-3 Suitable bioreactors for MSC 3D expansion, classified by the input energy type power (adapted from [17]).

Mechanically driven reactors

Mechanically driven devices operate in a fed-batch fashion and cells (in aggregates or scaffold-immobilized) are grown in suspension. These reactors include the stirred tank (STR), rotary wall vessel (RWV) and wave (WR) bioreactors. STR consists on a tank containing media and cells. The agitation of one or more stirrers provides proper mixing, allowing for mass transfer and control over culture conditions (*e.g*. pH, dissolved oxygen, temperature). Advantages of this bioreactor are the ease of design, scalability and ability to integrate online monitoring probes, enabling the online control of culture parameters. However, it becomes troublesome to satisfy the oxygen demand in the presence of higher volumes. Aeration by oxygen sparging may be employed to circumvent this problem, but it generates shear forces. Shear stress, induced either by the impeller or aeration, is a problem that may

result in cell death [44]. The vertical wheel bioreactor is an improvement over the STR that limits the shear forces inflicted by the impeller [51].

The WR is constituted by a disposable bag fixed on a rocking platform that provides a wave motion for proper mixing and aeration. The bag is partially filled with medium and cells, and the remaining is inflated with air [17]. Advantages of WR are low shear stress [44], negligible foaming (no need for addition of anti-foaming agents) [17] and reduced cleaning and validation (due to the bags being disposable) [52].

Finally, the RWV is a horizontal rotating cylinder completely filled with medium that simulates microgravity conditions by rotating the medium at the same angular rate as the wall [32]. The inner cylinder is covered by a silicone membrane that allows oxygen to be transferred to the medium. Advantages of RWV are low shear stress and a shorter diffusion distance between the bulk media and the cells. This is due to the reduction of the boundary thickness that surrounds the cells, which is inflicted by the viscous flow produced by the RWV [32]. However, both WR and RWV are limited in scalability due to their size capacity [44]. Generally, mechanically driven bioreactors, where cells are grown in suspension, are more appealing for expansion of MSC towards cell-based therapies [52].

Hydraulically driven reactors

Hydraulically driven reactors are operated with perfusion in a continuous mode. A perfusion system mimics the function of the microcirculation so that cells can be grown near tissue density, and compared to mechanically driven bioreactors, the mass transfer is enhanced due to continuous exchange of media [32]. Examples include hollow fibers (HF) and fixed-bed reactor (FBR). HF consists on a bundle of parallel semi-permeable hollow fibers encased in a cylindrical chamber. Cells can be cultivated either on the intra- or extracapillary surfaces and the pore size determines which molecules shall be rejected. Advantages of HF are low shear stress environment, high surface to volume ratio and the creation of a 3D system that resembles physiological conditions [17].

The FBR consists on a column/chamber packed with cells immobilized in scaffolds or encapsulated in particles. The culture medium is perfused through the bed of the reactor, supplying cells with nutrients and removing metabolites [17, 52]. However, if the hydraulic permeability of the cell-construct is not uniform, spatial gradients may occur [32]. Both HF and FBR are limited in scalability in that their nutrient and oxygen gradients restrict the length/height of the fibers/fixed-bed. Furthermore, the cell monitoring and harvest from these bioreactors are challenging [17, 52]. Therefore, perfusion bioreactors are more suitable for smaller scale cultivations and tissue engineered applications rather than large expansion of MSC.

Although there are different bioreactor systems that can be customizable to better suit each cell type and application, providing an efficient transport of nutrients/metabolites, isolating cells after culture and controlling the induced shear stress caused by culture media flow or rotating stirrer, are current challenges that must be overcome.

1.3.3 Energy metabolism of mesenchymal stromal cells

Mesenchymal stromal cells reside in hypoxic niches that provide the necessary factors for the maintenance of a quiescent state, allowing them to preserve the undifferentiated state and self-renewal capacity that are important in tissue homeostasis and regeneration [53].

Current evidence has shown that in addition to cell-cell interactions and signals from the microenvironment, the metabolic pathway plays a role in the self-renewal and differentiation ability of stem cells. Thereby, the understanding of the metabolic profile of these cells is crucial for the development of enhanced protocols to cultivate and produce clinical grade MSC.

To rapidly fulfil energy requirements, mammalian cells first transform glucose into pyruvate in the cytosol via glycolysis. Subsequently, pyruvate is either reduced by lactate dehydrogenase (LDH) to lactate, or enters the mitochondria, where it is converted by pyruvate dehydrogenase (PDH) in acetyl-CoA, this is used in the tricarboxylic acid (TCA) and mitochondrial oxidative phosphorylation (OXPHOS), the most efficient energy provider of the cell. The fate of pyruvate depends on several factors such as the rate of cellular growth or proliferation, oxygen availability, and differentiation state.

Cellular growth and proliferation

High proliferating cells, like ESC and cancer cells, require the production of macromolecules and ATP, which can be rapidly acquired through aerobic glycolysis (Warburg effect). This favours the conversion of pyruvate into lactate, and products of glycolysis to be diverted to anabolic synthetic pathways rather than undergoing complete oxidation in the TCA cycle [54]. However, as MSC are mainly quiescent in their niche, the extent to which they need to divert products of glycolysis for anabolic growth is uncertain [55].

Oxygen availability

Mammalian cells cultivated under normoxic conditions have their energy requirements produced via aerobic metabolism, in which oxygen serves as the final electron acceptor of OXPHOS [53].

Due to the limited availability of oxygen when stem cells are cultivated under hypoxic conditions, the levels of respiratory enzymes, activity of electron transport chain and oxygen consumption rate (OCR) are decreased, whereas the production of glycolytic enzymes and lactate are increased, causing the cells to rely more on glycolysis [56]. Thus, the energetic metabolism is likely to change from OXPHOS to glycolysis when stem cells are under hypoxia.

An important response to hypoxia is the stabilization of the hypoxia inducible factor (HIF)-1, a heterodimer consisting of a constitutively expressed HIF-1β subunit and a HIF-1α subunit whose expression is highly regulated by external factors. Low oxygen tensions were demonstrated to cause the stabilization of HIF-1α and its accumulation in the nucleus [57]. Additionally, HIF-1 alters mitochondrial function by suppressing mitochondrial respiration [58], suggesting that this factor might regulate the transition between glycolysis and oxidative phosphorylation. Indeed pyruvate dehydrogenase kinase 1, the enzyme that phosphorylates and inactivates PDH, is upregulated by HIF-1,

thus inactivating PDH under low oxygen concentrations [59]. In such circumstances, pyruvate is converted to lactate and glycolysis is favoured. In addition, HIF-1 stimulates the expression of the LDH-A [60] whose respective enzyme (LDH) converts pyruvate into lactate. These HIF-1-regulated mechanisms suppress the delivery of acetyl-CoA to the TCA cycle and OXPHOS.

Another factor associated with oxygen deprivation is increased oxidative stress, which can lead to mitochondrial dysfunction and decrease in the level of intracellular ATP [61]. Reactive oxygen species (ROS) have their origin from electron transport complexes in the reduced form [62], increased expression of the oxidative stress enzyme NAD(P)H oxidase under hypoxic conditions [63], and decreased expression of the anti-oxidant enzyme catalase. This results in the intracellular accumulation of hydrogen peroxide that is harmful to the cells [63], thereby contributing to the switch of the energy metabolism to anaerobic glycolysis with significantly enhanced glucose consumption and respective lactate production [64].

Differentiation state

In undifferentiated MSC, mitochondrial activities are maintained at a low level, whereas glycolytic activities are maintained at a high level for most glycolytic enzymes and lactate production [65].

When MSC start differentiating, there is a down-regulation of the pluripotent specific genes, an up-regulation of the terminal-specific genes and a change of the subsets of metabolic enzymes [53]. For instance, in osteogenic MSC, the mitochondrial DNA copy number, content of respiratory enzymes, intracellular ATP and OCR increase, while the levels of intracellular ROS decrease [65]. In addition, the expression of HIF-1α is reduced and leads to a decreased glycolytic metabolism and increased oxidative metabolism after osteogenic differentiation [66]. Adipogenic differentiation of human MSC was demonstrated to show a shift toward higher OCR [67] and was initiated or enhanced by the mitochondrial ROS production during OXPHOS [68].

Therefore, the transition between the undifferentiated and differentiated states of stem cells is characterized by a dynamic mitochondrial morphology and a shift from glycolysis to OXPHOS [53].

1.3.4 Effect of the cultivation parameters

Oxygen

Current literature has shown evidence that the cultivation of hMSC at low oxygen concentrations (1-5% O_2) relatively to normoxic conditions (21% O_2), enable these cells to maintain or even improve most of their attributes such as cell proliferation, migration and genomic stability [69, 70].

It was shown that the oxygen concentration did not influence the hMSC cellular phenotype [70, 71, 72] regardless of the cell source [70]. On the contrary, hypoxia did improve the ability of MSC to migrate [73, 74, 75] and diminished the occurrence of cell senescence and apoptosis compared to normoxic conditions [69, 76]. As aforementioned, the culture under hypoxic conditions was associated with the induction of HIF-1 (which influences the cell cycle, apoptosis, and differentiation, among others) and a higher expression of energy metabolism-associated genes (mainly associated with anaerobic glycolysis)

[77]. Estrada *et al.* [69] reported that hypoxia may lead to a reduced formation and accessibility of ROS, thus increasing the metabolic efficiency and diminishing the possibility of cell injury inflicted by those same species [78, 79].

Concerning the proliferation capacity, in general, lower concentrations of oxygen lead to a significantly higher proliferation rate [72, 75, 80, 81, 82] indicating the cell yield is presumably higher when cells are cultivated in low O_2 concentrations.

As for the differentiation potential, the effect of the O_2 concentration is still ambiguous among the scientific community. Even though it is globally accepted that hypoxia supports chondrogenic differentiation [70, 71, 81, 83], Malladi *et al.* [84] showed decreased chondrogenesis in reduced oxygen tension. Controversial findings were obtained with regard to osteogenic and adipogenic differentiation. For instance, none or diminished osteogenic and adipogenic differentiation of MSC were reported when these cells were cultivated under hypoxia [83, 84, 85, 86]. In a different study, the differentiation ability of MSC under hypoxia favoured osteogenesis while adipogenesis was inhibited [75]. In turn, Grayson *et al.* [87] showed a positive effect of hypoxic conditions in human MSC culture, in which there was an improved survival and increased adipogenic and osteogenic differentiation capacity.

Medium composition

Fetal bovine serum (FBS) was commonly used as medium supplement due to its richness in cell growth and attachment factors, along with other biomolecules required for the isolation and expansion of MSC [88]. However, being a complex xenogeneic mixture, FBS has some limitations including pathogen contamination risk (*e.g.* prions, bacteria, viruses and mycoplasma), batch-to-batch variations and the potential for immunological reactions against xenogeneic compounds [89]. These disadvantages have motivated the implementation of different supplement media to cultivate MSC, for instance human blood-derived materials such as human serum, platelets lysate (hPL) and cord blood serum (CBS), and also serum-free chemical defined media.

Defined basal media with known formulations, such as DMEM (Dulbecco's modified Eagle medium) or α-MEM (minimum essential media), are common media to culture hMSC. These media must be supplemented with additives, such as adhesion proteins, growth factors and hormones that have its origin from humans, such as hPL.

Human blood component-derived supplements contain several essential factors capable of promoting cell growth [90]. It was shown that hPL components promote growth with an increased proliferation rate, when compared with FBS-cultured MSC [91]. Moreover, using hPL to expand hMSC maintains their differentiation and immunomodulatory capacity [92]. Hassan *et al.* [93] have replaced FBS with allogeneic human serum from UCB, which is a rich source of growth factors, and demonstrated that CBS enhanced self-renewal and differentiation potential of MSC, while maintaining their morphology and multipotent differentiation capacity. In general, recent studies show that human derived media supplements overcome some of the disadvantages associated with FBS and appear to enhance the MSC expansion efficiency. Nevertheless, there is still a risk associated with using allogeneic human growth supplements as they may be contaminated with human pathogens that might not be detected by

routine screening of blood donors, are poorly defined and present batch-to-batch variability [94]. Furthermore, some forms of hPL require the use of animal-derived heparin to prevent coagulation [95].

The problems associated with the poorly defined serum and human blood derived supplements has motivated the development of serum-free, xeno-free and chemically defined media. Several serum-free media are currently available in the market (*e.g.* StemPro® and Mesencult®); however, the fact that their composition is confidential remains a drawback. Basal medium components require strict quality control to ensure optimal cell growth and its formulation determine growth frequency and morphology of primary and passaged hMSC cultures [30]. On the contrary, the formulation of chemical defined media is designed to support the growth of a population enriched with a desired cell type, preventing the overgrowth of undesired cells in primary cultures and allowing for the production of more homogenous hMSC. Furthermore, well-defined media may be optimized to facilitate cell bioprocessing protocols and produce cells with the desired properties, therefore enhancing the clinical efficacy of stem cells, due to a more favourable and controllable environment [94].

Shear stress

The dynamic cultivation is advantageous in improving nutrient supply and metabolite removal needed to support the development of 3D constructs. Moreover, it also provides mechanical cues that regulate the cell behaviour and subsequent construct development [96]. The hydrodynamic characteristics are an important parameter to have in consideration when designing a reactor, since fluid flow-induced shear stress impacts several cell functions (such as proliferation, differentiation and release of specific growth factors and cytokines) and tissue-related processes, including migration and wound healing [97, 98].

Fluid shear stress is originated by fluid movement tangential to a surface, which is crucial for the reduction of mass transfer limitations associated with concentration gradients at the fluid-scaffold interface. In addition to that, as fluid is forced through the scaffold in a perfusion reactor, a more homogenous micro-environment is created, making this an attractive system for 3D culture [99].

Fluid flow in 3D systems for MSC cultivation was mainly applied in perfusion bioreactors to study the osteogenic differentiation [96]. Overall, it is accepted that fluid flow promotes or enhances this specific lineage [96, 100], even in the absence of chemical induction [101]. However, controversial results were obtained on the impact of fluid shear stress on other cell properties, such as proliferation, which can likely be explained by the distinct cultivation settings between different studies [96, 100].

Interestingly, Zhao *et al*. [102] reported that hMSC cultivated in a perfusion bioreactor exhibited a higher proliferation rate at lower flow rates and an upregulation of the osteogenic differentiation potential for higher rates. These findings indicate that mild fluid flow shear stress contributes to proliferation and increasing levels of stress beyond a given point promotes differentiation at the cost of growth and self-renewal. Thereby, if one intends to create bone tissue, shear stress should be maintained at a certain magnitude to promote proliferation and achieve the required cell number, followed by an increase of the shear stress above that threshold to lead to an osteogenic response [100].

1.4 Methodologies for 3D culture analysis

Two main approaches are possible when assessing a cell culture: either perform endpoint analysis, in which cells are sacrificed (*e.g*. lysed or fixed), or perform real-time monitoring without sacrificing cell samples, which allows to non-invasively conclude about the dynamics within a cell population over culture time. Hence, the latter is of most interest in cell-based and tissue engineering applications.

Despite the several advantages over 2D, the analysis of 3D cell culture is challenging and requires more complex procedures. Light scattering (bright field and phase contrast) and standard fluorescence microscopy techniques, commonly used to analyse two-dimensional monolayer and optically transparent cultures, are inadequate to analyse 3D cultures; this is due to the diffraction and diffusion to which light is subjected when crossing tissues, scaffolds or cell aggregates. Although microscopy has been successfully adapted for 3D samples by recording several layers through the *z*-axis (*e.g.* confocal microscopy, multi-photon microscopy and optical coherence tomography), the required equipment is expensive and the access is often limited [103], leading researchers to frequently use less advanced approaches (*e.g.* light and standard fluorescence microscopy) that are unable to describe the complexity of a 3D construct. Moreover, the fact that samples must be commonly stained to perform the analysis remains a drawback of optical techniques, as performing staining assays requires samples to be sacrificed, and is reagent, labour and time consuming.

Given the importance and rising interest of 3D cell culture, in combination with the lack of an affordable, robust, effective and simple-to-use optical microscopy technique to analyse it, a considerable effort has recently been given in developing non-invasive real-time assays to monitor 3D cultivations.

Electrical methods are non-destructive, label-free and relatively non-expensive and were successful used to monitor 3D cell cultures. Using a platform with a combination of electrodes to measure the impedance of a gelatin hydrogel with embedded hMSC, researchers were able to evaluate the cell coverage and conclude about the cell proliferation [104]. In a similar setting, researchers were able to acquire information about cellular behaviours such as cell proliferation, apoptosis and monitor cell migration of hMSC cultivated in alginate hydrogel [105]. More recently, the same research group reported that osteoblasts and adipocytes exhibit distinct dielectric properties, allowing to discriminate the differentiation of hMSC into those lineages by measuring the real-time impedance [106].

In another study, an ultrasound-integrated bioreactor was developed to infer the ECM evolution and chondrocyte proliferation during a cartilage tissue formation in a continuously and non-invasive way [107]. Digital holographic microscopy is yet another methodology that allowed to assess the cellular response of osteoblasts in terms of 3D shape and dimensions, in porous scaffolds, without interfering with the natural environment [108].

A distinct approach to analyse the dynamics of a 3D culture, instead of directly analyse the cells, is by measuring the compounds present in the medium culture (*e.g.* nutrients, metabolites, gases) or cellular products/components (*e.g.* proteins, nucleic acids, lipids). The variations of such molecules

within the sample provides an insight of the cell behaviour, and can indirectly contribute to conclude about the viability, phenotype or fate of the cells.

Vibrational spectroscopy, such as Raman and Fourier transform (FTIR), is a rapid and sensitive method of multi-analysis. By measuring non-destructively the vibrational energy in a compound, this methodology permits to characterize several components within a sample, thus showing promise to be used as a monitoring technique. Moreover, apart from being non-expensive, it is reagent- and label-free. FTIR in the mid-infrared region associated with multivariate data analysis to estimate the glucose, lactate and ammonia concentrations was successfully employed to monitor the cultivation of MSC [109].

Bioanalysers combine a biological component with a detector to measure quantitatively the number of biomolecules, such as proteins, sugars (*e.g.* glucose) and metabolites (*e.g.* lactate) in a given biological system. A commonly used biosensor is based on enzymatic interactions, in which enzymes with an inherent specificity for a single target participate in some kind of reaction when in the presence of that molecule. This is detected by the sensor, which produces a signal and enables the quantification of the target molecule, thus allowing its constant monitoring during cultivation. An advantage of this method is that the enzyme is not consumed and can therefore be used continuously as long as the enzyme remains stable.

Nonetheless, the retrieval of samples from the 3D cultures or reactors that are to be analysed by the aforementioned techniques, or the integration of some of the recent monitoring tools within the 3D platforms and/or reactors, might be challenging.

1.5 Aim of studies

The current work focuses on the establishment of a novel *in vitro* monitoring system for the non-invasive analysis of three-dimensional cell and tissue cultures. The system comprises a mini-bioreactor, that supports 3D cultivation and operates under perfusion to better mimic physiological conditions. Additionally, a catheter connected to a micro-perfusion pump device is inserted within the cell construct for a non-invasive and regular medium sampling during cultivation. Such sampling enables for the continuous control of viability, growth or functional differentiation of the cells and tissue via biological parameters analysis (*e.g.* nutrients, metabolites and oxygen tension), while preventing the need for the currently used endpoint methodologies to examine 3D cultures.

Prior to the cultivation inside the bioreactors, a cytocompatible material to manufacture the reactor is to be selected. In addition, the cultivation of MSC in 3D platforms is to be optimized and the transport dynamics within those platforms characterized. In parallel, the MSC differentiation in 3D platforms is evaluated in order to assess the feasibility of generating a functional tissue construct to be used as an *in vitro* model inside the mini-perfusion bioreactor.

Due to the promising applications of MSC in cell-based therapies and tissue engineered products for regenerative medicine, human adMSC are used in the present work.

Chapter 2

Materials and methods

This chapter provides an overview of the materials and the methods used in the development of the present work.

2.1 Materials

An extensive list of all the instruments, equipment, solutions and software used throughout the development of the present work is enumerated in the Appendix A.1 Materials and methods.

2.2 Methods

The MSC used in the developed work were previously isolated from human adipose tissue by explant culture and cryopreserved in the cell bank of the Research Group Kasper. The cells used were retrieved from stored vials of the following cell lines: adMSC140113, adMSC170113, adMSC041013, adMSC180118 and adMSC260618.

All the procedures concerning cell cultivation were performed inside a safety bench and the instruments were sterilized with 70% (v/v) ethanol prior to being used. The flasks and the bioreactor circuit equipment were autoclaved for 20 min at 121 ºC, the liquid solutions were sterile filtered (0.2 µm) and the alginate (powder form) and collagen membranes were sterilized under UV light (250 nm) for 30 min, at least once each side in case of the membranes. Cells cultivated in T-flasks, well-plates, petri-dishes or bioreactors were incubated at 37 ºC, 5% CO_2 and 21% O_2, unless stated otherwise.

2.2.1 Cell culture

Cell thawing: The desired cell vial was first selected and retrieved from the liquid nitrogen tank. Subsequently, the vial was thawed by submerging and swirling it in the warm bath for 1-2 min. When the vial was thawed but still cool to the touch, 1 ml of basal medium was added to it. After two minutes, the cell suspension was transferred to a 50 ml centrifugation tube, the cryotube was washed with 2 ml of basal medium followed by two minutes of waiting. Afterwards, this 2 ml suspension was also transferred to the centrifugation tube. The centrifugation tube was topped up to 10 ml with basal medium and centrifuged at 500 $\times\, g$ for 5 min. Next, the supernatant was aspirated using a sterile glass Pasteur pipette coupled to a vacuum pump, the pellet was flicked and resuspended in 500 µl of expansion medium. The cells were counted in a Neubauer chamber to determine the volume to be transferred to one or more T-flasks to cultivate the desired cell concentration (1,000-3,000 cells/cm^2). Subsequently, medium was added to the flask(s) in order to preface the working volume (Table 2-1). Finally, the flask(s) was(were) incubated overnight. When necessary, the medium was changed after 24 h.

Cell passaging: The cells were passaged when the confluence reached 80-90%, which was checked regularly by phase contrast microscopy. Prior to perform the cell passaging, the solutions to be used (PBS, accutase and medium) were placed on the warm bath at 37 ºC. The medium inside the flask was first aspirated using a sterile glass Pasteur pipette coupled to a vacuum pump. Then, the flask was

rinsed with PBS using a volume of about 50-70% of the working volume, which was subsequently aspirated as aforementioned. Next, accutase solution was added to the flask (Table 2-1) and the flask was incubated. After 10-15 min, expansion medium was added to the flask (Table 2-1) and the cell suspension was transferred to a 50 ml centrifugation tube. The suspension was centrifuged at 500 $\times g$ for 5 min, after which the supernatant was aspirated as aforementioned. The pellet was flicked and resuspended in expansion medium (volume dependent on the size of the pellet). The cells were counted in a Neubauer chamber to determine the suspension volume to be transferred to one or more new culture flasks to seed the desired cell concentration (1,000-3,000 cells/cm^2). Finally, medium was added to the new culture flask(s) in order to preface the working volume (Table 2-1), being then incubated.

Table 2-1 Working volume, accutase and volume of medium added after the accutase incubation for each flask.

T-flask	Working volume (ml)	Accutase/Medium (ml/ml)
T25	5	1/2
T75	15	2/3
T175	25	4/6

Cell counting: The Neubauer chamber was first rinsed with water and then covered with the cover glass. A 20 µl sample of cell suspension was retrieved and mixed with 20 µl of Trypan Blue solution. Next, 20 µl of the resulting suspension was transferred to both sides of the Neubauer chamber and cell counting was performed under a bright field microscope with the aid of a manual counter.

Cell cryopreservation: When there were remaining cells after performing an experiment, these were cryopreserved. Cells were counted to determine the number of vials that were possible to produce (one vial per million of cells). The cell suspension was then centrifuged at 500 $\times g$ for 5 min and the cryo medium was prepared fresh while the centrifuge was working. Subsequently, the supernatant was aspirated using a sterile glass Pasteur pipette coupled to a vacuum pump, the pellet was flicked and resuspended in as many volume units (ml) as number of vials. Finally, 1 ml of this cell suspension was added to each cryo tube, allowing for each vial to have one million cells per ml of medium. Vials were then stored at -80 ºC for 3-4 days inside freezing containers that allowed their inner temperature to decrease 1 ºC/min. Finally, vials were transferred to the liquid nitrogen tank.

2.2.2 Cell culture in three-dimensional platforms

Collagen membranes: MatriStypt® or MatriDerm® membranes were first cut to the desired size (using a scalpel or a puncher), placed on well-plates or petri-dishes, and then sterilized prior to cell seeding. MSC in passage were centrifuged at 500 $\times g$ for 5 min, resuspended in expansion medium and seeded to dry or medium soaked matrices in order to have the desired cell density, between 5,000-20,000 cells/cm^2 depending on the experiment. The cells were seeded either statically or dynamically, and in both settings cell suspension was added on top of the membranes, with the latter being followed by a centrifugation step at 500 rpm for 5 min (Heraeus™ Megafuge™ 16, Thermo Scientific). Subsequently, the cell constructs were incubated for 1 h to allow cell adhesion. Afterwards, expansion medium was added to the membranes and these were incubated for 3 days before usage in further experiments.

For the optimization of the cell seeding experiment, MatriStypt® seeded by the distinct methods were cultivated for 10-11 days; calcein-AM/PI staining was performed occasionally to assess the cell viability and compare the different methodologies of cell loading.

For the cultivation of MSC in MatriDerm® or MatriStypt® inside the reactors and respective controls, and in the differentiation experiments MSC were seeded statically to medium soaked matrices, as described previously.

Alginate hydrogel: Sodium alginate (powder form) was sterilized before preparing a 1.2% (w/v) alginate solution. This was accomplished by dissolving sodium alginate in expansion medium supplemented with 1% (v/v) gentamycin, followed by a vortexing step to obtain a homogenous mixture. Subsequently, the alginate solution was stored at 4 °C until usage. MSC in passage were centrifuged at 500 × g for 5 min, resuspended in expansion medium and added to the alginate solution in a volume that allowed to have the desired cell density, between 100,000-300,000 cells per ml of alginate-cell suspension, depending on the experiment. Afterwards, the gels were casted by adding the alginate-cell suspension to well-plates and topping that suspension with a 100 mM $CaCl_2$ solution in a volume ratio of 1:2. Finally, the plates were incubated for periods varying from 8 to 24 h to allow the hydrogel cross-linkage before being used in further experiments.

For the optimization of the cell seeding experiment, gels were cultivated for 5 days; calcein-AM/PI staining was performed occasionally to assess the cell viability and compare the different densities of cell loading.

Standard cultivation: Standard cultivation of seeded 3D platforms was performed in the optimization of the cell culture experiments and in the assemblage of controls for the cultivation inside the perfusion bioreactor. It comprised on cultivating seeded alginate gels or membranes in culture plates, such as well-plates or petri-dishes, filled with expansion medium up to the respective working volume. Medium was changed every 2-3 days during the cultivation period.

2.2.3 Experimental setup of the perfusion circuit

Perfusion chamber: The perfusion chamber and respective lid are 3D-printed with the parylene-coated High Temp resin. The chamber has a cubical shape with trimmed vertical edges and an inner volume of 3 ml. As depicted in Figure 2-1 (a and c), a scaffold holder fixes the scaffold between the lid and the chamber, so that medium flows parallel to its surface; the holder bottom has an open cross structure that supports the scaffold, while allowing medium to perfuse the scaffold (Figure 2-1 (b and d)). In addition, the reactor design allows for the insertion of a catheter in between the scaffold and its platform holder.

Perfusion system: The perfusion system accommodates a single flow chamber, a single medium container and a multi-channel peristaltic pump, which allows for several perfusion circuits to operate in parallel. In Figure 2-2 (a) are depicted the two circuits of the system: the main circulating circuit and the sampling circuit. The main circuit includes the medium container, the reactor chamber and the tubing for continuous circulation of medium to provide oxygen and nutrients during cultivation. The gas

exchanges occur through a 0.2 µm sterile filter. The sampling circuit consists on a catheter connected to the micro-perfusion pump (MPP 102 PC, Joanneum Research), which contains a 10 ml bag filled with the Elo-Mel solution and two peristaltic pumps that together supply the necessary driving force for medium sampling from within the scaffold. Tubing connects the buffer bag to the catheter and the catheter to the sampling tubes for further biological parameter analysis, such as glucose/lactate concentrations measurement. Figure 2-2 (b) depicts the real image of three perfusion systems operating in parallel.

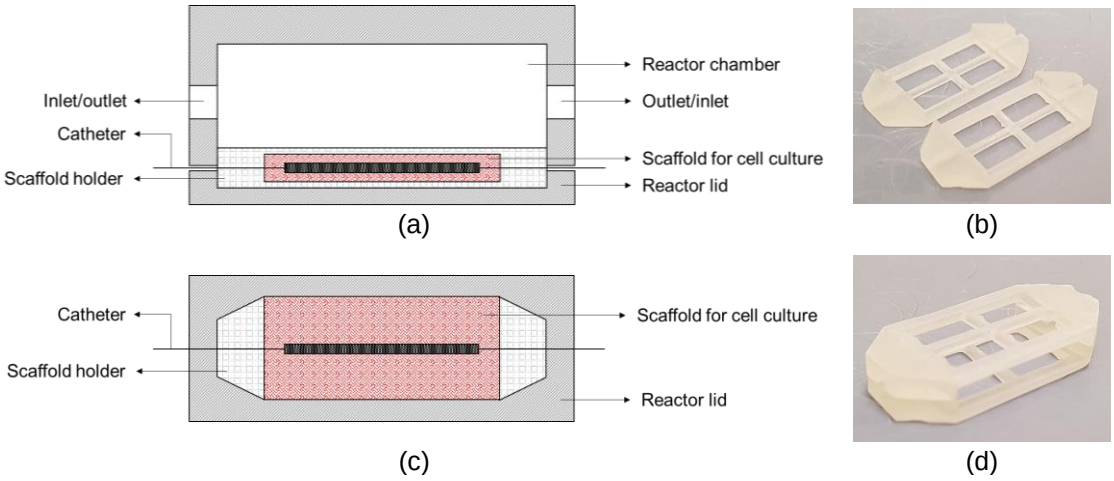

Figure 2-1 (a) Side and (c) bottom views of the perfusion chamber body (figures are not in scale). An (b) open and (d) closed scaffold holder fixes the scaffold between the lid and the chamber. Additionally, a catheter can be inserted within the scaffold and the older.

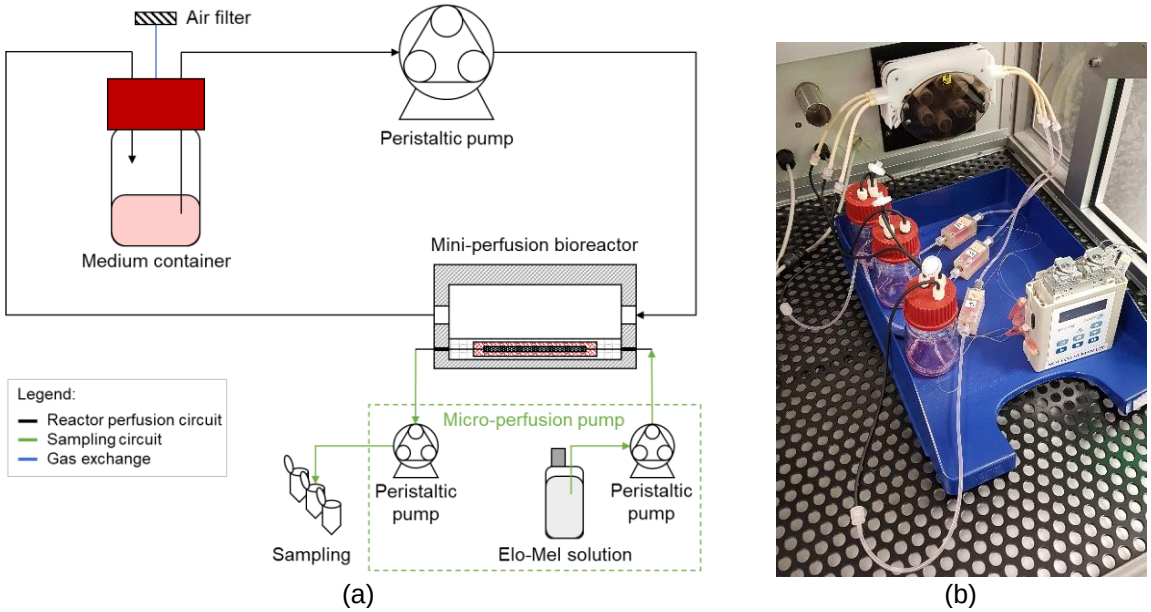

Figure 2-2 (a) Circuit of a single perfusion bioreactor system and (b) real image of three perfusion circuits operating in parallel. Each perfusion system comprises a medium container, a micro-perfusion reactor and a multi-channel peristaltic pump; the sampling system is composed by a mini-perfusion pump and a catheter that allow sampling from within the scaffold.

2.2.4 Cell culture inside the perfusion bioreactor

Cultivation in the perfusion bioreactor: The bioreactors (parylene-coated High Temp resin material), tubing circuits and medium containers were steam sterilized at 121 ºC for 20 min prior to usage. Cells were seeded to the membranes/alginate hydrogels as described previously. It is worthy to note that all seeding procedures to the membranes were performed statically to medium-soaked membranes and the gels were cut (using sterile scalpels) to fit the reactor after being casted. At the time of cultivation, the reactor circuit was assembled inside the safety bench and both media containers and reactors were left open. Each medium container of the perfusion circuit (for dynamic cultivation) was filled with 15 ml of expansion medium supplemented with 1% (v/v) gentamycin. For static cultivation, the inlet and outlet of the reactor were closed with caps, and the chamber was filled with 3 ml of expansion medium supplemented with 1% (v/v) gentamycin. Thereafter, a pair of collagen membranes or an alginate gel were transferred (using sterile tweezers) to a 3D platform holder, which was then inserted in the reactor. Depending on the experiment setting, a catheter was additionally inserted in between the pair of membranes or pierced through the gel to allow medium sampling from the centre of the cell constructs. The reactors were then closed (using a screwdriver), as well as the medium containers. Finally, the reactor circuits were incubated (IncuReTERM), and operated under dynamic (constant rate; 4, 5 or 10 rpm, depending on the experiment) and/or static conditions. When a catheter was present, this was connected to a micro-perfusion pump, which inflicted the necessary driving force to collect medium samples from the centre of the 3D platforms. The cultivation was carried out up to seven days in all experiment settings, without the cultivation medium being changed. Cell samplings (manually) and medium samplings (through the catheter or manually) were performed occasionally.

Cell sampling: The dynamic reactor circuit was disconnected from the pump and placed under the safety bench; the static reactor was also transferred to the safety bench. First, the medium container of the dynamic circuit was opened to depressurize the dynamic reactor and then the reactors were opened using a screwdriver. Carefully, a membrane was either removed from the reactor and placed on a petri-dish, where a fraction was cut (using a scalpel) for further analysis, or a piece of membrane was directly retrieved from the reactor if already cut in fragments. As for the hydrogel, a piece of the gel was cut directly from the inside of the bioreactor (using a scalpel). The reactors and containers were then closed, incubated and connected to the pumps (only for dynamic conditions). The cell viability on the cell samples was analysed via calcein-AM/PI staining.

Medium sampling: The medium samples from within the cell constructs cultivated in the mini-perfusion bioreactor were obtained through the catheter using the micro-perfusion pump. Before taking samples from the core of the 3D platforms, the catheter was first flushed with the Elo-Mel solution for 5 min at 10 µl/min. Subsequently, samples were collected for 15 min at 2 µl/min. In case of medium sampling from the chamber of the static reactor, one of the caps was opened to allow the acquisition of manual samples using a micropipette. The samples from the containers of the perfusion circuit, were retrieved manually (using a micropipette) after opening the container lid; manual medium samples were performed inside the safety bench. Finally, the samples were stored at 4 ºC until being analysed (measurement of glucose and lactate concentrations).

2.2.5 Bioreactor characterization

Cytotoxicity of the reactor material: Two approaches were performed to assess the cytotoxicity of different materials from which the reactor can be 3D-printed. At the end of each approach, the cell viability was assessed via calcein-AM/PI staining, and MTT and TOX8 assays. In addition to these methods, the glucose and lactate concentrations were measured in the second approach.

Approach 1: Expansion medium was incubated for 7 days inside 3D-printed bioreactors with: γ-irradiation-sterilized High Temp (HT) resin (HT-γ); pre-washed HT-γ (HT-γ-w); and autoclave-sterilized HT resin with a parylene-coating (HT-P); the step of pre-washing of the HT-γ-w was achieved by perfusing this reactor with PBS for 3 days. Cells were first cultivated (10,000 cells/cm^2) in wells of a well-plate with fresh expansion medium for 1 day, followed by a cultivation period of 3 days in the presence of medium incubated inside the different bioreactors.

Approach 2: Cells were first cultivated (3,000-6,000 cells/cm^2 depending on the study) in wells of a well-plate with expansion medium for 1-3 days, followed by a cultivation period of 3-4 days in the presence of cylinder-shaped pieces (1 mm thick, 5 mm of diameter) of different materials: parylene-coated High Temp resin 1× or 4× autoclave-sterilized (HT-P1× and HT-P4×, respectively), non-parylene-coated HT resin autoclave-sterilized (HT) or γ-irradiation-sterilized (HT-γ), Clear resin 1× or 8× UV light-sterilized (C-UV1× and C-UV8×, respectively), and UV-cured Clear resin (C(+)UVc).

Transport dynamics in 3D platforms under perfusion: The reactor circuit was assembled and both media containers and reactors were left open. Each medium container was filled with 15 ml of expansion medium. Thereafter, a pair of collagen membranes or an alginate gel, in the absence of cells, were transferred to a 3D platform holder, with a catheter inserted between the pair of membranes or pierced through the gel to allow medium sampling from the centre of the platforms. Subsequently, these platforms were inserted in separate reactors. The reactors were then closed, as well as the medium containers. Afterwards, the reactor circuits were incubated (IncuReTERM), and operated under dynamic (constant rate, 10 rpm) conditions. After 2 h, the expansion medium was changed for PBS (20 ml) to remove glucose/lactate from the platforms and perfusion was performed for 48 h. Finally, PBS was changed for expansion medium (15 ml) to replace the biomolecules in the platforms. Medium samples from within the platforms were acquired occasionally through the catheter to monitor the glucose/lactate variations.

2.2.6 Viability assays

MTT viability assay: MTT (yellow coloured) staining allows to assess the cell viability since it is metabolized by living cells, forming the violet coloured formazan. For MTT assay, the medium was first removed from the cell samples, which were then rinsed with PBS. Subsequently, the samples were covered with the MTT working solution (10% MTT stock solution in expansion medium) and incubated for 4 h at 37 ºC. Finally, the samples were documented by phase contrast microscopy.

To dissolve the precipitated formazan dye, SDS solubilisation solution was added to the samples (in a ratio 0.9:1 to the MTT working solution previously added) and these were incubated overnight at 37 ºC. Afterwards, 200 µl of the solution from each sample was transferred to a 96-well plate and absorbance (570-630 nm) was measured on a plate reader (Infinite® M1000 Pro, Tecan). The absorbance data was analysed using Microsoft Excel.

TOX8 viability assay: TOX8 stock solution was added to the samples (in a ratio 1:10 to the medium in the samples) and then these were incubated for 2-4 h at 37 ºC. Subsequently, 100 µl of the solution from each sample was transferred to a round bottom transparent 96-well plate. Finally, the increase of fluorescence (569/590 nm) was measured on a plate reader (Infinite® M1000 Pro, Tecan) and the data was analysed using Microsoft Excel.

Glucose consumption and lactate production: The monitoring of glucose and lactate concentrations is a mean to indirectly assess the cell viability. As addressed in section 1.3.3, undifferentiated hMSC in early passages cultivated *in vitro* use glucose as carbon source and metabolize it into lactate via glycolysis. Thereby, the concentration profile of these biomolecules in the medium allows to conclude about the cell metabolism, thus their viability. The glucose and lactate concentrations in the samples were measured using an enzymatic bioanalyser (YSI 2700 SELECT, YSI Incorporated), which aspirated 25 µl from each sample.

Calcein-AM and PI viability staining: To analyse the cell viability, samples were stained with calcein-AM (stains living cells in green) and PI (stains dead cells in red). Samples were first rinsed and covered with PBS. Subsequently, calcein-AM staining solution (4 µl of calcein-AM per ml of PBS) was added and the samples were incubated for 20 min at 37 ºC. Afterwards, PI stock solution was added (33 µl of PI per ml of PBS) and the samples were incubated in the dark for one minute at room temperature. Finally, the cells were rinsed twice with PBS and the staining was documented by fluorescence microscopy.

2.2.7 Adipose derived MSC differentiation

The employed methodology of trilineage differentiation of adMSC is based on the work developed by Egger [110] and Oliveira [111] and was performed in planar culture and in 3D platforms. Both protocols are similar, except in the initial setting of cell culture.

Planar culture: The surface of the well bottoms in a 12-well plate were first manually coated with 2 µg/cm^2 of fibronectin and left to dry at room temperature for one hour. The plate was then sealed with parafilm and stored at 4 ºC until usage. Before using the plates, the wells were rinsed once with PBS and then seeded with cells (4,000 cells/cm^2 for osteogenic and chondrogenic differentiations and 7,000 cells/cm^2 for adipogenic differentiation) within 1 ml of culture medium. Upon reaching 100% confluence, the medium was changed to the respective differentiation solution.

3D platforms: The differentiation in 3D platforms was carried out in MatriDerm® and alginate gel. Regarding the MatriDerm®, these were round shaped (0.28 cm^2) and seeded (statically to medium soaked membranes) with a cell concentration of 20,000 cells/cm^2. Concerning the alginate, 100 µl of

cell-alginate suspension (300,000 cells/ml) were casted in each well. Both the membranes and alginate gels were seeded/casted in 96-well plates, as described in section 2.2.2, and incubated overnight. On the day after, the medium was changed to the respective differentiation solution.

The cells were cultivated for 21 days in both settings, with the medium being changed every 2-3 days. Finally, on day 21, cells were fixated with ethanol (EtOH) or paraformaldehyde (PFA) according to the respective staining.

2.2.8 Fixation procedures

The fixation procedures were independent of the cell cultivation setting.

EtOH fixation: The medium was first removed, and the samples were rinsed thrice with PBS. Subsequently, the samples were covered with -20 ºC EtOH 96% and incubated for one hour at 4 ºC. Finally, the samples were rinsed thrice with PBS, covered with PBS and stored at 4 ºC.

PFA fixation: The medium was first removed, and the samples were rinsed thrice with PBS. Subsequently, the samples were covered with PFA (4% in PBS) and incubated for ten minutes at room temperature. Finally, the samples were rinsed thrice with PBS, covered with PBS and stored at 4 ºC.

2.2.9 Staining procedures

The staining procedures for the trilineage differentiation of adMSC were similar for both cell cultivation settings, except on the rinsing steps. Based on the work developed by Egger [110], the rinsing steps were performed at 200 rpm for 5 min with the aid of a shaker (Skyline Orbital Shaker, Elmi).

DAPI staining: DAPI staining permits to determine the cell viability by staining in blue the cell nuclei of living cells. To perform this staining, the samples were first fixated in EtOH. After fixation, the samples were covered in DAPI solution and incubated in the dark for 15 min at 37 ºC. Finally, the samples were rinsed twice with PBS, covered with PBS and the staining was documented by fluorescence microscopy with a 360/460 nm excitation/emission filter.

Oil Red O staining (adipogenic differentiation): Oil Red O stains in red the lipid vacuoles of cells, allowing to detect the lipid droplet accumulation inside the cells as a result of adipogenic differentiation. To perform this staining, the samples were first fixated in PFA. At the time of the assay, the samples were rinsed thrice with ddH_2O and then covered with Oil Red O solution (0.5% in propylene glycol). After 20 min of incubation at room temperature, the samples were rinsed with ddH_2O until the supernatant remained clear. Finally, the staining was documented by phase contrast microscopy.

Alcian Blue staining (chondrogenic differentiation): Alcian Blue allows to distinguish the cartilage formed during chondrogenic differentiation, which has a distinct ECM, by staining glycosaminoglycans in blue. To perform this staining, the samples were first fixated in EtOH. At the time of the assay, the samples were rinsed with washing solution (3% acetic acid in ddH_2O) for 3 min and then covered with Alcian Blue staining solution (1% (w/v) Alcian Blue 8 GX in washing solution). After 30 min of incubation

at room temperature, the samples were rinsed with washing solution until the supernatant remained clear. Finally, the staining was documented by phase contrast microscopy.

Calcein (osteogenic differentiation): Calcein stains the deposited calcium by forming a chelate complex with that mineral, which allows for the detection of ECM mineralization. To perform this staining, the samples were first fixated in EtOH. At the time of the assay, the samples were rinsed thrice with ddH_2O and then covered with calcein solution (5 µg calcein/ml ddH_2O). Afterwards the samples were incubated over night at 4 ºC in the dark. Finally, the samples were rinsed thrice with ddH_2O before documentation by fluorescence microscopy with a 485/535 nm excitation/emission filter.

von Kossa (osteogenic differentiation): von Kossa staining stains the phosphate deposition of the ECM, allowing to assess the formation of phosphate deposits by osteocytes. To perform this staining, the samples were first fixated in EtOH. At the time of the assay, the samples were rinsed thrice with ddH_2O and then covered with silver solution (5% $AgNO_3$ in ddH_2O). After 30 min of incubation at room temperature, the samples were exposed to UV light (250 nm) for 2 min and then rinsed with decolourization solution (5% Na_2CO_3, 0.2% formaldehyde in ddH_2O) for 2 min. Finally, the staining was documented by phase contrast microscopy.

Alizarin Red S (osteogenic differentiation): Alizarin forms a chelate complex with bivalent cations such as calcium, resulting in a bright red staining of the calcium deposited in the ECM. To perform this staining, the samples were first fixated in EtOH. At the time of the assay, the samples were rinsed thrice with PBS and then covered with Alizarin Red S staining solution (0.5% (w/v) Alizarin Red S in ddH_2O). After 15 min of incubation at room temperature, the samples were rinsed with PBS until the supernatant remained clear. Finally, the staining was documented by phase contrast microscopy.

Chapter 3

Results and discussion

This chapter comprises the presentation of the developed work and respective discussion.

3.1 Overview of the developed work

An overview of the developed work is provided in Figure 3-1; it highlights the major investigated topics, each one represented by a block, and how they are interrelated. First, the cytotoxicity of materials from which the mini-perfusion reactor can be 3D-printed was evaluated (described in section 3.2). Prior to the cultivation inside the bioreactor, the cell seeding and cultivation in 3D platforms were optimized (described in section 3.3), and the transport dynamics within those platforms was analysed (described in section 3.4). Thereafter, the cultivation of 3D cell-constructs under perfusion was performed (described in section 3.5). Finally, the capacity of adMSC to differentiate in planar and 3D culture was assessed (described in section 3.6).

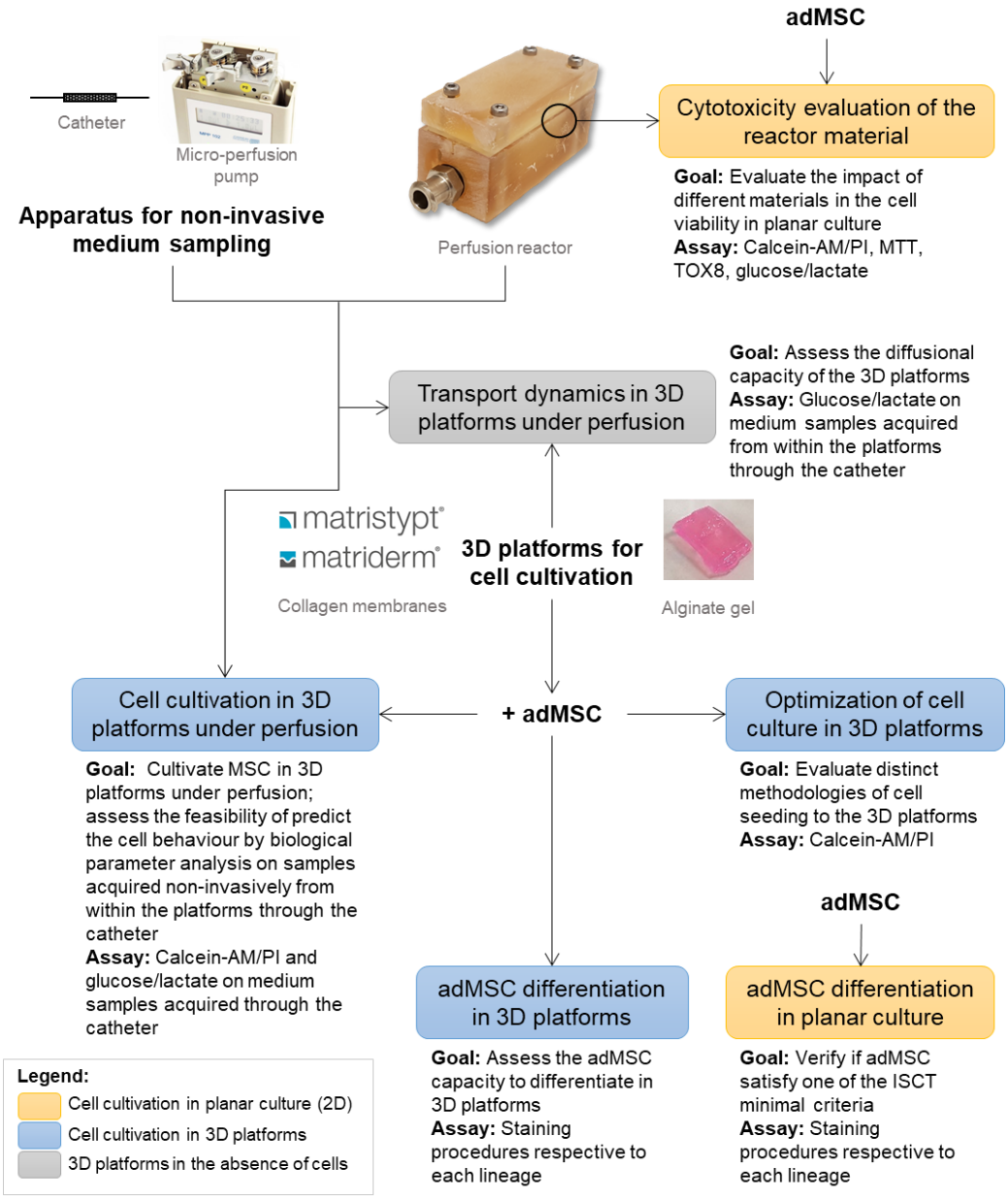

Figure 3-1 Block diagram of the developed work. Each experiment is accompanied by a summary of the main goal(s) and respective analytical assays.

3.2 Cytotoxicity evaluation of the bioreactor material

Prior to performing the cell cultivation inside the bioreactors, the cytotoxicity of their manufacturing material was assessed. Initially, the manufacturer of the bioreactors had available reactors 3D-printed with the High Temp resin (Formlabs) with or without a parylene coating. The non-parylene-coated reactors were either sterilized via γ-irradiation by the manufacturer or steam-sterilized in the laboratory's autoclave, whereas the parylene-coated reactors were solely sterilized in the autoclave. Later, an additional material became available, the Clear resin (Formlabs), which was sterilized via UV light and with the option of being further cured/hardened with UV light after the 3D printing.

Two different approaches were carried out to assess the cytotoxicity of the different materials used in the manufacturing of the reactors, and the respective sterilization process. In the first experiment (section 3.2.1), cells were cultivated in different media that were pre-incubated, or not, inside reactors manufactured with distinct materials. In the second experiment (section 3.2.2), cells were cultivated in the presence or absence of small pieces of different materials.

3.2.1 Cell cultivation with different media conditions

In the first approach to assess the cytotoxicity of the different materials, expansion medium was incubated for one week in bioreactors 3D-printed with: γ-sterilized High Temp (HT) resin (HT-γ); pre-washed HT-γ (HT-γ-w); and autoclave-sterilized HT resin with a parylene-coating (HT-P). Cells were first cultivated (10,000 cells/cm^2) for one day in expansion medium, after which the medium was changed for the different incubated media or fresh expansion medium (Ctrl). After three days of cultivation in these conditions, the cell viability was assessed via optical (calcein-AM/PI staining and MTT) and quantitative (cell count, MTT and TOX8) assays.

Calcein-AM is a membrane-permeable compound that is converted by live cells into the green-fluorescent calcein, thus enabling to detect live cells with fluorescence microscopy. Propidium iodide (PI) is a red fluorescent agent that binds to DNA but is not able to cross the membrane. It allows to detect dead cells once it crosses their disrupted membranes and stains their genetic material in red.

MTT permits to conclude about the metabolic activity of cells. This yellow-coloured compound is uptaken and metabolized by live cells into the insoluble purple-coloured formazan. The degree of this conversion can be documented by bright field microscopy: the more formazan crystals are formed, the higher is the cell metabolism. Formazan can be further solubilized, giving rise to a coloured solution whose absorbance can be measured and the extent of metabolic activity quantified.

The results obtained from the optical assays are depicted in Figure 3-2. Regarding the control, cells cultivated in fresh medium were viable, as expected. Concerning the HT-γ-w and HT-γ, the cells cultivated in the media pre-incubated in these reactors appeared dead, due to their red staining in the calcein-AM/PI assay and the reduced amount of formazan crystals formed in the MTT assay. Moreover, the pre-washing step of the HT-γ reactor resulted in a higher number of viable cells than the non-washed (more green-coloured cells in the calcein-AM/PI stainings for the samples cultivated in media

pre-incubated in the HT-γ-w than in the non-washed HT-γ reactor), indicating that the HT-γ material might leak toxic compounds that are diminished after the washing step, thus inflicting less cell damage. Finally, the cells cultivated in medium pre-incubated in the HT-P reactor exhibited a high degree of viability. In the calcein-AM/PI results, no dead cells were detected, and the cell morphology closely resembled the cells cultivated in fresh medium; in the MTT assay, although in less amount compared with the cells cultivated in fresh medium, formazan crystals were clearly visible. Furthermore, a higher amount of formazan was produced by the cells cultivated in medium incubated in the HT-P reactor, when compared to the cells cultivated in both HT-γ conditions.

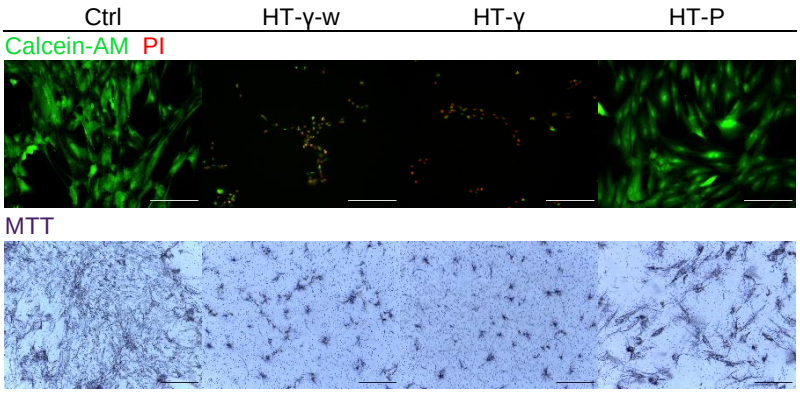

Figure 3-2 Calcein-AM/PI staining (top row) and MTT (bottom row) on cells cultivated for 3 days in fresh medium (Ctrl) or media pre-incubated for one week in γ-sterilized High Temp (HT) resin reactor (HT-γ); pre-washed HT-γ reactor (HT-γ-w), and parylene-coated HT resin reactor (HT-P). Calcein-AM/PI and MTT assays were performed to conclude about the cell viability: calcein-AM stains live cells in green; PI stains dead cells in red; live cells metabolize the yellow-coloured MTT into the purple-coloured formazan crystals. Scale bar represents 250 µm in all pictures acquired by fluorescence microscopy (calcein-AM/PI staining) and bright field microscope (MTT) in 100x magnification.

Alike MTT, TOX8 enables the quantification of the metabolic activity of living cells, thus their viability. This method is based on the bioreduction of the oxidized form of the dye resazurin (blue colour) into its reduced form (red colour) by viable cells. The extent of this conversion can be accounted by measuring the fluorescence of the solution.

The results obtained in the quantitative assays (Figure 3-3) are consistent with the ones obtained in the optical assays. As expected, the highest viability was achieved when cells were cultivated in fresh medium. The cell viability was considerably higher when cells were cultivated in medium pre-incubated in the HT-P reactor compared to the ones cultivated in media incubated in the HT-γ reactors (both non- and pre-washed), as can be concluded from the significant difference in the results for cell count, absorbance (MTT) and fluorescence (TOX8) between these three conditions.

These findings indicate that the γ-sterilized HT resin is cytotoxic, whereas the HT-P resin is cytocompatible, thus suggesting that the parylene-coating on the HT resin is crucial for cell viability.

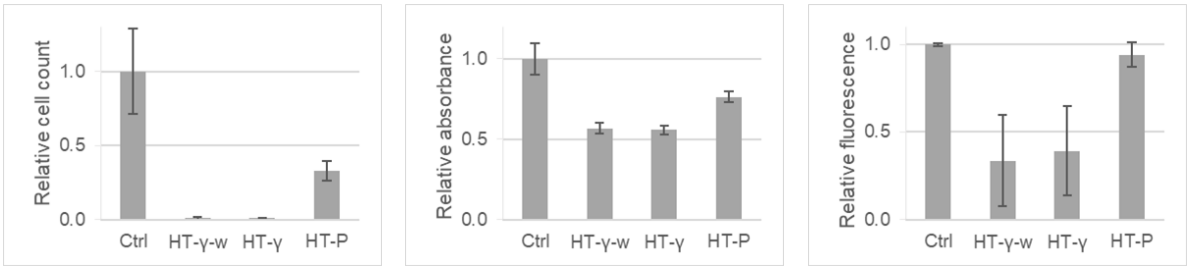

(a) (b) (c)

Figure 3-3 (a) cell count; (b) MTT; (c) TOX8 on cells cultivated for 3 days in: fresh medium, Ctrl; or media pre-incubated for one week in γ-sterilized High Temp (HT) resin reactor (HT-γ), pre-washed HT-γ reactor (HT-γ-w), and parylene-coated HT resin reactor (HT-P). Data represents mean ± SD from n = 3-6 replicates for each condition; data presented is relative to the control.

With the present approach of cell cultivation in media pre-incubated in reactors, the parylene-coated High Temp resin (HT-P) is the best suited reactor material.

3.2.2 Cell cultivation in the presence of the materials

The second approach was performed thrice, with the conducted studies differing in the materials that were evaluated. The methodology employed in the three studies was similar and based on cultivating cells for one to three days in expansion medium, followed by a cultivation period of 3-4 days in the presence of pieces of different materials. After the cultivation period, the cell morphology was documented by phase contrast microscopy; calcein-AM/PI staining and MTT were employed as optical assays (Figure 3-4); cell count, MTT, TOX8 and measurement of glucose and lactate concentrations were performed as quantitative assays (Figure 3-5).

As the experiment methodology and the analytical assays were identical between the three studies, the obtained results are presented together in the same chart. Hence, each quantitative assay is presented as a chart comprising three series, each corresponding to one of the studies. Due to the fact that the settings related to the cell line (origin and number of passage) and cultivation (initial cell density and number of days before and after adding the different pieces of material) varied between the different studies, it is only possible to perform a qualitative comparison between the different series/studies. Quantitative analysis between the different materials is however possible within each series/study.

First study

In the first study, cells were cultured (3,000 cells/cm^2) for one day in expansion medium followed by three days of cultivation in the presence of pieces of the following materials: parylene-coated High Temp resin 1× or 4× autoclaved (HT-P1× and HT-P4×, respectively), and non-parylene-coated HT resin autoclaved (HT) or γ-sterilized (HT-γ). Cells were also cultivated in the absence of material pieces in expansion medium as control (Ctrl).

Regarding the optical assays (Figure 3-4), only the cells cultured in the presence of HT-P resembled the control and presented a fibroblast-like morphology characteristic of MSC. Cells became

round-shaped when cultivated in the presence of the uncoated HT resin, indicating that this material damaged the cells as they lost their characteristic morphology.

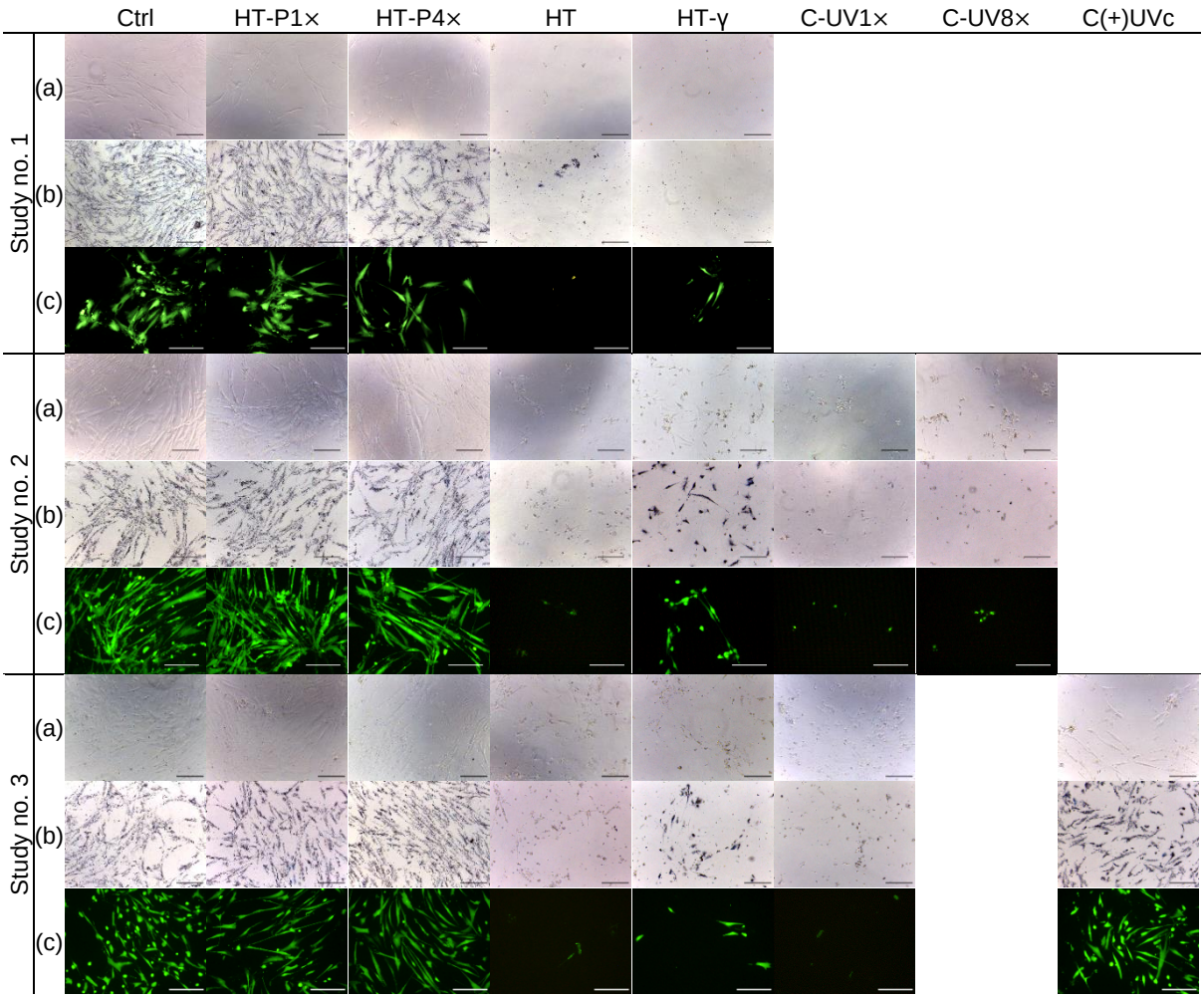

Figure 3-4 (a) Morphology, (b) MTT and (c) calcein-AM/PI staining on cells cultivated for 3-4 days in the absence of pieces of material in fresh medium (Ctrl) or in the presence of pieces of parylene-coated High Temp (HT) resin 1x or 4x autoclaved, HT-P1x and HT-P4x, respectively; non-parylene-coated autoclaved or γ-sterilized HT resin, HT and HT-γ, respectively; Clear (C) resin 1x or 8x UV light sterilized, C-UV1x (studies no. 2 and 3) and C-UV8x (study no. 2 only), respectively; and C resin UV light-cured, C(+)UVc (study no. 3 only). Calcein-AM/PI and MTT assays were performed to conclude about cell viability: calcein-AM stains live cells in green; PI stains dead cells in red; live cells metabolize the yellow-coloured MTT into the purple-coloured formazan crystals. Scale bar represents 250 µm in all pictures acquired by fluorescence microscopy (calcein-AM/PI staining) and bright field microscope (MTT and morphology) in 100x magnification.

Concerning the MTT assay, although in less amount compared to the control, only the cells cultivated in the presence of HT-P formed formazan crystals, meaning that they remained metabolically active, thus viable. This was not verified for the cells cultivated in the presence of the uncoated HT. Furthermore, the cells cultivated in the presence of HT-P1× produced more formazan crystals than the ones cultured with HT-P4×, suggesting that the parylene-coating might get corrupted after being subjected to successive autoclave steps. Indeed, after a series of autoclave steps, the parylene-coating of reactors 3D-printed with the HT resin seemed to start detaching (*see Figure A 1 in the Appendix*).

Finally, in the calcein-AM/PI staining, viable cells were detected when cultured in the presence of HT-P and HT-γ, although in a considerably less amount in the latter. The morphology and density of viable cells cultivated in the presence of HT-P1× and HT-P4× resembled the control, although a less viable density was observed in the latter samples. No viable cells were noticed on the samples cultivated in the presence of HT. In general, these findings suggest that the High Temp resin is cytotoxic if not covered with parylene.

The results obtained in the quantitative assays (Figure 3-5) are consistent with the ones obtained in the optical assays. As expected, the cell count and metabolic activity (MTT and TOX8) was highest for the control, followed by the cells cultured in the presence of HT-P, without a significant difference between the number of autoclave steps. Compared to the HT-P, the results obtained for the HT and HT-γ are negligible, as both the cell count and metabolic activity were considerably lower in the samples cultivated in the presence of these materials. Again, these findings demonstrate the importance of having a parylene coating in the High Temp material to prevent deleterious effects on the cells.

Alike MTT and TOX8, monitoring glucose and lactate concentrations is yet another means to assess the cellular metabolic activity. Generally, MSC in early passages cultivated *in vitro* acquire their energy mainly through glycolysis, in which they consume glucose and produce lactate. Hence, the decrease and increase of their concentrations in the medium, respectively, implies that cells are metabolically active, thus viable. Nonetheless, due to the presence of other C-sources in the medium that can as well be metabolized by the cells into lactate, such as glutamine, the variation of glucose is expected to be not as pronounced as that of lactate.

Concerning the glucose concentration, the consumption of this sugar in the control and the cells cultivated in the presence of HT-P was comparable, and there was a significantly lower consumption of the sugar by the cells cultivated in the presence of HT. Regarding the lactate concentration, the highest production of this metabolite was noticed for the control, followed by the samples cultivated in the presence of HT-P. There was a considerably lower production of lactate by the cells cultivated in the presence of HT and HT-γ, compared to the cells cultured in the presence of the High Temp resin when parylene-coated (HT-P).

In the first study of the second approach it was possible to demonstrate the cytotoxicity of the HT resin in the absence of the parylene coating. In the same way as the first approach, the best suited material for cell cultivation is the parylene-coated High Temp material.

Second study

Due to the decay of the parylene coating on the High Temp material after a series of autoclave steps, the manufacturer provided a novel material (Clear resin) that could be UV light sterilized and was expected to be cytocompatible without the need for a parylene coating.

(a)

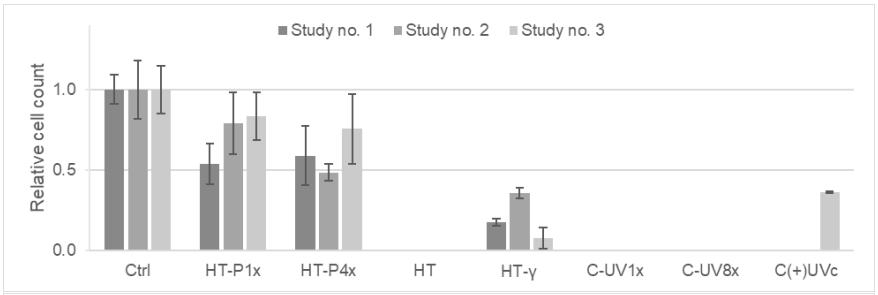

(b)

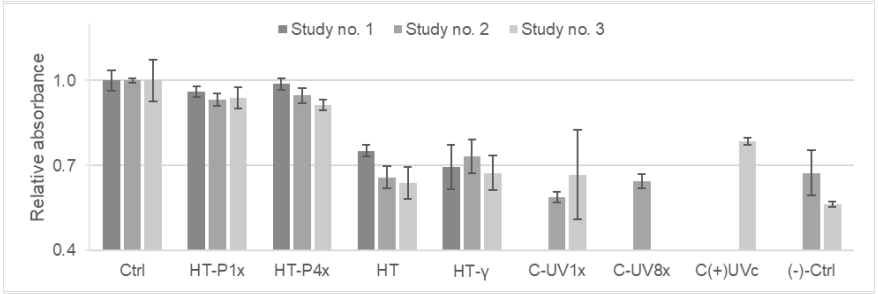

(c)

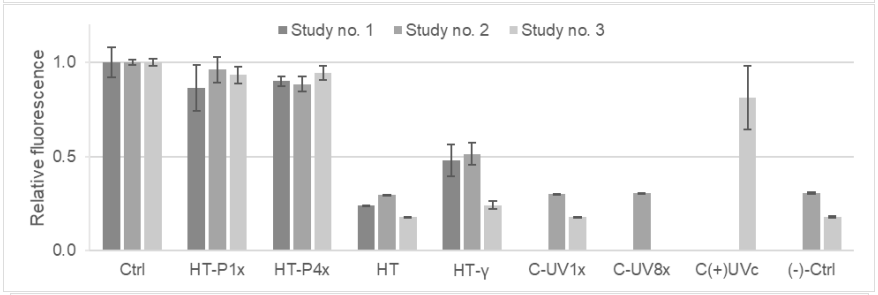

(d)

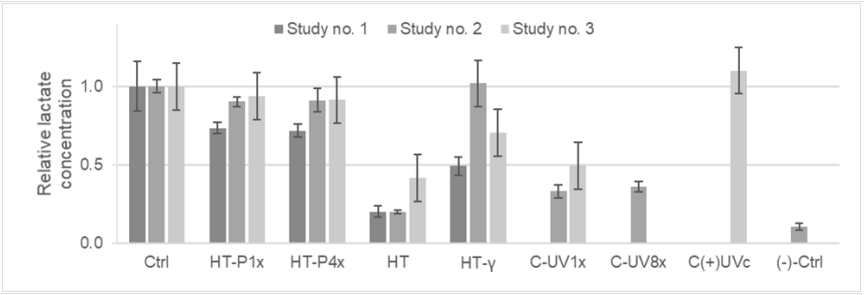

(e)

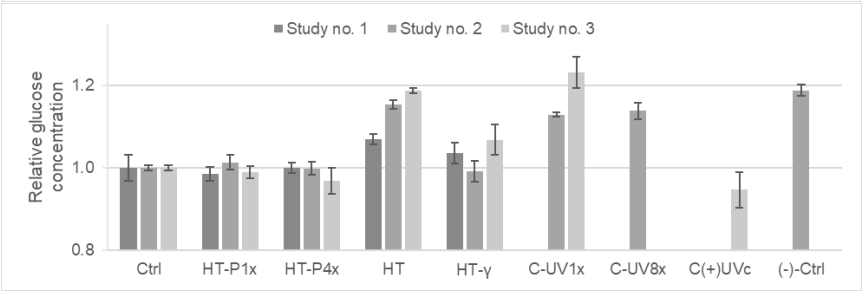

Figure 3-5 (a) Cell count; (b) MTT; (c) TOX8; (d) lactate and (e) glucose concentrations on cells cultivated for 3-4 days in the absence of pieces of material in fresh medium (Ctrl) or in the presence of pieces of parylene-coated High Temp (HT) resin 1x or 4x autoclaved, HT-P1x and HT-P4x, respectively; non-parylene-coated autoclaved and γ-sterilized HT resin, HT and HT-γ, respectively; Clear (C) resin 1x and 8x UV light sterilized, C-UV1x (studies no. 2 and 3) and C-UV8x (study no. 2 only), respectively; and C resin UV light-cured, C(+)UVc (study no. 3 only). Expansion medium was used as negative control, (-)-Ctrl (studies no. 2 and 3). Data represents mean ± SD from n = 3 replicates for each condition; data presented is relative to the control.

The second study was performed to assess the cytotoxicity of this novel material. Cells were cultured (6,000 cells/cm^2) for three days in expansion medium followed by four days of cultivation in the

presence of pieces of the following materials: HT-P1×, HT-P4×, HT, HT-γ, and Clear resin 1× or 8× UV light sterilized (C-UV1× and C-UV8×, respectively). Cells were also cultivated in the absence of material pieces in expansion medium as control (Ctrl), and expansion medium was incubated in wells without cells to serve as negative control ((-)-Ctrl).

Firstly, it is important to note that the results obtained for the already assessed conditions in the first study were reproduced, which contributes for the credibility of the present study. Moreover, as a result of this reproducibility, the discussion that follows will focus on the analysis of the Clear material.

Regarding the morphology (Figure 3-4), only the cells cultivated in the presence of HT-P remained with a fibroblast-like structure. The cells cultivated in the presence of HT or C-UV acquired a round shape, which indicates that the C-UV affected the cells negatively since they lost their characteristic morphology. The negative impact of the presence of HT-γ in the cell morphology was not as notorious as in the first study.

Concerning the MTT assay, the degree of formazan production by the cells cultivated in the presence of HT-P was comparable to the control, suggesting they remained with their metabolic capacity unaltered. Comparatively to the HT-P, the formazan produced by the cells cultivated with HT-γ was less pronounced, and no formazan was detected in the samples cultivated either in the presence of HT or C-UV. The Clear resin damaged the cells, as they became metabolically inactive, thus indicating cell death.

Finally, in the calcein-AM/PI staining, cells cultured in the presence of HT-P closely resembled the control in the viability and morphology, and there was a considerably higher number of viable cells in that condition than in the sample cultured with HT-γ. Again, no viable cells were detected on the samples cultivated in the presence of HT or C-UV, supporting the hypothesis that these materials are cytotoxic.

Regarding the number of UV light sterilization steps on the Clear material, it is not possible to conclude about their effect in the cell viability as both C-UV1× and C-UV8× presumably caused cell death at the same extent.

The results obtained in the quantitative assays (Figure 3-5) are consistent with the results obtained in the optical assays. The viability and metabolic activity (MTT and TOX8) were highest for the control. Compared to the control, a fewer number of viable cells were observed in the presence of HT-P, but the extent of the metabolic activity was comparable in both conditions. Less viable cells were detected when cells were cultured in the presence of HT-γ, which resulted in a lower conversion of MTT and resazurin in the MTT and TOX8 assays, respectively. No viable cells were detected when cells were cultured in the presence of HT or C-UV and the extension of the conversion of MTT and resazurin (TOX8) was negligible (in the sense that the results obtained for these conditions resembled the negative control).

As for the glucose consumption and lactate production, the behaviour of cells cultivated in the presence of HT-P or HT-γ resembled the control, whereas the cells cultivated in the presence of HT or C-UV presented a profile similar to the negative control.

As with the optical assays, it is not possible to conclude how the UV-light sterilization affects the Clear resin since there was no significant difference between the results obtained for the C-UV1× and

C-UV8× materials. These findings indicate that the Clear material is cytotoxic independently of the UV light sterilization steps, and therefore, it should not be the material of choice when manufacturing the reactors for cell cultivation.

Third study

After inferring and notifying the manufacturer that the novel material was cytotoxic, the manufacturer provided a Clear resin that was hardened/cured with UV light after being 3D-printed, and was expected to be cytocompatible without the need for a parylene coating.

The availability of this new material motivated a third and final study following the same approach to assess its cytotoxicity. Cells were cultivated (4,000 cells/cm^2) for two days in expansion medium followed by four days of cultivation in the presence of pieces of the following materials: HT-P1×, HT-P4×, HT, HT-γ, C-UV1×, and UV-cured Clear resin (C(+)UVc). Cells were also cultivated in the absence of material pieces in expansion medium, as control (Ctrl), and expansion medium was incubated in wells without cells, to serve as negative control ((-)-Ctrl).

Again, it is relevant to note that the results obtained for the already assessed conditions in the first and second studies were reproduced, which contributes for the credibility of the present study. Moreover, as a result of this reproducibility, the discussion that follows will focus on the analysis of the cured Clear material.

With regard to the optical assays (Figure 3-4), both cells cultivated in the presence of pieces of HT-P or C(+)UVc kept a fibroblast-like morphology, characteristic of MSC, whereas the cells cultivated in the presence of HT or C-UV1× became round-shaped upon the cultivation period.

Concerning the MTT assay, the production of formazan by the HT-P and C(+)UVc samples was of the same extent and similar to the control; there was a considerably less production of the purple crystal in the HT-γ samples, and no significant conversion of MTT was detect in the HT or C-UV1× samples.

Finally, in the calcein-AM/PI staining, cells cultivated in the presence of HT-P or C(+)UVc presented a morphology and a density of viable cells comparable to the control. Although the cells cultivated in the presence of HT-γ presented that same morphology, the cell viability was considerably lower in this condition. No viable cells were observable when cells were cultivated in the presence of HT or C-UV1×.

While it was expected a loss of viability for the HT and C-UV1× conditions, upon the results of the optical assays it is interesting to note a positive effect of the UV light hardening treatment on the cytocompatibility of the Clear resin. In all optical assays the cells remained viable in the presence of C(+)UVc, which was not verified when the UV light hardening treatment was not applied.

The results obtained in the quantitative assays (Figure 3-5) are consistent with the ones obtained in the optical assays. As expected, the viability and metabolic activity (MTT and TOX8) were highest for the control, followed closely by the samples cultivated in the presence of HT-P. Compared to these conditions, there was a lower number of viable cells in the C(+)UVc condition, and a consequent lower metabolism rate in the MTT and TOX8 assays. The cell viability was negligible for the HT and C-UV1× conditions, which translated into a low metabolic activity resembling the negative control.

Regarding the glucose/lactate metabolism, the highest consumption of the sugar and production of the metabolite were detected in the samples cultivated in the presence of HT-P and C(+)UVc, which were similar to the control. The degree of glucose metabolism by the cells cultured in the presence of HT-γ was less pronounced when compared to the three conditions previously addressed. Finally, the lowest glucose conversion into lactate was observed in the samples cultivated in HT or C-UV1×.

It is relevant to note that cytotoxic materials, such as HT, HT-γ or C-UV1×, might have a negative impact on the cell metabolic activity, thereby inducing cell death. On the contrary, the decrease of the cell metabolism might be associated with the decrease in the number of viable cells, and not be directly related to a negative effect inflicted by these less cytocompatible materials. If this is the case, these materials induce cell damage or even death by means not associated with the cell metabolism.

In both approaches the results suggest that the parylene-coated High Temp resin is the best suited for cell cultivation, since for all the different conditions studied, it was the best material to enable the cells to maintain their viability, morphology and metabolic activity. Although the UV-cured Clear resin has shown promise of being cytocompatible in the third study of the second approach, the results obtained for the parylene-coated High Temp resin were globally preferable. Accordingly, the bioreactors employed to cultivate cells under perfusion (described in section 3.5) were chosen to be manufactured with the parylene-coated High Temp material.

3.3 Optimization of cell culture in 3D platforms

The mini-perfusion bioreactor used in the present work requires a 3D platform to cultivate cells. Three distinct platforms were employed for that purpose: collagen and collagen-elastin membranes (MatriStypt® and MatriDerm®, respectively) and alginate hydrogel.

The first step of cultivation in three-dimensional scaffolds is the cell seeding, which determines the initial number of cells and spatial distribution in the construct. Thereby, the chosen methodology of cell loading is of outmost importance.

Before performing the cell cultivation inside the bioreactors, the conditions of cell seeding on the distinct 3D platforms were studied. Regarding the collagen membranes, different cell densities, static *vs.* dynamic seeding, and seeding to dry or hydrated matrices were assessed (section 3.3.1). Concerning the alginate hydrogel, different cell densities were evaluated (section 3.3.2).

3.3.1 MatriStypt®

Squares (1.5 cm^2) of Matristypt® were pre-incubated, or not, in expansion medium and then statically or dynamically seeded at a given cell concentration: 5,000; 10,000; or 15,000 cells/cm^2, as described in section 2.2.2. The volume of cell suspension added to each matrix was constant, despite the difference in the cell density, 50 µl. After 4 and 11 days of standard cultivation in well-plates, both the top and bottom of the membranes were documented via calcein-AM/PI staining. The present

approach enables to: i) conclude which initial cell density is best suited for this platform; ii) compare cell seeding on dried *vs.* hydrated membranes; and iii) compare dynamic *vs*. static seeding.

The results obtained from the calcein-AM/PI staining on the bottom and top of the membranes are depicted in Figure 3-6 and Figure A 2 (*see Appendix*), respectively.

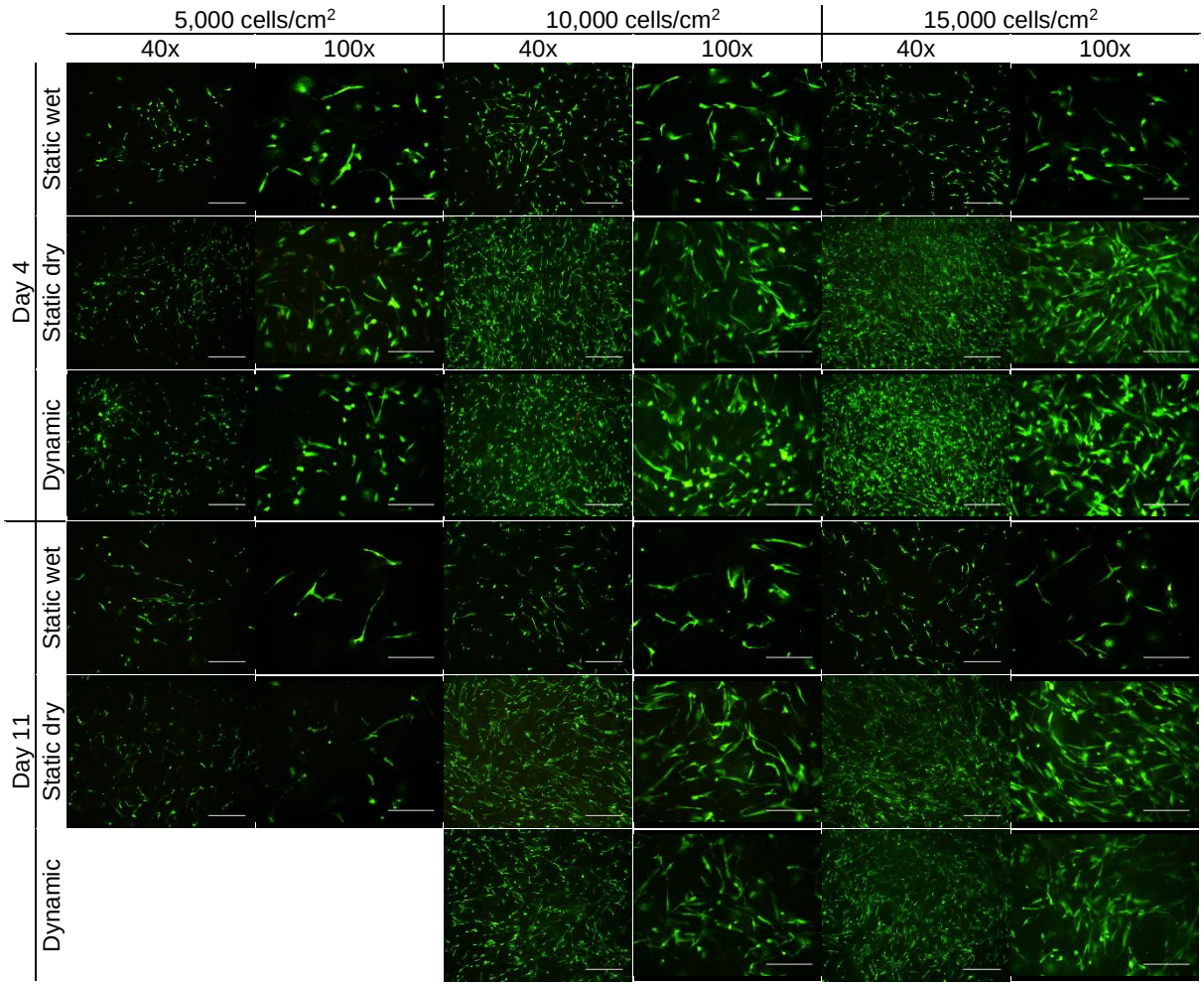

Figure 3-6 Calcein-AM/PI staining of the bottom of Matristypt® membranes on days 4 and 11 of cell cultivation. Cells were seeded at a concentration of 5,000; 10,000 or 15,000 cells/cm^2 to dried (static and dynamic [centrifugation at 500 rpm; 5 min] seeding) or hydrated matrices (wet; static seeding only). Calcein-AM stains live cells in green; PI stains dead cells in red. Pictures were acquired by fluorescence microscopy; scale bar represents 500 and 250 µm in 40x and 100x magnification, respectively.

Firstly, none of the seeding methods had a negative impact in the viability or in the morphology of the cells, as they presented a fibroblast-like shape and no red-coloured cells were observed upon calcein-AM/PI staining.

With regard to the cell density, the results obtained for the 10,000 and 15,000 cells/cm^2 were comparable, and these densities appeared more appropriate than the 5,000 cells/cm^2, as the latter had a considerable area without cells that translated in a lower fluorescent signal. For the experiments in which cell viability is assessed, a higher signal facilitates the interpretation of the results, thus a density of 10,000 or 15,000 cells/cm^2 are preferable when cultivating MSC in MatriStypt®.

Concerning the seeding on dried or hydrated (membranes soaked in medium prior to the cell seeding) membranes, the latter seemed to have a fewer number of cells. This is justified by the fact that the medium present in the matrix allowed for an even cell distribution along its surface and might have aided the cells penetrating the membrane; in the dried matrix, the cells remained concentrated on the spot they were seeded, and a negative cell density gradient was created between that spot and the borders of the membrane. As the seeding to dried matrices did not allow to evenly distribute the cells throughout the matrix surface, and the extent of cell attachment appeared comparable between both conditions, the cell seeding to medium-soaked matrices is advantageous.

Regarding the static and dynamic seeding, there was no apparent difference between these conditions. The parameters of the dynamic seeding were adapted from the work developed by Zhang *et al*. [112], in which 1 mm-thick scaffolds obtained from cancellous bone were centrifuged thrice at 500 rpm for 2 min and then turned over for centrifuging as one cycle. Although the thickness is similar to that of MatriStypt®, the stiffness of the cancellous bone and the collagen matrix is distinct, hence the seeding parameters that fits the cancellous bone scaffold might not adjust to the collagen membrane. Further studies tackling different centrifugation speeds and durations, using robust methods to analyse the scaffold centre, should be performed to assess the effect of dynamic cell seeding to MatriStypt®.

Finally, it is worth noting that when cells are seeded to MatriStypt®, they cross through the membrane and settle on the bottom, that is why no cells are observable on the top of the matrices at day 4 (*see Figure A 2 in the Appendix*). The same occurred when hMSC were statically seeded to poly(ethylene terephthalate) (PET) membranes [113]. In contrast, cells were uniformly distributed within dynamically seeded PET membranes [113], suggesting that cells might be homogenously distributed within MatriStypt® if using the right dynamic loading methodology.

The high cellular mass on the bottom of MatriStypt® may pose a disadvantage of this platform, since cells might be lost after crossing the membrane and attach to the bottom of the wells. To prevent this, well-plates could be covered with agarose [114].

Interestingly, at day 11, cells were visible on the top, indicating that they migrated inside MatriStypt® in the upward direction. Moreover, a higher number of cells were present on the top of the hydrated matrices compared to the dried matrices, suggesting that soaking MatriStypt® in medium prior to cell seeding might aid the cells to migrate inside the matrix.

Upon the results obtained in the first study, in which there was no apparent difference between the static and dynamic seeding, nor between the cell densities of 10,000 and 15,000 cells/cm^2, a second study was performed exploiting static seeding (either on dried or hydrated matrices) and cell densities of 10,000 or 20,000 cells/cm^2.

Squares (1.5 cm^2) of Matristypt® were pre-incubated, or not, in expansion medium and statically seeded at 10,000 or 20,000 cells/cm^2, as described in section 2.2.2. The volume of cell suspension added was constant despite the difference in cell density: 50 µl for the hydrated matrices and 100 µl for the dried matrices (this is to allow cells to be more evenly spread on the dried matrix surface). After 3 and 10 days of standard cultivation in well-plates, both the top and bottom of the membranes were

documented via calcein-AM/PI staining. The present approach enables to: i) conclude which initial cell density is best suited for this platform; and ii) compare cell seeding to dried *vs.* hydrated membranes.

The results obtained from the calcein-AM/PI staining on the bottom and top of the membranes are depicted in Figure 3-7 and Figure A 3 (*see Appendix*), respectively.

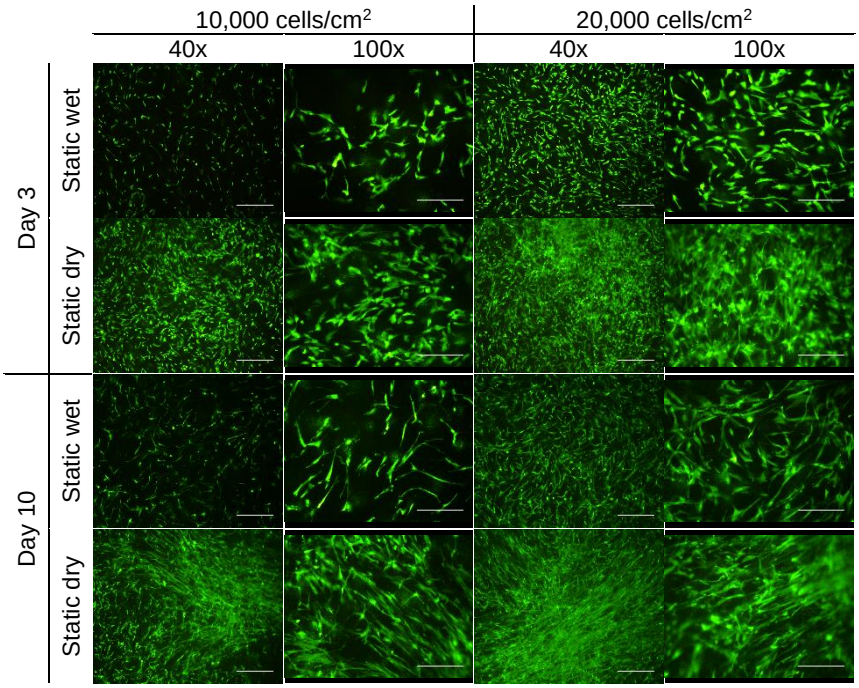

Figure 3-7 Calcein-AM/PI staining of the bottom of Matristypt® membranes on days 3 and 10 of cell cultivation. Cells were seeded at a concentration of 10,000 or 20,000 cells/cm^2 to dried or hydrated (wet) matrices. Calcein-AM stains live cells in green; PI stains dead cells in red. Pictures were acquired by fluorescence microscopy; scale bar represents 500 and 250 µm in 40x and 100x magnification, respectively.

Similarly to the first study, both seeding methods enabled cells to maintain their viability and characteristic morphology, as they presented a fibroblast-like shape and no red-coloured cells were detected upon calcein-AM/PI staining. With regard to the cell density, there was a significantly higher fluorescence signal in the 20,000 cell/cm^2, which is advantageous when assessing the cell viability. However, the cells seeded, in this density, to dried matrices seemed excessively confluent in the membrane bottom surface. This is not ideal for longer term cultivations as cells should have enough space to spread out and proliferate, to prevent cells from being contact-inhibited, or detach from the membrane and migrate to the surface of the wells due to lack of space. Thereby, if the employed methodology of cell seeding is to dried matrices, the cell density should be up to 20,000 cell/cm^2.

Concerning the seeding to dried or hydrated membranes, the cells on the medium-soaked matrices were evenly spread throughout the matrix surface, while a negative cell density gradient was again observed between the seeding spot and the borders in the dried matrices. Thus, it is preferable to seed cells to medium-soaked MatriStypt® membranes.

Finally, it was again observable the cell migration inside the MatriStypt® matrices in the upward direction between the days 3 and 10 of cultivation (*see Figure A 3 in the Appendix*).

Although cells were chosen to be seeded statically to the membranes in the forthcoming experiments of the present work, it is relevant to note that low efficiencies and poor cell distribution throughout the scaffold's porous network were previously reported with static seeding [112, 113, 115]. Thus, it is relevant to find more suitable means of cell loading to the scaffolds.

Regarding the scaffold quality, it was shown that the pre-soaking step allows for a better distribution of cells on the surface compared to dry membranes, but it was not possible to conclude about the cell adhesion and distribution within the membranes, between the static and dynamic seedings. Additional treatments on the MatriStypt® could improve the seeding efficiency, for example, oxygen-plasma treatment on fibrous polystyrene scaffolds was demonstrated to increase the cell adhesion [115].

With concern to the physical method of cell loading, dynamic loading was reported to be preferable than static seeding. Zhang *et al.* [112] investigated static, injection, centrifugal and vaccum seeding and concluded that the centrifugal method improved the distribution and proliferation of MSC to demineralized cancellous bone.

Mechanical loading using perfusion systems was also documented; for instance, Zhao *et al*. [113] used fluid flow to seed cells to poly(ethylene terephthalate) membranes by continuously recirculating a cell suspension through those scaffolds inside a perfusion bioreactor, and cells were uniformly distributed. In a different perfusion setting, oscillating perfusion was shown to be more efficient than static seeding by yielding higher seeding efficiencies, more homogeneous distribution and stronger cell-matrix interactions [115]. Moreover, lower cellularities were obtained in statically seeded scaffolds compared to dynamically seeded scaffolds when both were cultivated under perfusion [115]. Interestingly, in the statically seeded scaffolds a great number of single cells attached to the fibers had a rounded shape, while most of the dynamically seeded cells stretched along the surface of the fibers [115], which might have contributed for the stronger interaction between the cells and the matrix. These findings indicate that in an experiment setting in which the scaffolds are to be cultivated under perfusion, dynamic cell seeding via perfusion might be advantageous.

The mini-perfusion bioreactor used in the forthcoming experiments can be assembled in such a way that two chambers are connected to one another with a scaffold fixed in between the chambers. This design would allow for a cell suspension to continuously enter in one of the chambers, cross the scaffold and leave the reactor through the second chamber, thus allowing for a perfusion seeding as described by Zhao *et al*. [113]. In addition to obtaining higher cell efficiencies, better homogeneity within the scaffold and stronger cell-matrix interactions, performing the seeding in the flow perfusion system would diminish the risks of contamination due to less membrane handling. Hence, it would be interesting to study, in the future, a perfusion seeding to MatriStypt® using the mini-perfusion bioreactor.

3.3.2 Alginate hydrogel

Gels were casted with a cell density of 100,000 or 200,000 cells/ml as described in section 2.2.2. To assess the different cell densities, calcein-AM/PI staining was performed on days 0, 1, 3 and 5 of

standard cultivation in well-plates. The results obtained from the calcein-AM/PI staining on the gels are depicted in Figure 3-8.

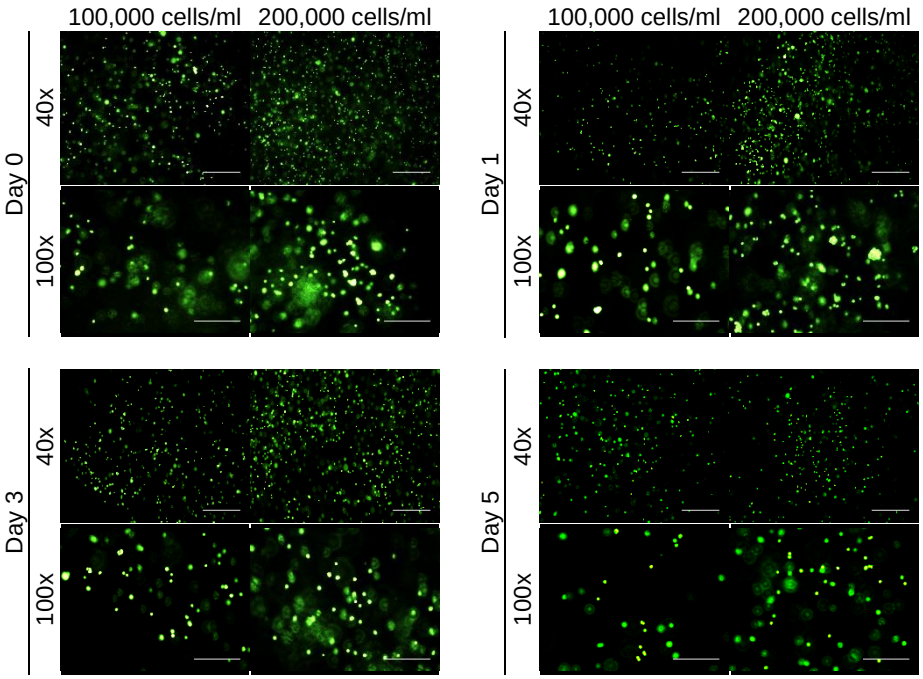

Figure 3-8 Calcein-AM/PI staining of alginate gel on days 0, 1, 3 and 5 of cell cultivation. Cells were suspended in alginate 1.2% (w/v) in a cell density of 100,000 or 200,000 cells/ml; gels were polymerized by adding 100 mM of $CaCl_2$ to the cell-alginate suspension in a volume ratio of 1:2, followed by a 7-8h period of incubation. Calcein-AM stains live cells in green; PI stains dead cells in red. Pictures were acquired by fluorescence microscopy; scale bar represents 500 and 250 µm in 40x and 100x magnification, respectively.

Firstly, the methodology employed to entrap cells within the alginate polymer allowed cells to maintain their viability throughout the five days of cultivation, since all cells were stained green and the number of viable cells appeared to remain constant, independently of the initial cell concentration. Therefore, casting gels by mixing cell suspension in alginate 1.2% (w/v) followed by the addition of 100 mM $CaCl_2$ in a ratio 1:2, and subsequent incubation for 7-8 hours, is an adequate methodology to entrap cells within the alginate polymer, at least in the addressed experiment settings.

In the 40x magnification pictures, a reasonably stronger fluorescence signal was observed for the 200,000 cells/ml, which is preferable in an experiment setting where the cell viability needs to be assessed. The 100x magnification images allowed to detect small cells agglomerates in the gels casted with 200,000 cells/ml, suggesting that with this density cells might get close enough to interact and attach to one another. Depending on the aim of future experiments, a cell density of 100,000 cell/ml is desirable if one intends to have single cells within the gel. Nonetheless, gels casted with higher cell densities should be assessed to test this hypothesis.

Although no significant difference was noticed between the cell densities studied, 200,000 cells/ml allowed a higher fluorescence signal and small cell agglomerates were noticed for this density. In future

settings, if aiming to have single cells within the gel, the cell density of choice should be up to 200,000 cells/ml and at least 100,000 cell/ml in order to guarantee a sufficient fluorescence signal.

3.4 Transport dynamics in 3D platforms under perfusion

Upon selecting the best suited material to construct the bioreactor and optimize the cell culture in the addressed 3D platforms, the next step is to insert those platforms inside the bioreactors and cultivate cells under perfusion. The cultivation is to be monitored by taking samples from the centre of the platforms with the aid of a catheter, and measuring the concentrations of glucose and lactate, the energy source of the cells and respective metabolite, thus allowing to predict the cell viability.

Before performing the cell cultivation inside the bioreactors, it is relevant to better understand the transport of these biomolecules inside the 3D platforms to be used - alginate hydrogel and collagen membranes. By assessing the transport of glucose and lactate inside the platforms under perfusion and in the absence of cells, this study aims to: i) compare the diffusional capacity between the different platforms; ii) evaluate the platforms capacity to supply glucose and retrieve lactate; and iii) aid in the discrimination of the glucose/lactate profile due to cell metabolism or diffusional transport when cultivating cells in the forthcoming experiments.

The alginate hydrogel was casted as described in section 2.2.2., without the addition of cells to the alginate 1.2% (v/v) solution, and the membranes (a pair of each type) were cut to fit the scaffold holder, hydrated in expansion medium and left in incubation until usage. Each perfusion circuit was assembled, and the scaffolds and respective holder were inserted in the reactor gap with a catheter in between them, as depicted in Figure 3-9.

(a) (b)

Figure 3-9 Assembly of the bioreactor with a catheter (a) in alginate gel or (b) surrounded by a pair MatriStypt®.

The glucose and lactate profiles inside the 3D platforms (alginate gel, MatriStypt® and MatriDerm®) under perfusion (constant rate; 10 rpm), and in the absence of cells, are depicted in Figure 3-10. Initially, perfusion was operated with expansion medium at a constant rate of 10 rpm. After 2-3 hours, the expansion medium was changed for PBS to exclude glucose and lactate from the platforms; the perfusion was operated for 48 hours with samples being taken occasionally. The concentrations of glucose/lactate throughout the first 22 hours are depicted in Figure 3-10 (a). At the end of the 48-hour period, PBS was changed for expansion medium to replace glucose and lactate in the platforms; the perfusion was operated for 100 hours with samples being taken occasionally. The concentrations of glucose/lactate throughout this period are depicted in Figure 3-10 (b).

(a)

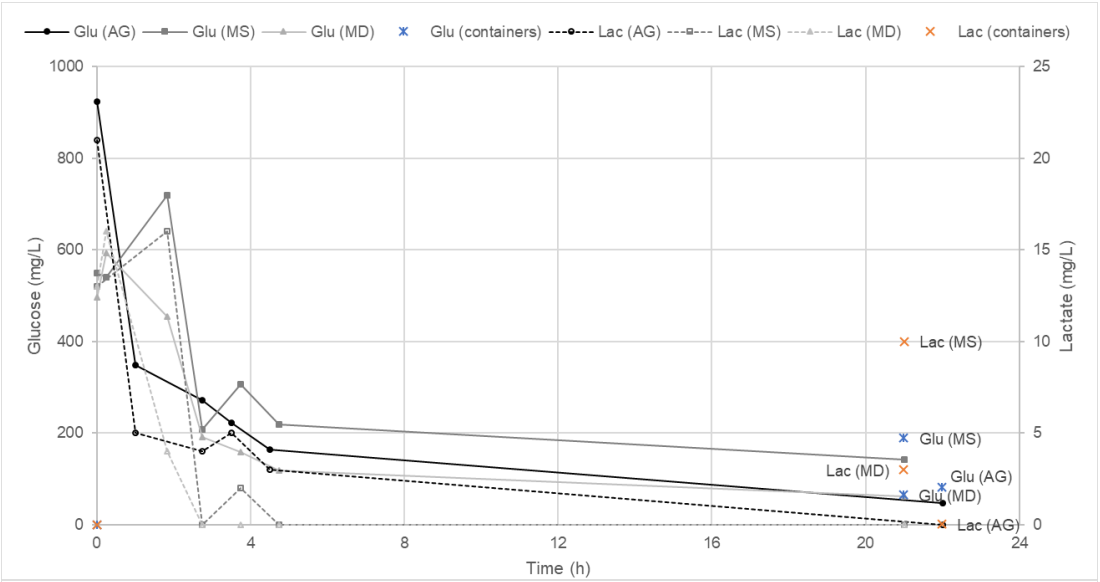

(b)

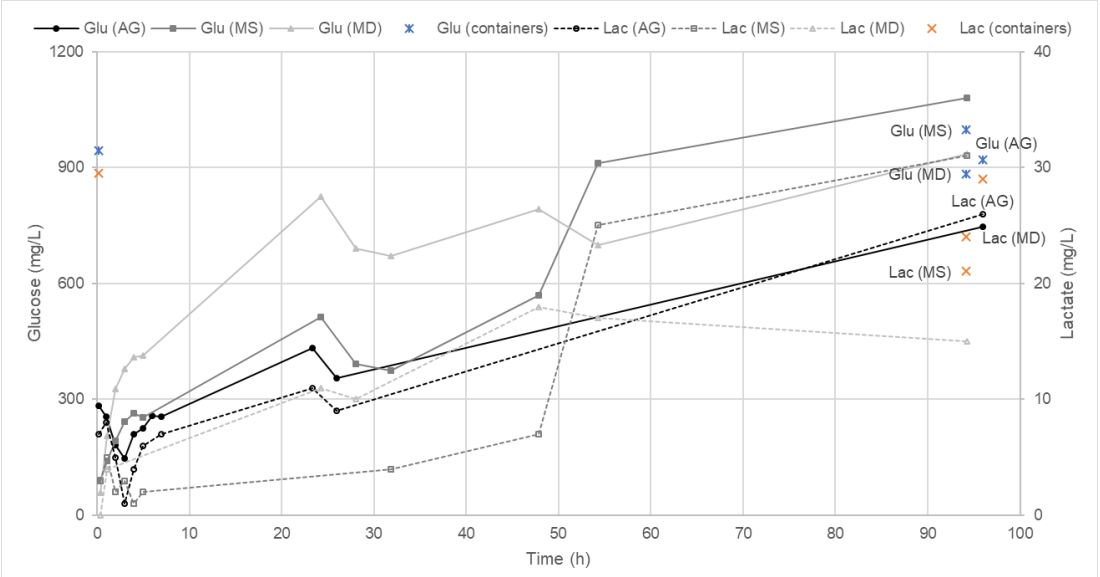

Figure 3-10 Glucose (Glu) and lactate (Lac) profiles through time in 3D platforms: alginate gel, AG; MatriStypt®, MS; and MatriDerm®, MD. The final concentrations of each molecule inside the PBS/media reservoirs are also displayed. Gel and collagen membranes were perfused (constant rate, 10 rpm) for 2-3 h with medium, then (a) medium was changed for PBS and perfusion was carried for 48 h (only the first 22 h are presented) and finally (b) PBS was changed for medium and the perfusion was carried for 100 h. The time points 0 h in charts (a) and (b) correspond to the changes of medium for PBS and *vice versa*, respectively.

Perfusion with PBS

When the platforms were perfused with PBS, there was an abrupt decrease of glucose/lactate inside the gel after just one hour, followed by a lower but still considerable exclusion rate of the molecules in the next four hours and finally an even slower exclusion rate was noticed until the end of the first day. It is worth to note that lactate was completely excluded from the alginate by then.

Contrarily to the alginate, there was an increase of glucose/lactate in both membranes in the first hours, more pronounced and prolonged in time in MatriStypt® (MS) than in MatriDerm® (MD). Then, a sudden decrease of the molecules was observed in both membranes, reaching the total exclusion of

lactate after three hours and globally surpassing the alginate capacity of excluding the molecules. Similarly to the alginate, from hour five onwards the removal rate of glucose/lactate became considerably lower and comparable to that of alginate. It is pertinent to refer that apart from the first two data points, the presence of the biomolecules in MD was always lower than in MS, indicating that MatriDerm® has the better diffusion capacity of the studied collagen membranes.

Interestingly, at the end, the glucose and lactate concentrations inside the platforms were always lower or equal to those inside the respective container. This indicates that the removal of the molecules augments their concentration in the PBS reservoir and there is a delay in equalizing the concentration of the molecules flowing in the circuit to those inside the platforms.

Perfusion with expansion medium

When the platforms were perfused with expansion medium, after a 48-hour period of perfusion with PBS, there was a decrease of glucose/lactate inside the alginate during the first three hours. Then, a sudden increase occurred until the initial values were met, and finally, from around hour eight onwards, the reposition rate of the biomolecules stabilized, remaining constant until the end of the experiment. It is interesting to note that the final concentration of glucose/lactate inside the reservoir of the circuit containing alginate was higher than that inside the alginate, indicating that even after 100 hours, the concentration of the molecules inside the alginate was not able to match that of the medium, thus indicating diffusional issues inside the alginate gel.

As for the collagen membranes, overall there was a sudden increase of the glucose/lactate concentrations in the first five hours, surpassing the concentrations inside the alginate. Afterwards, the reposition rate of those molecules became similar to the alginate, but their concentration was in general higher inside both collagen membranes than inside the alginate.

Apart from the last lactate data point inside MatriDerm®, which is believable to be a measurement inaccuracy (as its profile contrasts with the other molecule profiles inside the collagen membranes) it is interesting to note that the final concentrations of glucose/lactate inside both membranes were higher than that inside the respective containers. This is opposed to what happened for the alginate, suggesting that the membranes have better diffusional capacities then alginate gel. In the forthcoming experiments, in which cell cultivation inside the reactor is tackled, the membranes are therefore expected to supply glucose and retrieve lactate with better ease than the alginate gel.

3.5 Cell cultivation in 3D platforms under perfusion

After inferring that the parylene-coated High Temp resin reactors are cytocompatible, optimizing the cell cultivation in different 3D platforms and understanding the transport dynamics inside those same platforms, it is time to evaluate the ability of coupling the 3D platforms with the perfusion bioreactor to cultivate cells.

Two different approaches were carried out to assess the cell viability in dynamic culture. First, an endpoint analysis via calcein-AM/PI staining was performed in alginate gel and MatriStypt® to allow an optical monitoring of the cell cultivation inside the bioreactors (section 3.5.1). This methodology has the advantage of allowing a relatively easy qualitative comparison between the different studied conditions but presents a series of drawbacks: it obliges the frequent opening of the bioreactor, enhancing the risk of contamination; it is time, reagent and labour consuming; samples of gel/membrane have to be manipulated to be retrieved from the reactor, again subjecting the platforms to risk of contamination and the cell samples end up being corrupted/sacrificed.

In order to circumvent the hurdles of performing calcein-AM/PI or another endpoint analysis, a second and novel approach was performed. This was based on taking samples of medium contained within the platforms with the aid of a catheter connected to a micro-prefusion pump (section 3.5.2). Thereafter, the glucose and lactate concentrations in the samples were measured to infer about the cell metabolism, thus enabling to predict the cell viability. Compared to the first approach, this methodology greatly decreases the risk of contamination, it is considerably less time, reagent and labour consuming and most importantly, non-invasive. The second approach was performed in all of the previously addressed 3D platforms: alginate gel, MatriStypt® and MatriDerm®.

3.5.1 Cell viability monitoring via calcein-AM/PI staining

Alginate hydrogel

Gels were casted with a cell density of 100,000 cells/ml as described in section 2.2.2. Afterwards, gels were cut to fit the reactor and inserted in two separate bioreactors, one to be operated under static and the other under dynamic (constant rate, 10 rpm) conditions; the reactors were incubated in IncuReTERM. Gels were also cultivated in a standard manner in well-plates and incubated in Heracell, to serve as controls. Cell viability was assessed via calcein-AM/PI staining on days 0, 1, 3 and 5. The results obtained from the calcein-AM/PI staining on the gels are depicted in Figure 3-11.

As previously discussed in the section 3.3.2, the employed methodology of gel polymerization allowed cells to remain viable for up to five days, as can be observed by the green dots corresponding to live cells present in all conditions upon calcein-AM/PI staining. Furthermore, this methodology allowed for the gels to have a texture that enabled their manipulation when inserting them inside the reactors and taking samples, while being stiff enough to permit them to maintain their conformation after sampling, and during the subsequent analysis of the samples. It is also relevant to note that the cultivation inside the reactor, either under static or dynamic conditions, did not alter the stiffness of the gel in comparison to the control.

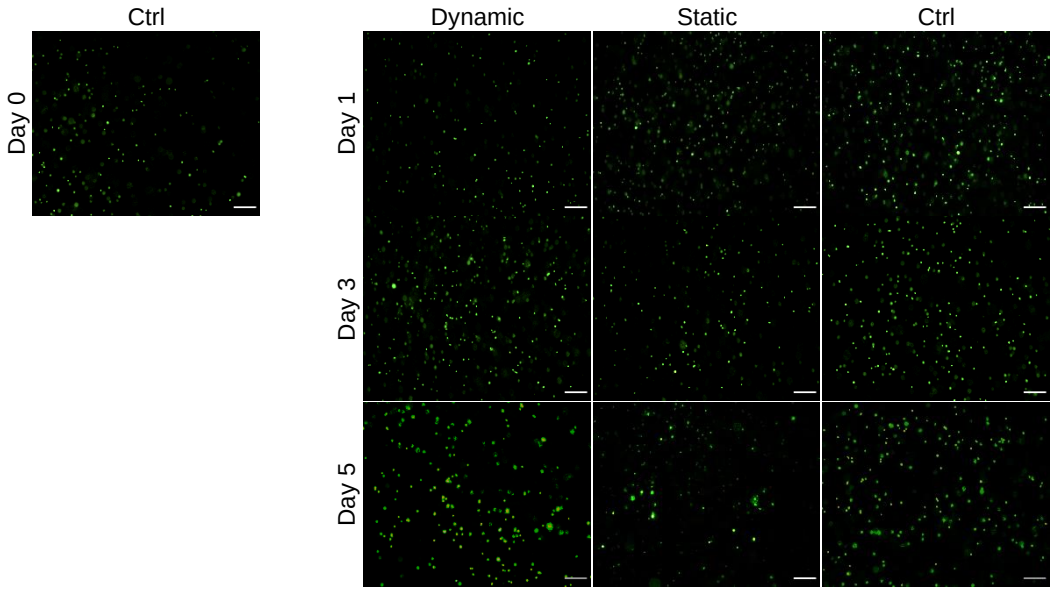

Figure 3-11 Calcein-AM/PI staining of alginate gels on days 0, 1, 3 and 5 of cell cultivation inside parylene-coated High Temp resin reactors under dynamic (constant rate, 10 rpm) or static conditions, and in well-plates (Ctrl). The reactors were incubated in IncuReTERM and the control was incubated in Heracell. The gels were casted by suspending cells in alginate 1.2% (w/v) in a cell density of 100,000 cells/ml followed by the addition of 100 mM of $CaCl_2$ to the cell-alginate suspension in a volume ratio of 1:2, and finally a 7-8 h period of incubation. Calcein-AM stains live cells in green; PI stains dead cells in red. Pictures were acquired by fluorescence microscopy; scale bar represents 250 µm in 40x magnification.

Concerning the viability throughout the five days of cultivation, the density of viable cells in the control was constant. With regard to the cultivation inside the bioreactors, an increase of viable cells was observed in the gel cultivated under perfusion, while a decrease of live cells was detected in the gel of the static bioreactor. This might be due to the fact that cells cultivated under dynamic conditions have access to a reposition of glucose and oxygen and retrieval of lactate within the gel, whereas in static conditions cells might get deprived from the necessary nutrients and a toxic amount of lactate might accumulate inside the gel, thus inducing cell death.

Nevertheless, these results might be misleading. The fluorescence microscope, a device aimed for two-dimensional analysis, can only focus on a single layer in the *z* axis; therefore, green dots present in other layers become background noise. For a given gel sample, the higher the number of these layers, the higher the number of green dots. In thinner gel samples, there are fewer layers and subsequently lower background noise that translates in a lower density of viable cells. Even though the gel sampling and subsequent analysis under the microscope were performed consistently, since gel samples were acquired manually, their thickness was variable. Hence, the interpretation of the degree of viability in gels using the fluorescence microscope is not ideal.

The results depicted in Figure 3-11 were obtained upon cutting a thin slice of the top of a given gel. In case of the bioreactors, that part of the gel was always facing the lid of the reactor, not being in direct contact with the flow in the dynamic reactor. With the aim of assessing the effect of the medium flow on the cells, in addition to the analysis of a top layer, the gel that remained inside the dynamic reactor,

which was facing the chamber and thus in direct contact with the medium flow, was subject to a calcein-AM/PI staining on day 5.

In Figure 3-12 is depicted a comparison between the sides of the gel facing the lid and the chamber of the reactor, the latter being in direct contact with the flow. As documented, the gel facing the lid presented a higher density of live cells. Moreover, several red spots were detected in the gel facing the chamber, which indicates cell death. These results demonstrate that the perfusion has a negative impact on the cell viability, possibly due to fluid-induced shear stress.

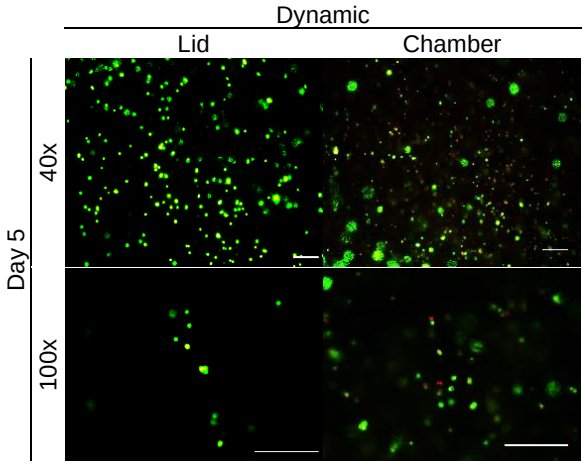

Figure 3-12 Comparison between the sides of the gel facing the lid and the chamber (direct contact with flow) obtained via calcein-AM/PI staining on day 5 of cell cultivation inside a parylene-coated High Temp resin reactor under perfusion (constant flow, 10 rpm). The reactor was incubated in IncuReTERM. The gel was casted by suspending cells in alginate 1.2% (w/v) in a cell density of 100,000 cells/ml followed by the addition of 100 mM of $CaCl_2$ to the cell-alginate suspension in a volume ratio of 1:2, and finally a 7-8h period of incubation. Calcein-AM stains live cells in green; PI stains dead cells in red. Pictures were acquired by fluorescence microscopy; scale bar represents 250 µm in 40x and 100x magnification.

Although a negative impact of the flow was detected on the cells, overall the cell viability in the gel under perfusion was comparable to a standard cultivation platform (control), and advantageous compared to the gel cultivated inside the reactor under static conditions. These findings indicate that coupling an alginate gel to the mini-perfusion bioreactor shows promise in MSC cultivation.

MatriStypt®

Squares (6.7 cm^2) of MatriStypt® were seeded at a concentration of 15,000 cells/cm^2, as described in sections 2.2.2 and 2.2.4. Two matrices were inserted in two separate bioreactors, one to be operated under static and the other under dynamic (constant rate, 10 rpm) conditions. Two matrices were cultivated in a standard manner in well-plates, to serve as controls. The reactors and one of the controls were incubated in IncuReTERM and a second control was incubated in Heracell. Both the top and bottom of the membranes were documented via calcein-AM/PI staining to evaluate the cell viability on days 1, 3 and 7. The results obtained from the calcein-AM/PI staining on the bottom and top of the membranes are depicted in Figure 3-13 and Figure A 4 (*see Appendix*), respectively.

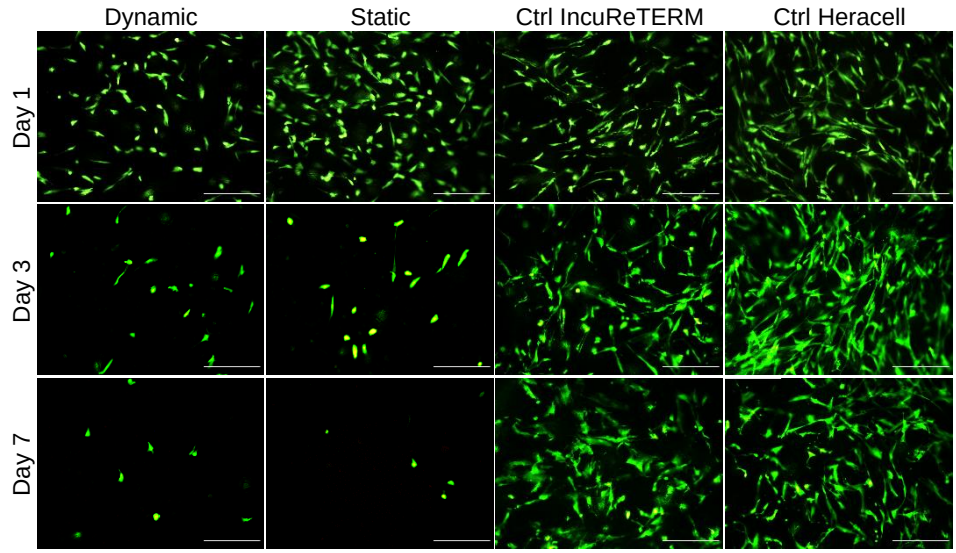

Figure 3-13 Calcein-AM/PI staining of the bottom of Matristypt® membranes on days 1, 3 and 7 of cell cultivation inside parylene-coated High Temp resin reactors under dynamic (constant rate, 10 rpm) or static conditions, and in well-plates (Ctrl). Cells were seeded at a concentration of 15,000 cells/cm^2 on hydrated matrices; the reactors and one of the controls were incubated in IncuReTERM and a second control was incubated in Heracell. Calcein-AM stains live cells in green; PI stains dead cells in red. Pictures were acquired by fluorescence microscopy; scale bar represents 250 µm in 100x magnification.

Firstly, the results obtained in the controls were independent of the incubator in which cells were cultivated, since there was no apparent difference in the cell viability throughout the seven days of the study between the controls cultivated in the standard incubator (Heracell) or IncuReTERM, an incubator with incubated pumps aimed for dynamic culture. These findings indicate that IncuReTERM is capable of supplying the necessary conditions to MSC cultivation. Moreover, it ensures the feasibility of comparing cell samples incubated in either of the addressed incubators.

With regard to the cultivation inside the reactors, the degree of cell viability throughout the seven days of cultivation was comparable between the dynamic and static conditions, suggesting that the medium renewal did not offer an advantage to the perfused cells nor inflicted cell damage. After one day of cultivation, the density of viable cells on the membranes was similar to the controls, however from day three onwards there was a significant loss of viability in both conditions and also a loss of the fibroblast-like morphology characteristic of MSC, especially at day seven.

The loss of viability might be due to the employed cultivating setting; membrane handling and manipulation when acquiring the samples; or even due to cell detachment from the membranes. The last hypothesis is unlikely since the membranes were inserted in the reactors with their bottom facing the lid, preventing them from being released to the chamber (remember that cells gather on the bottom when seeded to MatriStypt®). Relatively to the cultivation setting, the coupling of MatriStypt® membranes with the perfusion reactor appears to be not as promising as the alginate. Compared to the collagen membrane, cells cultivated in alginate gels are likely more protected due to being encapsulated within a polymer chain, thereby less susceptible to external hazards, such as medium perfusion and constant handling of the reactor and membranes when performing cell sampling.

It is interesting to refer that from day three onwards, different areas of viability were detected in the membranes cultivated inside the reactors operated under dynamic or static conditions (Figure 3-14).

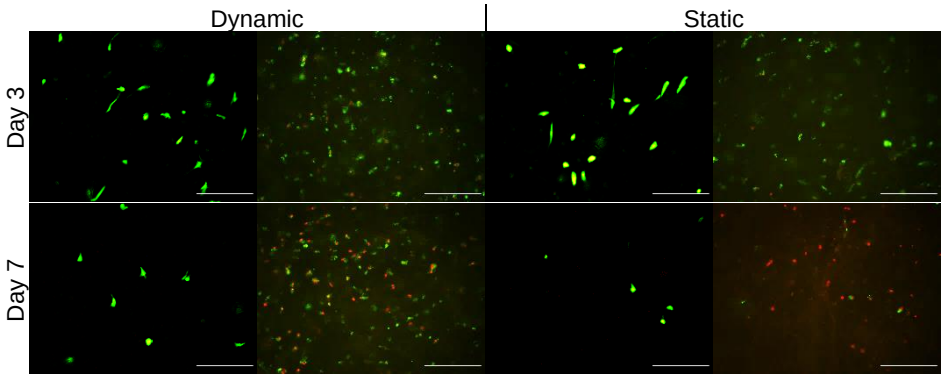

Figure 3-14 Comparison between representative areas of cell viability (first column) and death (second column) in the bottom of Matristypt® membranes obtained via calcein-AM/PI staining on days 3 and 7 of cell cultivation inside parylene-coated High Temp resin reactors under dynamic (constant flow, 10 rpm) or static conditions. Cells were seeded at a concentration of 15,000 cells/cm^2 on hydrated matrices; the reactors were incubated in IncuReTERM. Calcein-AM stains live cells in green; PI stains dead cells in red. Pictures were acquired by fluorescence microscopy; scale bar represents 250 µm in 100x magnification.

While in some areas, only viable cells were detected, there were zones containing less green-coloured cells and with the presence of red-coloured cells, specially at day seven, which indicates cell death. If one compares the zones of cell death between the membranes cultivated under dynamic and static conditions, the degree of cell death was more pronounced in the membrane cultivated inside the static reactor. These findings indicate that even though there was a loss of viability at the same extent inside both reactors operated with distinct flow regimens, the cultivation under dynamic conditions is advantageous.

It is important to note that these results are merely representative and do not allow for a total description of the matrix, demonstrating a relevant drawback of these type of endpoint optical assays.

3.5.2 Cell viability monitoring via glucose/lactate measurements

The cultivation of the cell constructs inside the mini-perfusion reactors coupled to a catheter to gather medium samples from within the platforms, and the monitorization of the cell viability by measuring the glucose and lactate concentrations in those samples, constitute a novelty. As such, it is convenient to discuss how the profile of these biomolecules aid in the prediction of the cell behaviour to better understand the obtained results.

Assuming that cells are viable, and their metabolism is constant throughout the period of cultivation, three distinct profiles are possible to occur depending on the medium flow rate being perfused through the reactor. If:

i. *Flow rate > metabolism rate*: in the beginning there is a fast increase of glucose and decrease in lactate inside the platform, until concentrations similar to those in the medium are met

(remember that before being inserted in the reactors, there is an incubation period in which cells consume some of the glucose that was inside the platforms and produce lactate, thus the concentrations of these molecules changed in relation to the culture medium). After equalizing the values to those in the medium, as glucose is metabolized into lactate, the concentrations of glucose and lactate diminish and augment, respectively, both inside the platform and in the medium at the same rate and with similar values;

ii. *Flow rate = metabolism rate*: the rate of glucose consumption equals the rate of glucose reposition in the platform, and the rate of lactate production equals the rate of lactate exclusion from the platform. Globally, there is a decrease of glucose and an increase of lactate both inside the platform and in the medium at similar rates; opposed to the previous hypothesis, a value gap of the biomolecules concentration is maintained between the platform and the medium, due to the incubation period that preceded the cultivation inside the reactor;

iii. *Flow rate < metabolism rate*: this hypothesis is detrimental since lactate gets accumulated inside the platform, possibly reaching inhibitory concentrations, and glucose decreases, depriving cells of their preferred C-source. Thus, a glucose decrease and a lactate increase are expected in the beginning, while cells are metabolically active, both inside the platform and in the medium, and more pronounced in the former due to transport limitations within the scaffolds. Then, if cells start losing their viability, the metabolism diminishes until the flow rate is enough to supply glucose and retrieve lactate and concentrations similar to those in the medium are met. Finally, as most cells become unviable or metabolically weakened, the glucose and lactate values remain globally constant.

It is relevant to note that due to diffusional limitations inside the cell constructs, there might be a delay in equalizing the concentration of the biomolecules to those in the medium, *i.e.* at a given point in time, the values inside the platform equal those that were in the medium a given compass earlier. This situation occurs when the flow rate is such that allows the reposition of glucose and retrieval of lactate.

Relatively to the controls (standard cultivation of the cell constructs in well-plates or petri-dishes) or the static cultivation inside the reactor, it is expected an accumulation of lactate and a reduction of glucose, more pronounced in the latter due to transport limitations across the scaffolds. This is because the samples of the controls are obtained manually from the culture media that surrounds the cell construct, whereas for the static cultivation inside the reactors the samples are acquired from within the scaffold through the catheter.

Finally, upon addressing the diffusional capacities of the distinct platforms in section 3.4, a more limited transport capacity is expected in alginate gel than in the collagen and collagen-elastin membranes (MatriStypt® and MatriDerm®, respectively).

Alginate hydrogel

Gels were casted with a cell density of 100,000 cells/ml as described in section 2.2.2. Afterwards, two gels were cut to fit the reactor, pierced with a catheter and inserted in two separate bioreactors, each connected to a perfusion circuit. Two seeded gels were also cultivated in a standard manner, and

fresh medium was incubated in separate wells of a well-plate to serve as controls and negative controls, respectively. The reactors were incubated (IncuReTERM) and perfused at a constant rate (5 rpm), whereas the controls were incubated (Heracell) under static conditions. The experiment was performed for seven days, with samples being taken occasionally either through the catheter (reactors) or manually (controls). The glucose/lactate profiles inside the perfused alginate gels or in the culture medium of the controls are depicted in Figure 3-15.

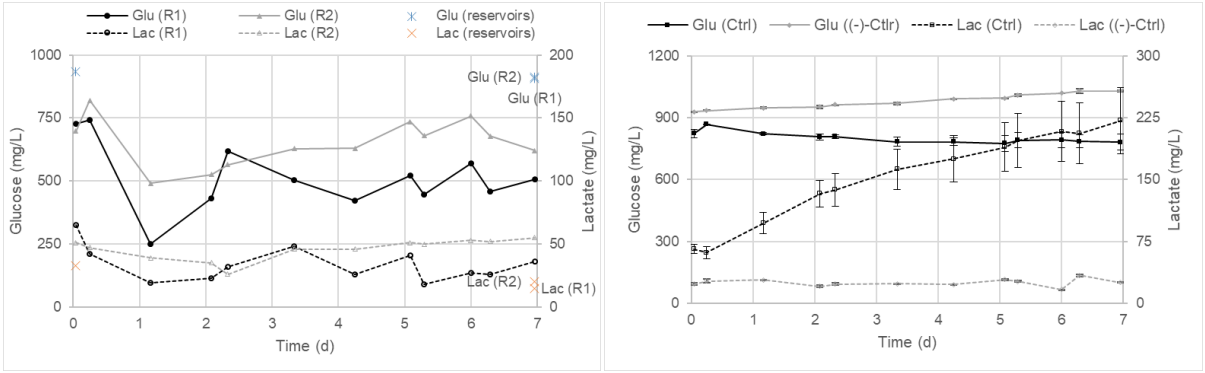

(a) (b)

Figure 3-15 Glucose (Glu) and lactate (Lac) profiles throughout the seven days of cultivation: (a) in samples acquired through a catheter from the inside of alginate gels cultivated in two separate reactors (R1 and R2) under perfusion (constant rate, 5 rpm); and (b) in medium samples acquired manually from well-plates with seeded gels (Ctrl) or only fresh medium ((-)-Ctrl). Data in chart (b) represents mean ± SD from n = 2 replicates for each condition.

It is relevant to note that with the current experiment setting it is not possible to perform a quantitative comparison between the cultivation inside the reactors and the controls. This is due to a different number of cultivated cells in the reactors compared to the controls, and a different medium volume flowing in the perfusion circuit (15 ml) and the medium in the controls (3 ml), resulting in different magnitudes of glucose metabolism by the cells in the distinct conditions. In addition, the medium samples of the reactors were acquired through the catheter from within the gels, whereas the samples of the controls correspond to the culture medium surrounding the gels (acquired manually through a micropipette), which more closely resemble the medium present in the containers of the perfusion circuits rather than the medium within the gel cultivated under perfusion.

With regard to the controls (Figure 3-15 (b)), it was demonstrated an accumulation of lactate in the standard cultivation setting (Ctrl). If this accumulation reaches inhibitory values, it can be detrimental to the cultivation since lactate is toxic to MSC. Naturally, the increase in lactate was accompanied by a decrease in glucose, since the latter is transformed into the former. These deprivation of glucose and accumulation of lactate are what motivate regular medium changes in standard MSC cultures, which is labour, time and reagent consuming, augments the risk of contamination and motivates the search of novel methodologies to overcome this, such as the usage of dynamic culture.

The negative control allows to demonstrate that glucose and lactate remained practically constant throughout the seven days of experiment, but with a slight positive slope, which can be explained by a certain degree of evaporation inside the incubator. Since the amount of glucose/lactate is constant, the evaporation of medium causes these molecules to be more concentrated.

Concerning the dynamic cultivation (Figure 3-15 (a)), the glucose and lactate profiles were comparable in both reactors. Initially, there was a decrease in glucose and lactate in the first 1-2 days, followed by an increase of this molecules until values closer to the initials were reached, which occurs between days 3 and 4. Then, the concentrations of glucose and lactate remained constant until the end of the experiment. The initial decrease followed by an increase of both biomolecules within the cell construct might be explained by the diffusional capacities of the gel, since a similar behaviour was observed in section 3.4 when gels were perfused with culture medium (Figure 3-10 (b)). The fact that the concentration of the molecules remained constant within the platforms from day two onwards, could indicate that the metabolism rate equalised the rates of reposition of glucose and retrieval of lactate; if this was the case, then a decrease of glucose and an increase of lactate would be expected in the medium container. However, no apparent variation in the values of glucose and a nonsensical decrease of lactate were observed in the medium container between the first and last datapoints, suggesting that the metabolization of glucose into lactate was frail or even inexistent, thus indicating cell death. Nevertheless, this might as well not be factual since the results are arduous to interpret. As an example, the lactate diminished globally when it should have either remained constant, with a slight increase due to a small degree of medium evaporation in the incubator, or significantly increase within the platforms and in the medium containers in case the cells were metabolically active.

Regarding the diffusional capacities of the alginate gel, in general it seemed that the concentration of glucose and lactate inside the gels were lower and higher, respectively, than those inside the medium container. This assumption is based on the considerable gap that was observed between the concentrations of the molecules in these two distinct zones among the perfusion circuit, both in the first and final datapoints. Nonetheless, in order to certify this hypothesis it would have been necessary to know the profile of these molecules in the medium inside the containers throughout the seven days of experiment, and not only the first and final datapoints.

Finally, the different intensities of the molecules within the alginate gels/medium containers between both perfusion circuits could be explained by the different positions of the circuits inside the incubator. One of the circuits had its container and reactor closer to the thermal plate and air vents, whereas the other was more susceptible to environmental changes whenever the incubator was opened, and the circuits manipulated. Hence the degree of evaporation or environmental cues could be on the basis for this disparity of the biomolecules concentrations between both reactors.

These findings lead to the believe that the constant flow rate of 5 rpm is not able to supply glucose and retrieve lactate as desirable, and that the alginate gel has significant diffusional limitations that prevent an adequate reposition and retrieval of glucose and lactate, respectively. Remember that transport limitations in alginate gel were already addressed in section 3.4, when evaluating the transport dynamics inside the mini-perfusion reactor. Possible ways to improve these results are, for instance, the usage of higher flow rates, with the care of preventing mechanical stress on the cells; and, change the biochemical or physical properties of alginate to enhance the diffusional transport of biomolecules. Moreover, the measurement of the final volume within the culture systems would ensure if the water evaporation is negligible. Finally, in addition to the monitoring within the gel, it would be beneficial to

measure the glucose and lactate concentrations in the medium container, at least during the first experiments tackling this original setting of cultivating MSC in alginate under perfusion, coupled to a catheter for medium sampling. Although the manual medium sampling of the container would enhance the risk of contamination, the control of these molecules in the whole system would contribute to better understand how their profile within the gel aid to predict the cell behaviour.

Beyond the monitoring via glucose/lactate measurements, a calcein-AM/PI staining was performed at the end of the experiment, to visualize the degree of viability in the cell constructs (Figure 3-16).

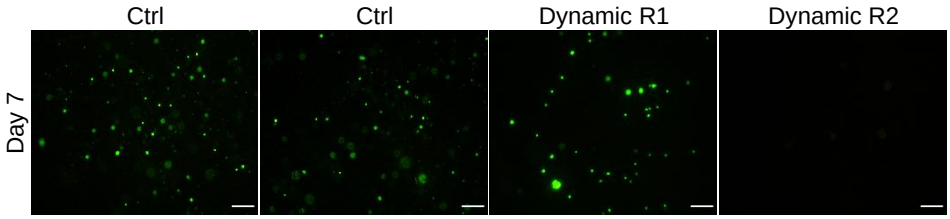

Figure 3-16 Calcein-AM/PI staining of alginate gels on day 7 of cell cultivation inside two parylene-coated High Temp resin reactors (R1 and R2) under dynamic conditions (constant flow, 5 rpm) or in well-plates (Ctrl). The reactors were incubated in IncuReTERM and the controls were incubated in Heracell. Cells were first suspended in alginate 1.2% (w/v) in a cell density of 100,000 cells/ml and then the gels were polymerized by adding 100 mM of $CaCl_2$ to the cell-alginate suspension in a volume ratio of 1:2, followed by a 7-8h period of incubation. Calcein-AM stains live cells in green; PI stains dead cells in red. Pictures were acquired by fluorescence microscopy; scale bar represents 250 µm in 40x magnification.

As depicted in Figure 3-16, it was observed a similar degree of viability in the controls and in one of the gels cultivated under dynamic conditions, namely the reactor R1, as these three conditions contained green-coloured cells at similar densities. Hence, the aforementioned hypothesis that cells were unviable inside both reactors is unlikely.

In the staining of the gel from the reactor R2, no viable nor death cells were detected. This might be due to stress inflicted on the cells when the gel and the reactors were assembled; or after the cell cultivation, probably due to corruption of the cell sample when handling it or due to the usage of inappropriate methods to document the staining. As addressed in section 3.2.2, the usage of the fluorescence microscope is not ideal when assessing three-dimensional platforms since it can only focus a single *z*-layer.

These findings show promise in cultivating MSC encapsulated in alginate gels inside the mini-perfusion reactor coupled to a catheter for medium sampling. Further studies exploiting different conditions, such as different flow rates or gels with different diffusional capacities; and different experiment settings, for instance the monitoring of the molecules in the medium container in addition to the monitoring within the gel, or the assemblage of controls that closely resemble the gels in the reactor to allow a quantitative analysis, should be performed to better understand how the profile of glucose/lactate within the gel aid in the prediction of the cell viability.

MatriStypt®

Squares (6.7 cm^2) of MatriStypt® were seeded at a concentration of 15,000 cells/cm^2, as described in sections 2.2.2 and 2.2.4. Pairs of seeded membranes were inserted in two separate bioreactors, with a catheter inserted in between each pair, and two pairs of matrices were cultivated in a standard manner in well-plates, to serve as controls. The reactors were incubated (IncuReTERM) and perfused at a constant rate (5 rpm), whereas the controls where incubated (Heracell) under static conditions. The experiment was performed for seven days, with samples being taken occasionally either through the catheter (reactors) or manually (controls). The glucose/lactate profiles in between the pair of the perfused MatriStypt® matrices or in the culture medium of the controls are depicted in Figure 3-17.

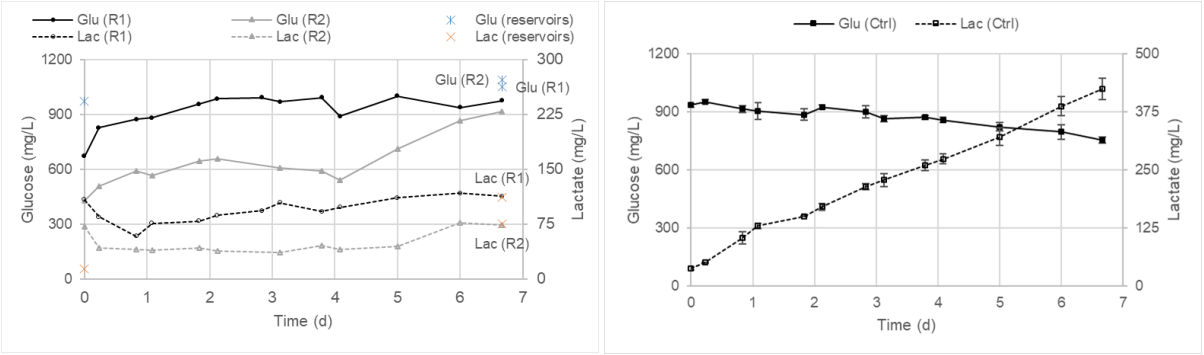

(a) (b)

Figure 3-17 Glucose (Glu) and lactate (Lac) profiles throughout the seven days of cultivation: (a) in samples acquired through the catheter from the in between of MatriStypt® pairs cultivated in two separate reactors (R1 and R2) under perfusion (constant rate, 5 rpm); and (b) in medium samples acquired manually from well-plates with seeded membranes (Ctrl). Data in chart (b) represents mean ± SD from n = 2 replicates.

It is relevant to note that, similarly to the previous study in alginate gel, the current experiment setting does not allow for a quantitative comparison between the cultivation inside the reactors and the controls. This is due to a different number of cultivated cells in the reactors compared to the controls and a different medium volume flowing in the perfusion circuit (15 ml) and the medium in the controls (3 ml), resulting in different magnitudes of glucose metabolism by the cells in these two conditions. In addition, the medium samples of the reactors were acquired through the catheter from between the membranes, whereas the samples of the controls (acquired manually through a micropipette) correspond to the culture medium surrounding the matrices, which more closely resembles the medium present in the containers of the perfusion circuits, rather than the medium from within the cell constructs.

Relatively to the controls (Figure 3-17 (b)), it was demonstrated an accumulation of lactate in the standard cultivation setting (Ctrl) accompanied by a decrease in glucose, since the latter is transformed into the former. This presents a disadvantage of the static regime characteristic of the standard planar cultivation of MSC, as previously discussed.

With regard to the dynamic cultivation of seeded MatriStypt® inside the mini-perfusion reactor (Figure 3-17 (a)), the glucose and lactate profiles were comparable in both reactors, although a reasonable but consistent difference in their intensities was maintained throughout the seven days of cultivation between the two reactors. In the beginning there was a fast increase in glucose and decrease

in lactate, indicating that the employed flow rate (5 rpm) enabled the reposition of glucose and retrieval of lactate that were, respectively, consumed and produced during the incubation period that preceded the cultivation of the cell constructs inside the reactors. Afterwards, both glucose and lactate either remained constant or varied with a slight positive slope, with the final concentrations of glucose near reaching those in the medium container, and the final concentrations of lactate perfectly matching those in the medium container. This behaviour suggests that the values of glucose and lactate within the cell constructs varied with similar rates and intensities as of those in the medium container, indicating decent diffusional properties in the MatriStypt® membranes. However, since the concentrations of the molecules in the medium containers are not known throughout the experiment, it is not possible to confirm this hypothesis.

The considerable rise of lactate from 14 mg/L to 112 and 75 mg/L in the medium containers of the reactors R1 and R2, respectively, is mainly due to the glucose metabolism by the cells, although a certain degree of evaporation might have contributed to the concentration of this molecule in the medium container. Nonetheless, it is clear that the lactate increase is not solely due to this event because for the metabolite to have a six fold increase, the medium volume would have to have a six fold decrease*, i.e.* a volume of 2.5 ml at the end of the seven days of the experiment, which did not occur.

Due to the unknown concentration of the lactate in the medium containers throughout the experiment, it is not possible to conclude if there was a constant increase of lactate, which would indicate a constant metabolism, thus the maintenance of the cell viability during the seven days of the experiment, or if the rate of lactate increase was variable, which would indicate changes in the metabolism and possibly in the cell viability.

Since the cells were metabolically active at some point, the glucose was expected to decrease as it was being metabolized. The rise in glucose can therefore be explained by the degree of evaporation that occurs inside the incubator. Furthermore, the variation of glucose is plausible not to be as prominent as the variation of lactate since MSC are able to use other C-sources, such as glutamine, to produce lactate.

Finally, as with the previous experiment with alginate gel, the different intensities of the molecules within the cell constructs/medium containers between both perfusion circuits could be explained by the different positions of the circuits inside the incubator, since the circuits were susceptible to different degrees of evaporation and environmental cues.

If cells are metabolically active in a scaffold being perfused with a flow rate that prevents the accumulation of lactate and deprivation of glucose, it is expected an increase of lactate and decrease of glucose in the medium container. In addition, if the scaffold has low diffusional limitations, then the molecules within the scaffold are expected to accompany the variations of those in the medium container (*i.e.* an increase in lactate and decrease in glucose) at comparable rates and intensities. This was indeed observed in the current experiment for the lactate profile, suggesting that the flow rate of 5 rpm allows for a sufficient supply of glucose and retrieval of lactate that surpasses the metabolic rate of the cells, and that the MatriStypt® membranes have decent diffusional capacities. Furthermore, although glucose

varied positively, possibly to a degree of evaporation, the fact that its profile within the cell construct appeared to resemble the one in the medium container supports the aforementioned assumptions.

Future work might focus on studying different conditions, such as how different flow rates inflict mechanical stress on cells, cell detachment and reposition/retrieval of glucose/lactate. In addition to the monitoring within the MatriStypt®, it would be beneficial to measure the glucose and lactate concentrations in the medium container, at least during the first experiments tackling this novel concept of cultivating MSC in MatriStypt® under perfusion, coupled to a catheter for medium sampling. Although the manual medium sampling of the container would enhance the risk of contamination, the control of these molecules in the whole system would contribute to better understand how the molecules profile in the collagen membranes aid to predict the cell behaviour.

On the final day of the experiment, a calcein-AM/PI staining was performed to compare the cell viability between the different conditions. As discussed in section 3.3.1., cells gather on the bottom when seeded to MatriStypt®. Therefore, when the reactors were assembled, the pair of membranes were carefully inserted in the reactors with their bottoms facing each other to prevent cell detachment; the catheter was inserted in between the pair. The results obtained on the bottom and top of the membranes are depicted in Figure 3-18 and Figure A 5 (*see Appendix*), respectively.

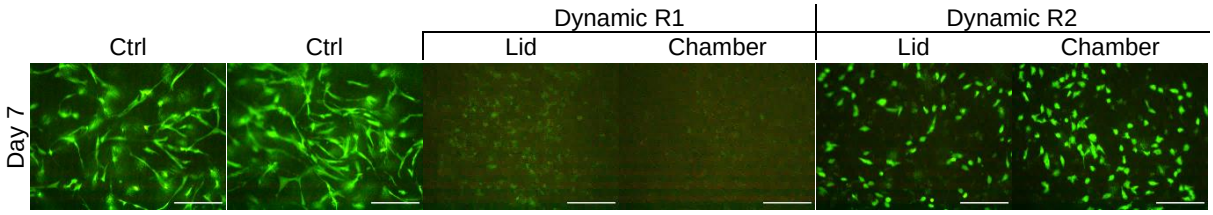

Figure 3-18 Calcein-AM/PI staining of the bottom of MatriStypt® membranes on day 7 of cell cultivation inside two separate parylene-coated High Temp resin reactors (R1 and R2) under dynamic flow (constant rate, 5 rpm) or in well-plates (Ctrl). Cells were seeded at a concentration of 15,000 cells/cm^2 on hydrated matrices; the reactors were incubated in IncuReTERM and the controls were incubated in Heracell. Calcein-AM stains live cells in green; PI stains dead cells in red. Pictures were acquired by fluorescence microscopy; scale bar represents 250 µm in 100x magnification.

As depicted in Figure 3-18, a higher degree of viability was detected in the controls compared to the pair of membranes cultivated under dynamic conditions. Moreover, most cells cultivated under perfusion lost the fibroblastic-like morphology characteristic to MSC.

Viable cells were visible in both membrane pairs cultivated under perfusion, but while in one of the reactors (R2) there was cells remaining on the surface of the membranes (intense green-coloured cells), in the pair cultivated in the reactor R1 only cells within the fibrous mesh of the matrices were detected. It is relevant to note that apart from the intense coloured cells on the surface of the membranes in the reactor R2, its background mesh resembled the mesh observed for the pair of the membranes cultivated in the reactor R1, however this was not possible to document due to contrast properties of the software used to acquire the fluorescent images. Hence, the cells on the top of the pair cultivated in reactor R1

were probably detached when assembling the cell construct or when handling the cell sample at the time of the staining.

With regard to the effect of the perfusion on the membranes, there was no apparent difference in the cell viability between the membranes facing the lid or the chamber, which is reasonable since the documented surfaces (Figure 3-18) were in contact with one another, both facing the catheter, and not in direct contact with the flow.

In section 3.3.1 the capacity of the cells to migrate in MatriStypt® was addressed, which was again confirmed in the controls, as green-coloured cells were visible on their top surface (*see Figure A 5 in the Appendix*). Contrarily to the controls, no cells were visible on the top surface of the membranes cultivated under perfusion. The membranes on the chamber side had their top surfaces in direct contact with the flow, and the membranes on the lid side were in direct contact with the lid. The fact that no cells were detected is presumably due to the harsh conditions to which these surfaces were subjected: either direct contact with the flow for the membrane top surface on the chamber side, or less availability of nutrients and oxygen on the membrane top surface on the lid side.

In general, these results show promise in cultivating MSC in MatriStypt® membranes inside the mini-perfusion reactor coupled to a catheter for medium sampling. Further studies exploiting different conditions, such as different flow rates, and experiment settings, for instance the monitoring of the molecules in the medium container in addition to the monitoring within the matrices, or the creation of controls that closely resemble the membranes inside the reactor to allow for a quantitative analysis, should be performed to better understand how the profile of glucose/lactate within these cell constructs aid to predict the cell viability.

MatriDerm®

Squares (6.7 cm^2) of MatriDerm® were seeded at a concentration of 16,000 cells/cm^2, as described in sections 2.2.2 and 2.2.4. Pairs of seeded membranes were inserted in two separate bioreactors with a catheter inserted between each pair, one of the bioreactors to be operated under static and the other under dynamic conditions (constant rate, 4 rpm). Two pairs of matrices were also cultivated in a standard manner, one in a well-plate and the other in a petri-dish to serve as controls. The reactors were incubated in IncuReTERM, whereas the controls where incubated in Heracell. The experiment was performed for seven days, with samples being taken occasionally either through the catheter (reactors) or manually (chamber of the static reactor, container of the perfusion circuit and controls). The glucose/lactate profiles in between the pair of MatriDerm® matrices cultivated inside the reactors or in the culture medium of the controls, chamber of the static reactor and container of the perfusion circuit are depicted in Figure 3-19.

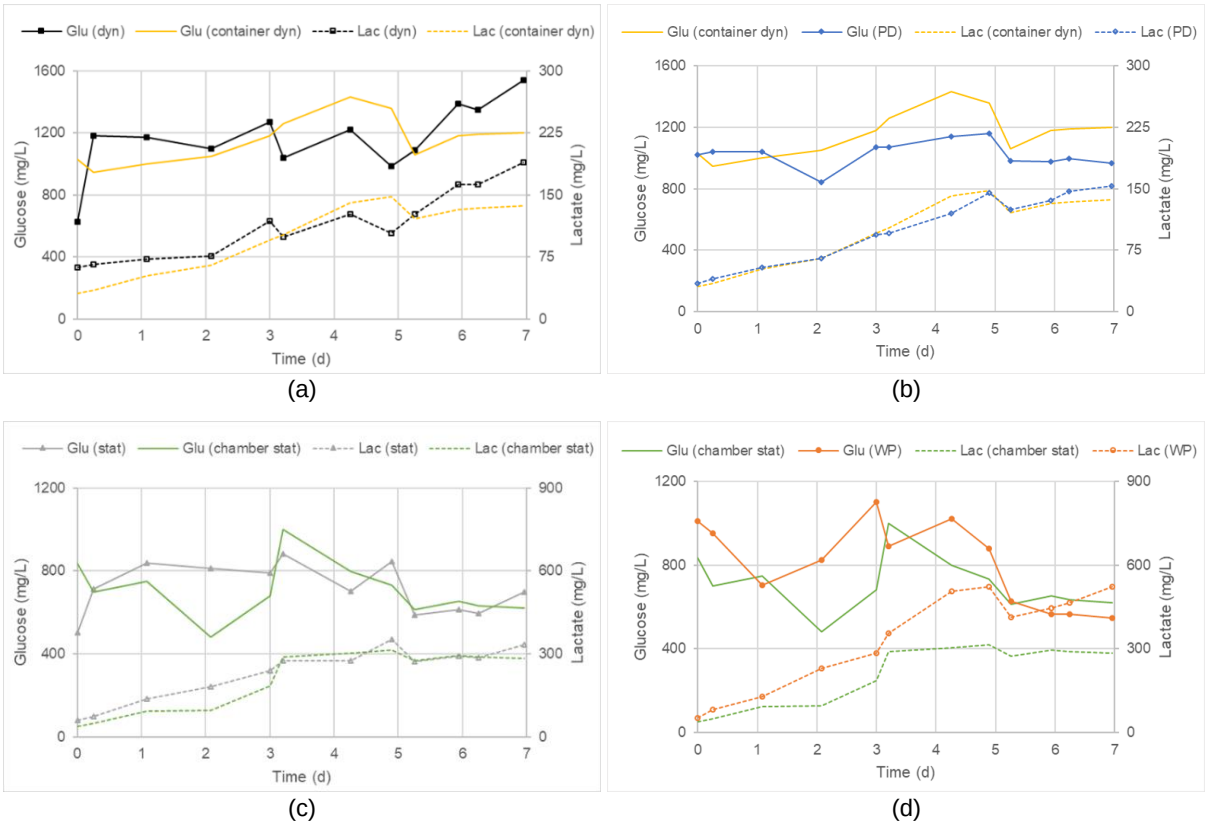

Figure 3-19 Glucose (Glu) and lactate (Lac) profiles throughout the seven days of cultivation in samples acquired through a catheter from the between of MatriDerm® pairs cultivated (a) under perfusion (constant rate, 4 rpm) or (c) under static conditions. Samples of culture medium were acquired manually from: (a and b) the medium container of the perfusion circuit; (b) a petri-dish with a pair of seeded membranes; (c and d) the reactor chamber of the static cultivation; and (d) a well-plate with a pair of seeded membranes.

In the current experiment setting, attention was paid to cultivating the same number of cells in all conditions and elaborating appropriate controls to the cell constructs being cultivated in the reactors, thus allowing for the quantitative analysis between the distinct conditions. A suitable control for the dynamic reactor was the cultivation of a pair of membranes in a petri-dish containing 15 ml of culture medium, the same volume being perfused in the dynamic circuit. In addition, the variations of glucose and lactate in the medium container of the perfusion circuit were monitored and compared to those inside the petri-dish, as both samples were acquired manually (using a micropipette). A suitable control for the static reactor was the cultivation of a pair of membranes in a well-plate containing 3 ml of culture medium, the same volume inside the chamber of the static reactor. In addition, the variations of glucose and lactate in the chamber of the static reactor were monitored and compared to those inside the well-plate, since both samples were acquired manually (using a micropipette).

With regard to the cultivation inside both reactors, the values of glucose and lactate in the beginning were lower and higher, respectively, in between the membranes than of those in the culture medium. This is due to the glucose metabolization during the incubation period that preceded the cultivation inside the reactors.

Concerning the dynamic cultivation (Figure 3-19 (a)), the concentrations of glucose and lactate were similar to those of the medium container throughout the seven days of the experiment, indicating that the flow rate of 4 rpm was such that allowed for the reposition of glucose and prevented the accumulation of lactate in between the MatriDerm® pair. Up to day five, both glucose and lactate profiles indicate that cells were metabolically active since the former varied with a negative tendency, whereas the later varied positively. The notorious increase of these molecules from day five onwards is possibly due to the acquisition of samples by the micro-perfusion pump, since there is no plausible explanation for that occurrence and the concentrations of these molecules in the medium container remained with the same tendency as before.

Interestingly, the increase of lactate in the medium container closely resembled the increase of this molecule in the respective control – standard cultivation of a pair of membranes in a petri-dish (Figure 3-19 (b)). As with the glucose variation, the resemblance with the control was not as evident. While in the control there was a slight tendency for a decrease in glucose, in the medium container of the perfusion circuit the opposite was observed, which might be explained by a stronger degree of evaporation in the container (IncuReTERM) than in the control (Heracell). The consumption of different C-sources, such as glutamine, by the perfused cells; or a higher metabolic activity in the consumption of glucose by the cells in the control compared to the cells cultivated dynamically might as well have contributed to that occurrence. Globally, these findings indicate that the cultivation of seeded MatriDerm® under perfusion at a constant flow rate of 4 rpm inside the mini-perfusion reactor allows cells to, at least, remain as metabolically active as in a standard cultivation setting, and presumably with a similar degree of cell viability.

Regarding the static cultivation inside the reactor (Figure 3-19 (c)), the initial increase of glucose inside the cell construct suggests that the fresh medium was able to cross through the membranes and supply glucose (up to 800 g/L), but naturally in less extent compared to the dynamic cultivation (1000 g/L). The increase in glucose in between the pair of MatriDerm® was accompanied by the decrease of glucose in the reactor chamber. Subsequently, from day one onwards the glucose diminished at a constant rate, both in between the pair of membranes and in the reactor's chamber, suggesting that glucose was being consumed by the cells. As expected, due to the lack of fluid motion, the accumulation of lactate within the cell construct could not be prevented in a static setting, with values of 300 mg/L being reached by day three, about three times more compared to the same period in the dynamic setting, thus indicating an advantage of cultivating cells under perfusion inside the micro-perfusion reactor. The increase of lactate up to day three indicates that cells were metabolically active, thus viable. However, from day three onwards, the variation of lactate stagnated, indicating that the cells became metabolically inactive and presumably death. The fact that the concentration of glucose remained constant from day five onwards supports the addressed hypothesis of cell death.

As observed in the control of the static reactor – standard cultivation of a pair of membranes in a well-plate (Figure 3-19 (d)) – a more intense decrease of glucose (up to 600 mg/L) and increase of lactate (up to 500 mg/L), compared to the static cultivation in the reactor, did not prevent the cells from being metabolically active and viable. Hence, the morbidity observed inside the static reactor is most

likely related to the depletion of oxygen inside the reactor under static conditions, since a lower air volume was available in that platform compared to the well-plate.

It is relevant to note that the comparable concentration behaviour of the molecules within the cell constructs in the static reactor and the respective chamber, even though without medium being perfused, demonstrate that the MatriDerm® membranes have an acceptable diffusional capacity.

These findings suggest that, when cultivating seeded MatriDerm® inside the reactors, it is preferable to perfuse the cells rather than cultivating them under static conditions. Furthermore, the usage of a constant flow rate of 4 rpm allows for a sufficient supply of glucose and retrieval of lactate that surpasses the metabolic rate of the cells, and the obtained metabolic activity and cell viability are comparable to those of a standard planar cultivation setting. Finally, the MatriDerm® membranes have decent diffusional capacities.

Similarly to the previous experiments with alginate gel and MatriStypt®, on the final day of the experiment a calcein-AM/PI staining was performed to compare the cell viability between the different conditions. When the reactors were assembled, the pair of membranes were carefully inserted in the reactors with their tops facing each other to prevent cell detachment (cells remain on the top surface upon seeding); the catheter was inserted in between the pair of membranes. The results obtained on the top and bottom of the membranes are depicted in Figure 3-20 and Figure A 6 (*see Appendix*), respectively.

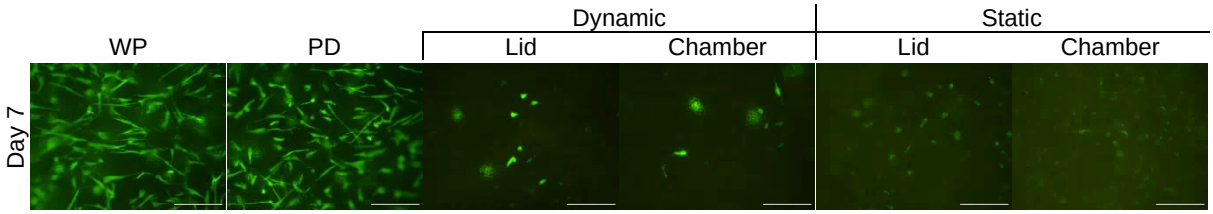

Figure 3-20 Calcein-AM/PI staining of the top of MatriDerm® membranes on day 7 of cell cultivation inside parylene-coated High Temp resin reactors under dynamic (constant flow, 4 rpm) or static conditions and in a well-plate (WP) or in a petri-dish (PD). Cells were seeded at a concentration of 16,000 cells/cm^2 to hydrated matrices; the reactors were incubated in IncuReTERM and the controls were incubated in Heracell. Calcein-AM stains live cells in green; PI stains dead cells in red. Pictures were acquired by fluorescence microscopy; scale bar represents 250 µm in 100x magnification.

As depicted in Figure 3-20, a comparable degree of viability was visible between both controls, as well as the maintenance of the fibroblastic-like morphology characteristic to MSC. Compared to the controls, a lower degree of viability and loss of the fibroblastic-like morphology were detected in the pair of membranes cultivated inside both reactors.

Viable cells were visible in both membrane pairs cultivated inside the reactors, but while there were intense green-coloured cells in the pair cultivated under perfusion, in the pair cultivated under static conditions the cells were stained with a dim colour. This suggests a higher degree of viability in the perfused membranes since they were constantly supplied with nutrients and oxygen and prevented from lactate accumulation. In contrast, a higher density of cells was detected in the membranes cultivated

under static conditions, indicating that the flow of the dynamic cultivation might have caused some cells to detach. Furthermore, the presence of bright cells on the surface of the perfused membranes might have prevented the detection of cells further within the fibrous mesh due to contrast properties of the software used to document the samples.

MSC cultivated in 3D scaffolds were shown to present two distinct forms of adhesion, either flattened, in which cells firmly adhere to a single section of the scaffold, thus resembling planar culture; or bridged, in which cells attach to multiple scaffold components, thereby exhibiting a 3D conformation [99, 116]. When under perfusion, flattened cells are subject to shear stress at their exposed surface similar to those cultivated in planar culture, whereas bridged cells experience shear stress as a 3D stimulus, and therefore are more sensitive and susceptible to the effects of fluid-induced shear forces [116]. This is mainly because cells bridging the scaffolds sense the flow perpendicularly to their cytoskeleton, as opposed to the flattened cells [99].

The fact that the calcein-AM/PI staining of MatriStypt® and MatriDerm® cultivated under perfusion showed a loss in the cell number (Figures 3-18 and 3-20, respectively), while the glucose/lactate monitoring suggested that cells were viable inside the dynamic reactors (Figures 3-17 (a) and 3-19 (a and b), respectively), might be explained by the detachment of cells that were more susceptible to the flow, such as bridging cells/or cells closest to the surface. Moreover, the loss of the fibroblastic-like morphology of the cells on the membrane surfaces under perfusion contributes to this hypothesis, that only flattened cells did remain attached to the surface even though the harsh conditions. These results are evidence that several cell characteristics dependent on mechanical forces and stimuli, such as adhesion and proliferation, are more variable and complex to interpret in 3D scaffolds under perfusion than those in conventional 2D platforms.

With regard to the effect of the position of the membranes in the reactors, there was no apparent difference in the cell viability between the membranes facing the lid or the chamber within the dynamic reactor, which is reasonable since the documented surfaces (Figure 3-20) were in contact with one another, both facing the catheter, and not in direct contact with the flow. As with the static reactor, a higher cell density was detected on the membrane in the chamber side, which is to be expected since the closer to the lid, the lesser the availability of oxygen and nutrients due to diffusional limitations within the membranes.

Interestingly, MatriDerm® showed capacity for the cells to migrate across its collagen-elastin mesh, since green-coloured cells were visible in the bottom surface independently of the cultivation condition (*see Figure A 6 in the Appendix*), which presents an advantage compared to MatriStypt®. Naturally, a higher number of cells were detected on the bottom surfaces of the membranes in the controls compared to the ones cultivated inside the reactors. Alike the results obtained for the top surfaces, more intense green cells, but in a less density, were visible in the bottom surfaces of the membranes cultivated under perfusion comparatively with the membranes cultivated inside the static reactor. Concerning the effect of the position of the membranes in the reactors, there was no apparent difference in the cell viability between the membranes facing the lid or the chamber within the reactors.

Globally, these results show promise in cultivating MSC in MatriDerm® membranes inside the mini-perfusion reactor coupled to a catheter for medium sampling. MatriDerm® shows a decent diffusional capacity and enables cells to migrate within its fibers, even when under perfusion. The monitoring of the medium inside the container of the perfusion circuit, in addition to the monitoring of the medium within the cell construct, aids in the elucidation of how the samples acquired through the catheter allow to predict the cell viability. Further studies using similar or optimized experiment settings should be performed to better understand the relation between the profile of glucose/lactate within the cell constructs and the cell viability. In addition, it would be interesting to exploit different conditions, such as different flow rates to assess its impact on the cell detachment, in order to improve the dynamic cultivation inside the mini-perfusion reactor.

3.6 Adipose derived MSC differentiation

One of the aims of coupling the mini-perfusion bioreactor to a catheter is not exclusively to non-invasively monitor three-dimensional cultivation of cells, but also monitor tissue cultivation. If combined with the available 3D platforms (alginate hydrogel or collagen matrices), the bioreactor is best suited to support the cultivation of skin or cartilage for instance, *i.e.* tissues that are not characterized by having a rigid ECM, as opposed to bone. This is mainly due to the low stiffness of the gel and the membranes, which is not ideal to cultivate the latter type of tissue.

To form a certain tissue, cells must be differentiated into cells that can give rise to that same tissue. Mesenchymal stromal cells are known to have a multi-differentiation potential, mainly into the osteogenic, chondrogenic and adipogenic trilineage. Hence, bone, cartilage and fat tissues can be originated when MSC are differentiated into those lines, respectively.

The present chapter focuses on performing the trilineage differentiation of adipose-derived mesenchymal stromal cells, first in planar culture to assure their capability to do so and verify one of the ISCT minimal criteria – trilineage differentiation (section 3.6.1) – and then in 3D platforms (section 3.6.2). The latter has the main goals of evaluate the capacity of the cells to differentiate in those platforms; assess the feasibility of generating a functional tissue to be used in future studies inside the novel monitoring device; and ultimately, to serve as an *in vitro* model inside the mini-perfusion bioreactor.

3.6.1 Differentiation in planar culture

The employed methodology to differentiate adMSC in planar culture is based on the work developed by Egger [110] and Oliveira [111], which is described in sections 2.2.7-2.2.9. Briefly, well bottoms of a well-plate were covered with fibronectin prior to cell seeding. adMSC were cultured for 21 days in the respective differentiation condition, with medium being changed every 2-3 days. On day 21, the cells were fixated and further documented through the distinct staining assays.

As aforementioned, this experiment is intended to evaluate the trilineage differentiation capability of adMSC. The impact of the oxygen concentration and media formulations on the differentiation potential were assessed.

Adipogenesis

The adipogenic differentiation was assessed via Oil Red O. By staining the lipid vacuoles of the cells in red, this staining allows to detect the lipid droplet accumulation as a result of adipogenesis. The Oil Red O staining on cells cultivated under normoxic (21% O_2) or hypoxic (5% O_2) conditions in adipogenic differentiation medium (ADM) or expansion medium (EM) for 21 days is presented in Figure 3-21.

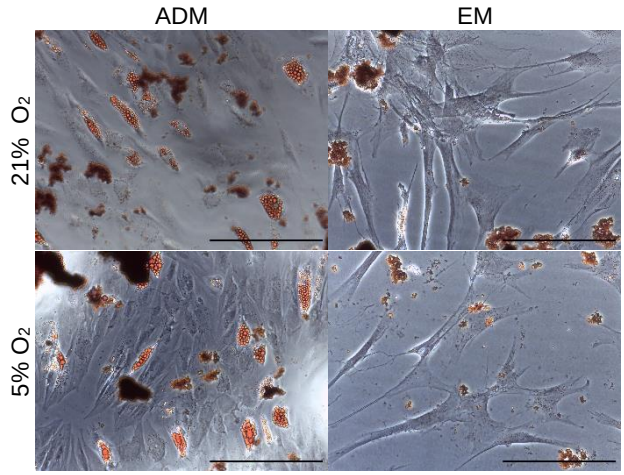

Figure 3-21 Oil Red O staining at day 21 on adMSC cultivated under normoxic (21% O_2) or hypoxic (5% O_2) conditions in adipogenic differentiation medium (ADM) or expansion medium (EM). Oil Red O stains lipid vacuoles in red. Pictures were acquired by phase contrast microscopy; scale bar represents 250 µm in 200x magnification.

Dark red granulates corresponding to insolubilized Oil Red O were visible in all pictures; these were not possible to discard even though the applied rinsing steps.

Apart from that, lipid droplets were detected in cells cultivated in ADM under both oxygen conditions, demonstrating that adMSC are capable to differentiate into the adipogenic lineage. As expected, no lipid droplets were detected on the control.

There was not a significant difference between the frequency nor the quality of the droplets between the hypoxic and normoxic conditions in the ADM samples, which stands in agreement with a body of literature that reported no relevant effect of hypoxia on the adipogenic potential of MSC [83, 85, 86].

Chondrogenesis

The chondrogenic differentiation was assessed via Alcian Blue. By staining glycosaminoglycans in blue, which are characteristic to the ECM of cartilage, this staining allows to detect chondrogenesis. The Alcian Blue staining on cells cultivated under normoxic (21% O_2) or hypoxic (5% O_2) conditions in manufactured chondrogenic differentiation medium (CDM I), handmade chondrogenic differentiation medium (CDM II) or expansion medium (EM) for 21 days is presented in Figure 3-22.

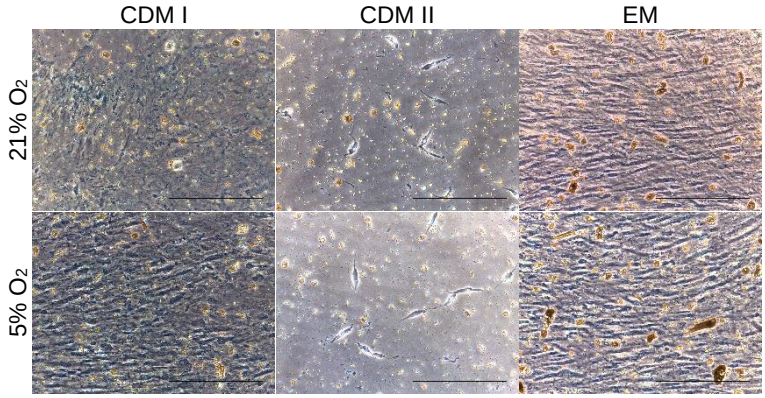

Figure 3-22 Alcian Blue staining at day 21 on adMSC cultivated under normoxic (21% O_2) or hypoxic (5% O_2) conditions in manufactured chondrogenic differentiation medium (CDM I), handmade chondrogenic medium (CDM II) or expansion medium (EM). Alcian Blue stains glycosaminoglycans in blue. Pictures were acquired by phase contrast microscopy; scale bar represents 250 µm in 200x magnification.

Brownish granulates from EtOH fixation residues and small blue insolubilized crystals of Alcian Blue were visible in all pictures; these were not possible to discard even though the applied rinsing steps.

During cultivation in CDM II, the adMSC formed agglomerates that detached from the plate and were discarded during medium changes, hence the low cell density obtained in the samples for this condition, independently of the oxygen concentration; this was also reported by Oliveira [111].

The results obtained for both chondrogenic media were comparable to the control, and no difference was observed between the different oxygen conditions within each medium (except for the lower cell density observed in the CDM II samples due to the aforementioned cell detachment). No stained glycosaminoglycans characteristic of the cartilage ECM were detected in any of the CDM conditions, either due to low cell densities that resulted in a negligible production of ECM; inappropriate Alcian Blue staining methodology; or due to a partial trilineage differentiation capacity of this adMSC cell line.

Osteogenesis

The osteogenic differentiation was assessed via von Kossa, Alizarin Red S, and the pairing of Calcein with DAPI. The distinct stainings were performed at day 21 on cells cultivated under normoxic (21% O_2) or hypoxic (5% O_2) conditions in manufactured osteogenic differentiation medium (ODM I), handmade osteogenic differentiation medium (ODM II) or expansion medium (EM).

The von Kossa stains phosphate deposits in dark grey, which are characteristic of the osteocytes ECM, thus allowing to detect osteogenesis. The von Kossa staining is depicted in Figure 3-23.

A top view of the samples after the von Kossa staining is depicted in Figure 3-23 (a). Black webs from von Kossa staining residues were observed in all pictures present in Figure 3-23 (b); these were not possible to discard even though the applied rinsing steps. The degree of phosphate staining can be detected from the grey intensity in between those webs, the darker the grey, the higher is the amount of phosphate deposits and subsequently the osteogenesis extent. As expected, the control samples presented the lightest shade of grey, indicating that there was no osteogenic differentiation.

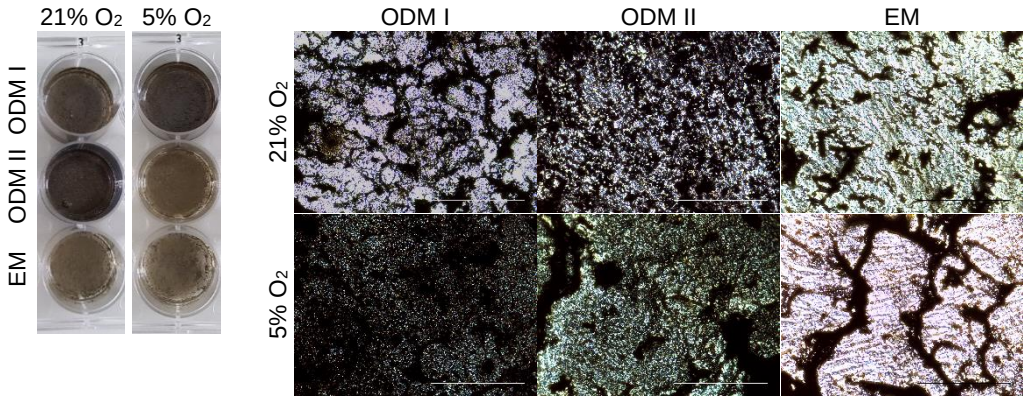

Figure 3-23 von Kossa staining at day 21 on adMSC cultivated under normoxic (21% O_2) or hypoxic (5% O_2) conditions in manufactured osteogenic differentiation medium (ODM I), handmade osteogenic medium (ODM II) or expansion medium (EM). von Kossa stains phosphate in dark grey: (a) top view of the wells with the stained samples; (b) documentation by phase contrast microscopy; scale bar represents 250 µm in 200x magnification.

In the samples cultivated in ODM I, a darker grey was obtained on both samples cultivated in different oxygen concentrations comparatively to the control. Furthermore, the samples under hypoxic conditions presented a higher amount of phosphate deposits than the normoxic ones, suggesting that hypoxic conditions favour osteogenesis of adMSC cultivated in ODM I.

Interestingly, only the samples cultivated under normoxic conditions in ODM II presented the production of phosphate deposits, and more pronounced than in any other condition (Figure 3-23 (a)). Thereby indicating that only normoxic conditions promote adMSC osteogenic differentiation in ODM II, and with a higher intensity compared to the samples cultivated in ODM I.

Alizarin Red S forms a chelate complex with bivalent cations, such as calcium, resulting in a bright red staining of the calcium deposited in the ECM as a result of osteogenesis. The Alizarin staining is documented in Figure 3-24.

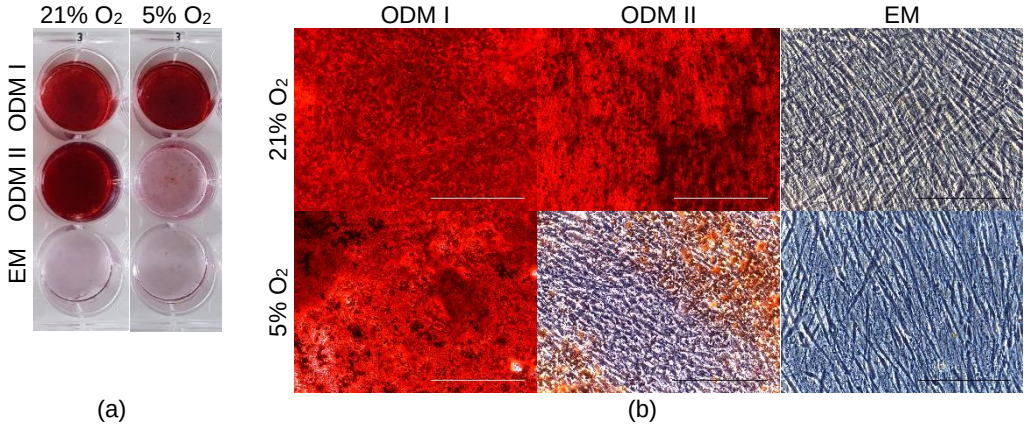

Figure 3-24 Alizarin Red S staining at day 21 on adMSC cultivated under normoxic (21% O_2) or hypoxic (5% O_2) conditions in manufactured osteogenic differentiation medium (ODM I), handmade osteogenic medium (ODM II) or expansion medium (EM). Alizarin Red S stains calcium in red: (a) Top view of the wells with the stained samples; (b) documentation by phase contrast microscopy; scale bar represents 250 µm in 200x magnification.

The results obtained with the Alizarin Red S staining are consistent with the von Kossa staining. As expected, the control samples were not stained in red, indicating that there was no calcification in their ECM, thus no osteogenesis occurred in these conditions. It is clearly visible, especially in the top view (Figure 3-24 (a)), that calcium was present on the ECM of samples cultivated in ODM I under both oxygen conditions. Moreover, there was a higher red intensity on samples cultivated under hypoxia, thus supporting the hypothesis that hypoxia favours osteogenesis of adMSC cultivated in ODM I. Again, only samples cultivated under normoxia in ODM II presented calcium in its ECM. Furthermore, this was the sample in which the most vivid red, thus production of calcium, was detected, indicating that the ODM II under 21% O_2 is the most efficient condition to perform the osteogenic differentiation of adMSC.

Like Alizarin, the fluorescent dye Calcein forms a chelate complex with calcium, thus allowing to detect the ECM mineralization that occurs during osteogenesis. The fluorescent dye DAPI stains the nuclei of live cells in blue, and was used together with calcein to permit the discrimination of cells within the greenish calcein-stained mesh. The Calcein and DAPI stainings and their composite are documented in Figure 3-25.

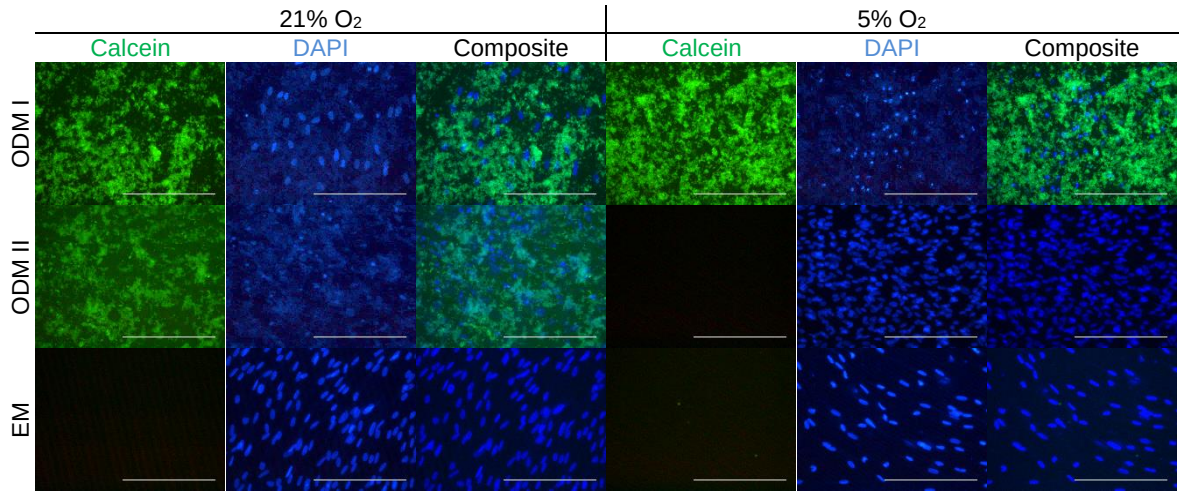

Figure 3-25 Calcein and DAPI stainings, and their composite, at day 21 on adMSC cultivated under normoxic (21% O_2) or hypoxic (5% O_2) conditions in manufactured osteogenic differentiation medium (ODM I), handmade osteogenic medium (ODM II) or expansion medium (EM). Calcein stains calcium in green; DAPI stains the nuclei of live cells in blue. Pictures were acquired by fluorescence microscopy; scale bar represents 250 µm in 200x magnification.

The results obtained with the Calcein and DAPI stainings are consistent with the previous stainings. As expected, ECM mineralization did not occur in the control samples, indicating that these maintained an undifferentiated state. Both oxygen conditions presented mineralization in the ECM of cells cultivated in ODM I, thus indicating osteogenesis. Again, a more intense green was obtained for hypoxic conditions, supporting the assumption that low oxygen conditions facilitate the osteogenic differentiation of adMSC in ODM I. Regarding the ODM II, only the sample cultivated under normoxia did differentiate into the osteogenic lineage, as visible by the green-stained ECM mineralization.

Three distinct stainings to detect osteogenesis of adMSC resulted in similar results: i) in ODM I, adMSC are capable to differentiate under both normoxic and hypoxic conditions, with higher extent in

the latter, indicating that low oxygen concentrations enhance the osteogenic potential of adMSC, which is in accordance to what was reported by Grayson *et al*. [87]; and ii) in ODM II, adMSC osteogenic differentiation is promoted, and with higher intensities compared to the ODM I, however, the cells are incapable of differentiating under hypoxia, which is in agreement with a body of literature [83, 84, 85, 86]. Moreover, Egger [110] and Oliveira [111] demonstrated that adMSC were not able to differentiate into the osteogenic lineage when cultivated under hypoxic conditions in a medium with the same composition as ODM II.

These findings indicate that the manufactured medium has in its composition factors that allow for the osteogenic differentiation of adMSC, independently of the oxygen condition, although differentiation under hypoxia is favoured. Nevertheless, it is not possible to conclude what is causing this behaviour due to the disclosed composition of ODM I. In turn, the handmade medium is optimized for the osteogenic differentiation of adMSC under normoxia but is missing one or more crucial components that prevent osteogenesis from occurring under low oxygen supply. Hence, these findings demonstrate that, in addition to the impact of the oxygen tension, adMSC differentiation is dependent on several other cultivation conditions, with a critical factor being the composition of the differentiation culture medium.

3.6.2 Differentiation in 3D platforms

The employed methodology to differentiate adMSC in 3D platforms is based on the work developed by Egger [110], which is described in sections 2.2.7-2.2.9. Briefly, cells were seeded to alginate gel or MatriDerm® and cultured for 21 days in the respective differentiation condition, with medium being changed every 2-3 days. On day 21, the samples were fixated and further documented through the same staining assays that were performed in the planar differentiation experiments.

As aforementioned, this experiment aims to evaluate the capacity of cells to differentiate in the addressed 3D platforms and assess the feasibility of generate, in future studies, a functional tissue to be cultivated inside the reactor, and ultimately, to serve as an *in vitro* model.

Adipogenesis

The Oil Red O staining on cells cultivated in alginate gel or MatriDerm® under normoxic (21% O_2) or hypoxic (5% O_2) conditions in adipogenic differentiation medium (ADM) or expansion medium (EM) for 21 days is presented in Figure 3-26.

The adipogenic differentiation was proven possible in alginate hydrogel. Golden lipid droplets, instead of the typical red staining observed in planar culture, were visible under bright field microscope in samples cultivated in ADM. The frequency and quality of the droplets were comparable between the different oxygen conditions, indicating that hypoxia did not affect the adipogenic potential of adMSC, as similarly observed in the planar differentiation. As expected, no lipid droplets were visible in the control samples.

Regarding the MatriDerm®, it is not possible to conclude about the adipogenesis extent due to the absorption of the red-coloured dye by the fibrous collagen-elastin mesh, thus preventing to discriminate between the stained mesh and stained cells.

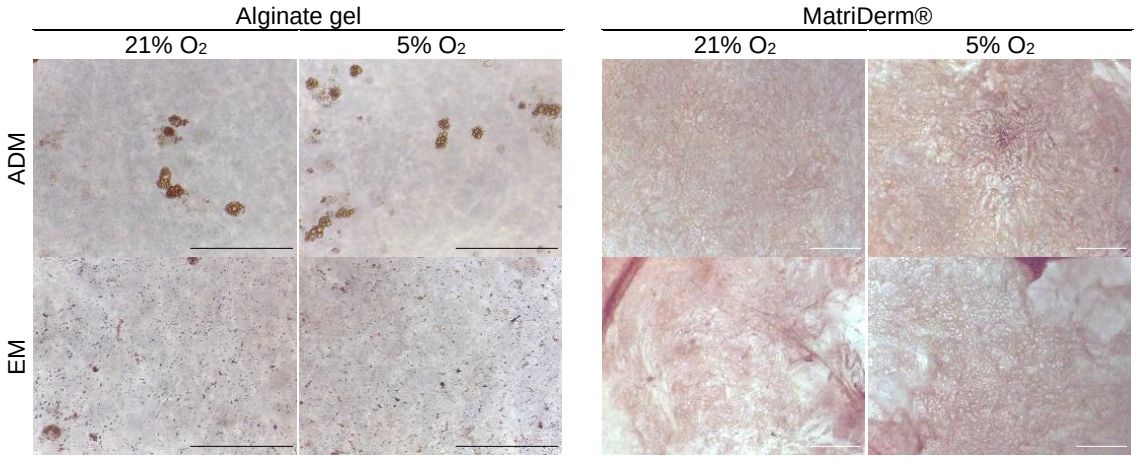

Figure 3-26 Oil Red O staining at day 21 on adMSC cultivated in alginate gel or MatriDerm® under normoxic (21% O_2) or hypoxic (5% O_2) conditions in adipogenic differentiation medium (ADM) or expansion medium (EM). Oil Red O stains lipid vacuoles in red; only perceptible in alginate. Pictures were acquired by phase contrast microscopy; scale bar represents 250 µm in 200x or 100x magnification for the gel and the membrane, respectively.

Chondrogenesis

The Alcian Blue staining on cells cultivated in alginate gel or MatriDerm® under normoxic (21% O_2) or hypoxic (5% O_2) conditions in manufactured chondrogenic differentiation medium (CDM I), handmade chondrogenic differentiation medium (CDM II) or expansion medium (EM) for 21 days is depicted in Figure 3-27.

Although dark points corresponding to cells were visible in alginate gel, this platform was stained in blue, thus preventing to detect the blue-stained glycosaminoglycans characteristic of the cartilage ECM.

Concerning the MatriDerm®, Alcian Blue staining was detected and distinguishable between both chondrogenic media and the control. As expected, no glycosaminoglycans were present in the samples corresponding to the latter condition. With regard to the media, the amount of glycosaminoglycan was more pronounced in the samples cultivated in the manufactured medium (CDM I). As for the oxygen supply, hypoxia favoured the chondrogenic potential of adMSC, independently of the chondrogenic medium used, since in both CDM there was a more intense blue colorization in samples cultivated under 5% O_2 compared to those cultivated in 21% O_2. This result is in accordance to what is globally accepted by the scientific community, that chondrogenesis is supported by hypoxia [70, 71, 81, 83].

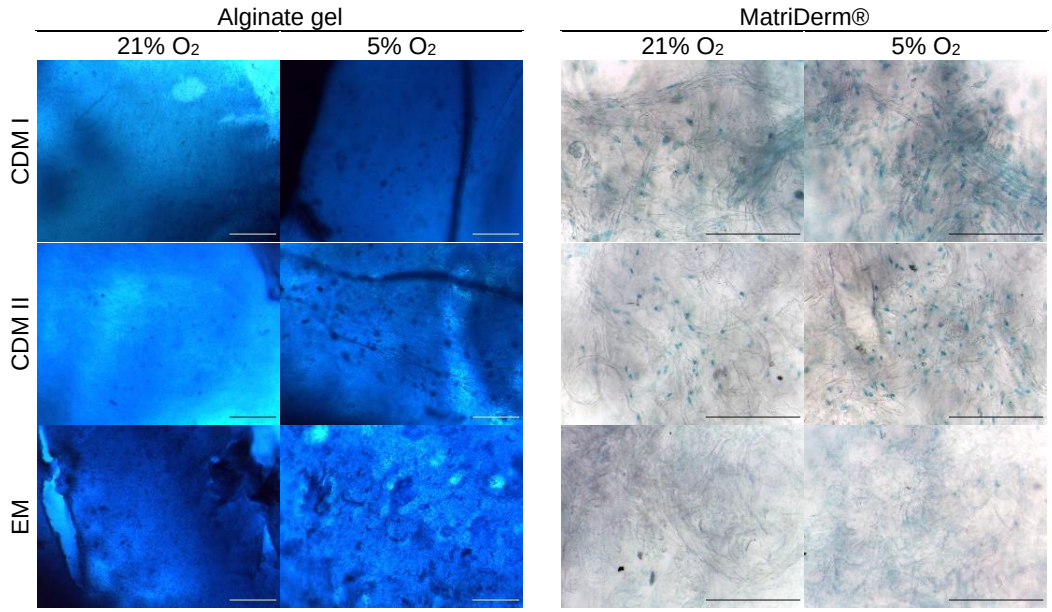

Figure 3-27 Alcian Blue staining at day 21 on adMSC cultivated in alginate gel or MatriDerm® under normoxic (21% O_2) or hypoxic (5% O_2) conditions in manufactured chondrogenic differentiation medium (CDM I), handmade chondrogenic medium (CDM II) or expansion medium (EM). Alcian Blue stains glycosaminoglycans in blue. Pictures were acquired by phase contrast microscopy; scale bar represents 250 µm in 100x or 200x magnification for the gel or the membrane, respectively.

Osteogenesis

The osteogenic differentiation was assessed via von Kossa, Alizarin Red S, and the pairing of Calcein with DAPI. However, only the Calcein/DAPI in MatriDerm® did result in a significant outcome.

The Calcein, DAPI and their composite on cells cultivated in MatriDerm® under normoxic (21% O_2) or hypoxic (5% O_2) conditions in manufactured osteogenic differentiation medium (ODM I), handmade osteogenic differentiation medium (ODM II) or expansion medium (EM).are documented in Figure 3-28.

As depicted in Figure 3-28, the MatriDerm® fibers exhibited affinity with calcein, since the control samples were coloured in green, thereby making it difficult to distinguish stained fibers from stained calcium deposits in the ECM. Even so, a cellular prominence containing a calcium deposit was detected in the membrane cultivated in ODM II under normoxia, suggesting the occurrence of osteogenic differentiation. Interestingly, this is in agreement with what was observed previously in the planar differentiation. ODM II and 21% O_2 was the setting that best promoted osteogenesis of adMSC when cultivated and differentiated in 2D culture, therefore it would be expected a greater ease in detecting the osteogenic differentiation in the cell constructs cultivated in these conditions.

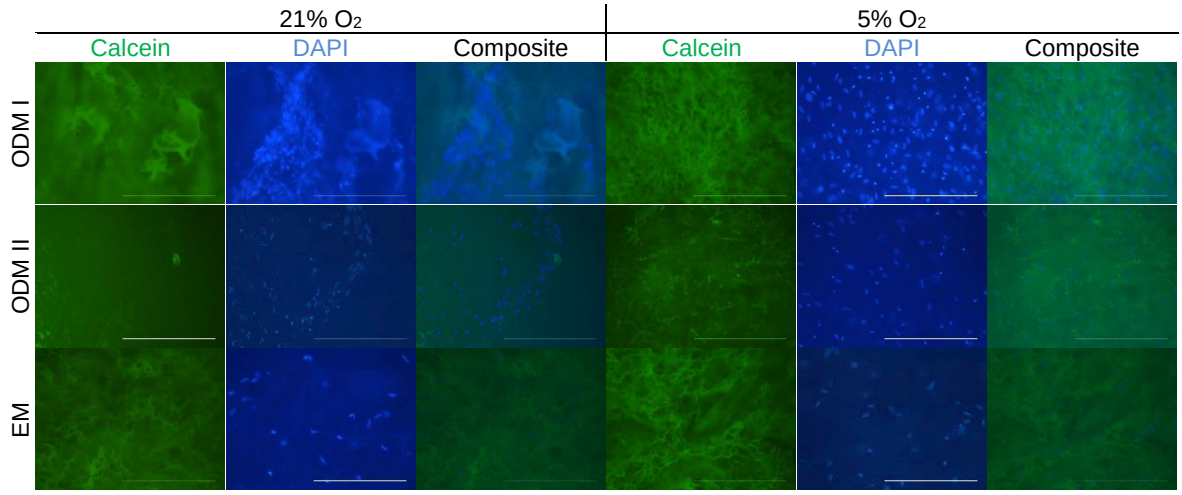

Figure 3-28 Calcein and DAPI stainings at day 21 on adMSC cultivated in MatriDerm® under normoxic (21% O_2) or hypoxic (5% O_2) conditions in manufactured osteogenic differentiation medium (ODM I), handmade osteogenic medium (ODM II) or expansion medium (EM). Calcein stains calcium in green; DAPI stains the nuclei of live cells in blue. Pictures were acquired by fluorescence microscopy; scale bar represents 250 µm in 200x magnification.

Regarding the other stainings to detect osteogenesis, the dyes used in the von Kossa (*see Figure A 7 in Appendix*) and Alizarin Red S (*see Figure A 8 in Appendix*) stainings were imprisoned within alginate gel or remained attached to the fibrous mesh of the MatriDerm®, even after performing several rinsing steps with mechanical agitation. As for the Calcein/DAPI staining in alginate gel (*see Figure A 9 in Appendix*), it was arduous to document cells and not possible to document the calcification of the ECM. The blurred nature of the gel contributes to light diffraction and background noise across several layers along the *z*-axis, which prevents entities such as cells and mineralization from being easily detected by fluorescence microscopy.

In general, the staining protocols to detect the trilineage differentiation of MSC in planar culture are not suitable for the addressed three-dimensional platforms. Nonetheless, Oil Red O in alginate gel and Alcian Blue in MatriDerm® allowed for a clear detection of adipogenesis and chondrogenesis, respectively. Although not as evident, the Calcein/DAPI staining on MatriDerm® enabled the detection of calcium deposits, does indicating osteogenesis.

Due to the fact that none of the staining procedures worked simultaneously in alginate gel and MatriDerm®, it is not possible to conclude about the best suited platform to perform each lineage differentiation of adMSC.

In order to facilitate the detection of MSC differentiation in three-dimensional platforms, more adequate experiment settings are necessary. For instance, an optimization of the fixation, staining and rinsing protocols for each platform; perform different methodologies to assess the differentiation, such as the examination of the expression of specific markers to each lineage; or the usage of 3D platforms that permit a clear optical evaluation and do not interfere with the methodology of analysis.

Chapter 4

Conclusions

This chapter finalises the present work, highlighting major conclusions and pointing out aspects to be developed in future work.

In this work, the cytotoxicity of the material from which the mini-perfusion reactor can be 3D-printed was successfully evaluated, and it was concluded that the parylene-coated High Temp resin is the most cytocompatible material.

The cell seeding to three-dimensional scaffolds determines the initial number of cells, their spatial distribution within the construct, and cell adhesion efficacy. Thereby, the chosen methodology of cell loading is of outmost importance. MSC seeding to 3D platforms, namely alginate gel and collagen membranes (MatriStypt®), was assessed. Regarding the alginate gel, casting gels by mixing cell suspension in alginate 1.2% (w/v) (between 100,000-200,000 cells/ml), followed by the addition of 100 mM $CaCl_2$ in a ratio 1:2 and subsequent incubation for 7-8 hours, is an adequate methodology to entrap cells within the alginate polymer. This allows gels to have a decent stiffness for further handling, does not interfere with the cell viability and provides a sufficient fluorescent signal for culture analysis. As for the membranes, the dynamic loading (centrifugation at 500 rpm for 5 min) does not compare favourably with static seeding. The static cultivation in MatriStypt® allows MSC to remain viable and maintain their characteristic fibroblastic-like morphology. Moreover, hydrating the matrices prior to the cell seeding is beneficial.

It is known that dynamic loading is advantageous and recent efforts have been made to seed cells to scaffolds in perfusion systems. It would be interesting to load cells in a perfusion setting using the addressed mini-perfusion bioreactor because, in addition to improve the cell loading efficiency, it would also significantly reduce the risk of contamination.

Regarding the transport capacity of the addressed 3D platforms, the alginate gel was demonstrated to have more diffusional limitations in comparison to the collagen and collagen-elastin membranes (MatriStypt® and MatriDerm®, respectively). The hydrodynamics of the mini-perfusion bioreactor and biomechanical properties of the 3D scaffolds should be further characterized to better understand the fluid-induced shear stress and the mechanical stimuli, to which cells are subjected when cultivated inside the reactor. This would allow to deduce optimal cultivation parameters that better resemble physiological conditions.

Endpoint analysis of a cell culture, such as the widely employed calcein-AM/PI staining, requires the frequent handling of cell samples, which enhances the risk of contamination, influences the cultivation conditions and sacrifices cells; furthermore, it is time, reagent and labour consuming. The present work confirms the feasibility of cultivating 3D cell constructs inside a mini-perfusion bioreactor coupled to a catheter to acquire medium samples from within the scaffolds. The measurement of glucose and lactate in those samples enables a non-invasive monitoring of the cultivation of the cell constructs under perfusion, demonstrating a great advantage compared to endpoint analysis. Using this novel concept, it was predicted that MSC-seeded alginate gels and collagen membranes under perfusion remained viable for up to seven days.

The developed work provided the proof-of-concept of inserting a catheter within a cell construct cultivated inside the mini-perfusion bioreactor, to non-invasively monitor 3D cultivations. In the future, additional experimentation should be conducted to optimize this novel and non-invasive 3D monitoring system, notably: exploit tissue cultivation, evaluate different biological parameters in the samples - such

as oxygen tension, pH and specific expression markers - implement devices that enable the real-time measurement of those parameters, and tackle different experiment settings - such as flow rate and oxygen supply.

Finally, the trilineage differentiation of adMSC was performed in planar culture and in 3D platforms (alginate gel and MatriDerm®). In the 2D differentiation, chondrogenesis was not detected, probably due to the staining procedure, and adipogenesis occurred with no apparent dependence on the oxygen supply. The osteogenic differentiation was favoured under hypoxia in the manufactured osteogenic medium, whereas only normoxic conditions did allow the differentiation in the handmade osteogenic medium. The fixation, staining and documentation procedures for the planar differentiation of adMSC proved not to be suitable for the 3D differentiation. Nevertheless, it was possible to detect adipogenesis in alginate gel, while chondrogenesis and osteogenesis were observed in MatriDerm®. These results show the feasibility of differentiating MSC in the considered 3D platforms and to possibly generate, in the future, a functional tissue construct.

Different protocols for the 3D differentiation in alginate gel and collagen membranes, and subsequent analysis should be tackled in order to generate and detect, respectively, functional tissues to be cultivated inside the mini-perfusion reactor. This would significantly contribute for the improvement and establishment of an advanced and standardized non-invasive monitoring device for 3D cell and tissue cultivations.

Bibliography

[1] J. M. Kaplan, M. E. Youd and T. A. Lodie, “Immunomodulatory activity of mesenchymal stem cells,” *Current Stem Cell Research & Therapy,* vol. 6, 2011.

[2] Y. Shi, Y. Wang, Q. Li, K. Liu, J. Hou, C. Shao and Y. Wang, “Immunoregulatory mechanisms of mesenchymal stem and stromal cells in inflamatory diseases,” *Nature Reviews Nephrology,* vol. 14, pp. 493-507, 2018.

[3] A. M. DiMarino, A. I. Caplan and T. L. Bonfield, “Mesenchymal stem cells in tissue repair,” *Frontiers in Immunology,* vol. 4, p. 201, 2013.

[4] L. d. S. Meirelles, A. M. Fontes, D. T. Covas and A. I. Caplan, “Mechanisms involved in the therapeutic properties of mesenchymal stem cells,” *Cytokine & Growth Factor Reviews,* vol. 20, pp. 419-27, 2009.

[5] J. M. Karp and G. S. L. Teo, “Mesenchymal stem cell homing: the devil is in the details,” *Cell Stem Cell,* vol. 4, no. 3, pp. 206-16, 2009.

[6] P. Bianco, P. G. Robey and P. J. Simmons, “Mesenchymal stem cells: revisiting history, concepts, and assays,” *Cell Stem Cell,* vol. 2, no. 4, pp. 313-9, 2008.

[7] K. Bieback and I. Brinkmann, “Mesenchymal stromal cells from human perinatal tissues: from biology to cell therapy,” *World Journal of Stem Cells,* vol. 2, no. 4, pp. 81-92, 2010.

[8] D. Minteer, K. G. Marra and J. P. Rubin, “Adipose-derived mesenchymal stem cells: biology and potential applications,” *Advances in Biochemical Engineering/Biotechnology,* vol. 129, pp. 59-71, 2013.

[9] C. E. Gargett, K. E. Schwab, R. M. Zilwood, H. P. T. Nguyen and D. Wu, “Isolation and culture of epithelial progenitors and mesenchymal stem cells from human endometrium,” *Biology of Reproduction,* vol. 80, pp. 1136-45, 2009.

[10] X. Du, Q. Yuan, Y. Qu, Y. Zhou and J. Bei, “Endometrial mesenchymal stem cells isolated from menstrual blood by adherence,” *Stem cells International,* vol. 2016, 2016.

[11] M. J. D. Griffiths, D. Bonnet and S. M. Janes, “Stem cells of the alveolar epithelium,” *Lancet,* vol. 366, pp. 249-60, 2005.

[12] J. Liu, F. Yu, Y. Sun, B. Jiang, W. Zhang, J. Yang, G.-T. Xu, A. Liang and S. Liu, “Concise reviews: Characteristics and potential applications of human dental tissue-derived mesenchymal stem cells,” *Stem cells,* vol. 33, no. 3, pp. 627-38, 2014.

[13] E. B. de Sousa, P. L. Casado, V. M. Neto, M. E. L. Duarte and D. P. Aguiar, “Synovial fluid and synovial membrane mesenchymal stem cells: latest discoveries and therapeutic perspectives,” *Stem Cell Research & Therapy,* vol. 5, p. 112, 2014.

[14] M. Secco, E. Zucconi, N. M. Vieira, L. L. Q. Fogaça, A. Cerqueira, M. D. F. Carvalho, T. Jazedje, O. K. Okamoto, A. R. Muotri and M. Zatz, “Multipotent Stem Cells from Umbilical Cord: Cord Is Richer than Blood!,” *Stem Cells,* vol. 26, no. 1, pp. 146-50, 2008.

[15] R. Secunda, R. Vennila, A. M. Mohanashankar, M. Rajasundari, S. Jeswanth and R. Surendran, “Isolation, expansion and characterization of mesenchymal stem cells from human bone marrow, adipose tissue, umbilicar cord blood and matrix: a comparative study,” *Cytotechnology,* vol. 67, pp. 793-807, 2014.

[16] J. H. Yoon, E. Y. Roh, S. Shin, N. H. Jung, E. Y. Song, J. Y. Chang, B. J. Kim and H. W. Jeon, “Comparison of explant-derived and enzymatic digestion-derived MSCs and the growth factors from Wharton's jelly,” *BioMed Research International,* vol. 2013, 2013.

[17] V. Jossen, R. Pörtner, S. C. Kaiser, M. Kraume, D. Eibl and R. Eibl, “Mass Production of Mesenchymal Stem Cells - Impact of bioreactor design and flow conditions on proliferation and differentiation,” in *Cells and Biomaterials in Regenerative Medicine*, IntechOpen, 2014.

[18] M. Dominici, K. Le Blanc, I. Mueller, I. Slaper-Cortenbach, F. C. Marini, D. S. Krause, R. J. Deans, A. Keating, D. J. Prockop and E. M. Horwitz, “Minimal criteria for defining multipotent mesenchymal stromal cells. The International Society for Cellular Therapy position statement,” *Cytotherapy,* vol. 8, no. 4, pp. 315-7, 2006.

[19] J. Kim, S. Park, Y. J. Kim, C. S. Jeon, K. T. Lim, H. Seonwoo, S.-P. Cho, T. D. Chung, P.-H. Choung, Y.-H. Choung, B. H. Hong and J. H. Chung, “Monolayer Graphene-Directed Growth and Neuronal Differentiation of Mesenchymal Stem Cells,” *Journal of Biomedical Nanotechnology,* vol. 11, pp. 2024-33, 2015.

[20] H. Shen, Y. Wang, Z. Zhang, J. Yang, S. Hu and Z. Shen, “Mesenchymal Stem Cells for Cardiac Regenerative Therapy: Optimization of Cell Differentiation Strategy,” *Stem Cells International,* vol. 2015, 2015.

[21] D. G. Harkin, L. Foyn, L. J. Bray, A. J. Sutherland, F. J. Li and B. G. Cronin, “Concise Reviews: Can Mesenchymal Stromal Cells Differentiate into Corneal Cells? A Systematic Review of Published Data,” *Stem Cells,* vol. 33, no. 3, pp. 785-91, 2014.

[22] A. S. Lee, C. Tang, M. S. Rao, I. L. Weissman and J. C. Wu, “Tumorigenicity as a clinical hurdle for pluripotent stem cell therapies,” *Nature Medicine,* vol. 19, pp. 998-1004, 2013.

[23] R.-J. Swijnenburg, S. Shrepfer, F. Cao, J. I. Pearl, X. Xie, A. J. Connolly, R. C. Robbins and J. C. Wu, “In vivo imaging of embryonic stem cells reveals patterns of survival and immune rejection following transplantation,” *Stem Cells and Development,* vol. 17, no. 6, pp. 1023-29, 2008.

[24] S. Aggarwal and M. F. Pittenger, “Human mesenchymal stem cells modulate allogeneic immune cell responses,” *Blood,* 2005.

[25] J. Kobolak, A. Dinnyes, A. Memic, A. Khademhosseini and A. Mobasheri, “Mesenchymal stem cells: Identification, phenotypic characterization, biological properties and potential for regenerative medicine through biomaterial micro-engineering of their niche,” *Methods,* vol. 99, pp. 62-8, 2015.

[26] F. Casiraghi, N. Perico, M. Cortinovis and G. Remuzzi, “Mesenchymal stromal cells in renal transplantation: opportunities and challenges,” *Nature Reviews Nephrology,* vol. 12, pp. 241-53, 2016.

[27] P. Salehinejad, N. B. Alithleen, A. M. Ali and S. N. Nematollahi-Mahani, “Comparison of different methods for the isolation of mesenchymal stem cells from human umbilical cord Wharton's jelly,” *In Vitro Cellular & Developmental Biology - Animal,* vol. 48, no. 2, pp. 75-83, 2012.

[28] D. G. Phiney and D. J. Prockop, “Concise review: mesenchymal stem/multipotent stromal cells: the state of transdifferentiation and modes of tissues repair - current views,” *Stem Cells,* vol. 25, no. 11, p. 2896, 2007.

[29] K. Baghaei, S. M. Hashemi, S. Tokhanbigli, A. A. Rad, H. Assadzaeh-Aghdaei, A. Sharifan and M. R. Zali, “Isolation, differentiation, and characterization of mesenchymal stem cells from human bone marrow,” *Gastroenterology and Hepatology from Bed to Bench,* vol. 10, no. 3, pp. 208-13, 2017.

[30] D. Mushahary, A. Spittler, C. Kasper, V. Weber and V. Charwat, “Isolation, cultivation, and characterization of human mesenchymal stem cells,” *Cytometry Part A,* vol. 93, no. 1, pp. 19-31, 2018.

[31] A. Iftimia-Mander, P. Hourd, R. Dainty and R. J. Thomas, “Mesenchymal stem cell isolation from human umbilical cord tissue: understanding and minimizing variability in cell yield for process optimization,” *Biopreservation and Biobanking,* vol. 11, no. 5, pp. 291-8, 2013.

[32] P. Godara, C. D. McFrland and R. E. Nordon, “Design of bioreactors for mesenchymal stem cell tissue engineering,” *Journal of Chemical Technology and Biotechnology,* vol. 83, pp. 408-20, 2008.

[33] J. W. Haycock, “3D Cell Culture: A Review of Current Approaches and Techniques,” in *3D Cell Culture. Methods in Molecular Biology (Methods and Protocols), vol 695*, Humana Press, 2011.

[34] K. von der Mark, V. Gauss, H. von der Mark and P. Müller, “Relationship between cell shape and type of collagen synthesised as chondrocytes lose their cartilage phenotype in culture,” *Nature,* vol. 267, pp. 531-32, 1977.

[35] C. Goepfert, V. Lutz, S. Lünse, S. Kittel, K. Wiegandt, M. Kammal, K. Püschel and R. Pörtner, “Evaluation of cartilage specific matrix synthesis of human articular chondrocytes after extended propagation on microcarriers by image analysis,” *International Journal of Artificial Organs,* vol. 33, no. 4, pp. 201-18, 2010.

[36] T. Mseka, J. R. Bamburg and L. P. Cramer, “ADF/cofilin family proteins control formation of oriented actin-filament bundles in the cell body to trigger fibroblast polarization,” *Journal of Cell Science,* vol. 120, pp. 4332-44, 2007.

[37] F. Y. McWhorter, T. Wang, P. Nguyen, T. Chung and W. F. Liu, “Modulation of macrophage phenotype by cell shape,” *Proceedings of the National Academy of Sciences,* vol. 110, no. 43, pp. 17253-8, 2013.

[38] V. M. Weaver, O. W. Petersen, F. Wang, C. A. Larabell, P. Briand, C. Damsky and M. J. Bissell, “Reversion of the Malignant Phenotype of Human Breast Cells in Three-Dimensional Culture and In Vivo by Integrin Blocking Antibodies,” *Journal of Cell Biology,* vol. 137, no. 1, pp. 231-45, 1997.

[39] A. Ernst, S. Hofmann, R. Ahmadi, N. Becker, A. Korshunov, F. Engel, C. Hartmann, J. Felsberg, M. Sabel, H. Peterziel, M. Durchdewald, J. Hess, S. Barbus, B. Campos, A. Starzinski-Powitz, A. Unterberg, G. Reifenberg, P. Lichter, C. Herold-Mende and B. Radlwimmer, “Genomic and expression profiling of glioblastoma stem cell-like spheroid cultures identifies novel tumor-relevant genes associated with survival,” *Clinical cancer research,* vol. 15, no. 21, pp. 6541-50, 2009.

[40] D. Egger, C. Tripisciano, V. Weber, M. Domicini and C. Kasper, “Dynamic cultivation of mesenchymal stem cell aggregates,” *Bioengineering,* vol. 5, no. 48, 2018.

[41] T. J. Bartosh, J. H. Ylöstalo, A. Mohammadipoor, N. Bazhanov, K. Coble, K. Claypool, R. H. Lee, H. Choi and D. J. Prockop, “Aggregation of human mesenchymal stromal cells (MSCs) into 3D spheroids enhances their antiinflammatory properties,” *PNAS,* vol. 107, no. 31, pp. 13724-9, 2010.

[42] S. Alimperti, P. Lei, Y. Wen, J. Tian, A. M. Campbell and S. T. Andreadis, “Serum-free spheroid suspension culture maintains mesenchymal stem cell proliferation and differentiation potential,” *Biotechnology Progress,* vol. 30, no. 4, 2014.

[43] A. Ovsianikov, A. Khademhosseini and V. Mironov, “The Synergy of Scaffold-Based and Scaffold-Free Tissue Engineering Strategies,” *Trends in Biotechnology,* vol. 36, no. 4, pp. 348-57, 2018.

[44] A. Kumar and B. Starly, “Large scale industrialized cell expansion: producing the critical raw material for biofabrication processes,” *Biofabrication,* vol. 7, no. 4, p. 044103, 2015.

[45] A. T.-L. Lam, J. Li, E. J.-H. Sim, A. K.-L. Chen, J. K.-Y. Chan, M. Choolani, S. Reuveny, W. R. Birsh and S. K.-W. Oh, “Biodegradable poly-ε-caprolactone microcarriers for efficient production of human mesenchymal stromal cells and secreted cytokines in batch and fed-batch bioreactors,” *Cytotherapy,* vol. 19, no. 3, pp. 419-32, 2017.

[46] L.-Y. Sun, S.-Z. Lin, Y.-S. Li, H.-J. Harn and T.-W. Chiou, “Functional Cells Cultured on Microcarriers for Use in Regenerative Medicine Research,” *Cell Transplantation,* vol. 20, no. 1, pp. 49-62, 2010.

[47] C. Frantz, K. M. Stewart and V. M. Weaver, “The extracellular matrix at a glance,” *Journal of Cell Science,* vol. 123, no. 24, pp. 4195-200, 2010.

[48] O. Z. Fisher, A. Khademhosseini, R. Langer and N. A. Peppas, “Bioinspired Materials for Controlling Stem Cell Fate,” *Accounts of Chemical Research,* vol. 43, no. 3, pp. 419-28, 2010.

[49] J. Lee, M. J. Cuddihy and N. A. Kotov, “Three-Dimensional Cell Culture Matrices: State of the Art,” *Tissue Engineering,* vol. 14, pp. 61-86, 2008.

[50] T. Andersen, P. Auk-Emblem and M. Dornish, “3D cell culture in alginate hydrogels,” *Microarrays,* vol. 4, pp. 133-61, 2015.

[51] K. M. Obom, P. J. Cummings, J. A. Ciafardoni, Y. Hashimura and D. Giroux, “Cultivation of Mammalian Cells Using a Single-use Pneumatic Bioreactor System,” *Journal of Visualized Experiments,* vol. 92, p. e52008, 2014.

[52] C. A. Rodrigues, T. G. Fernandes, M. M. Diogo, C. L. da Silva and J. M. Cabral, “Stem cell cultivation in bioreactors,” *Biotechnology advances,* vol. 29, no. 6, pp. 815-29, 2011.

[53] C. Hu, L. Fan, P. Cen, E. Chen, Z. Jiang and L. Li, “Energy Metabolism Plays a Critical Role in Stem Cell Maintenance and Differentiation,” *International Journal of Molecular Sciences,* vol. 17, no. 2, p. 253, 2016.

[54] S. Y. Lunt and M. G. V. Heiden, “Aerobic glycolysis: meeting the metabolic requirements of cell proliferation,” *Annual Review of Cell and Developmental Biology,* vol. 27, pp. 441-64, 2011.

[55] R. Burgess, M. Agathocleous and S. Morrison, “Metabolic regulation of stem cell function,” *Journal of Internal Maedicine,* vol. 276, no. 1, pp. 12-24, 2014.

[56] P. Jezek, L. Plecitá-Hlavatá, K. Smolková and R. Rossignol, “Distinctions and similarities of cell bioenergetics and the role of mitochondria in hypoxia, cancer, and embryonic development,” *The International Journal of Biochemistry and Cell Biology,* 2010.

[57] G. L. Semenza, “Hydroxylation of HIF-1: oxygen sensing at the molecular level,” *Physiology,* vol. 19, pp. 176-82, 2004.

[58] I. Papandreou, R. A. Cairns, L. Fontana, A. L. Lim and N. C. Denko, “HIF-1 mediates adaptation to hypoxia by actively downregulating mitochondrial oxygen consumption,” *Cell metabolism,* vol. 3, no. 3, pp. 187-197, 2006.

[59] J. Kim, I. Tchernyshyov, G. L. Semenza and C. V. Dang, “HIF-1-mediated expression of pyruvate dehydrogenase kinase: A metabolic switch required for cellular adaptation to hypoxia,” *Cell metabolism,* vol. 3, no. 3, pp. 177-85, 2006.

[60] G. L. Semenza, B.-H. Jiang, S. W. Leung, R. Passantino, J.-P. Concordet, P. Maire and A. Giallongo, “Hypoxia response elements in the aldolase A, enolase 1, and lactate dehydrogenase A gene contain essential binding sites for hypoxia-inducible factor 1,” *The Journal of Biological Chemistry,* vol. 271, no. 51, pp. 32529-37, 1996.

[61] L. Buravkova, E. Andreeva, V. Gogvadze and B. Zhivotovsky, “Mesenchymal stem cells and hypoxia:Where are we?,” *Mitochondrion,* vol. 19, pp. 105-112, 2014.

[62] R. Guzy, B. Hoyos, E. Robin, H. Chen, L. Liu, K. Mansfield, M. Simon, U. Hammerling and P. Schumacker, “Mitochondrial complex III is required for hypoxia-induced ROS production and cellular oxygen sensing,” *Cell Metabolism,* vol. 1, no. 6, pp. 401-8, 2005.

[63] K. M. Peterson, A. Aly, A. Lerman, L. O. Lerman and M. Rodriguez-Porcel, “Improved survival of mesenchymal stromal cell after hypoxia preconditioning: role of oxidative stress,” *Life Science,* vol. 88, no. 1-2, pp. 65-73, 2011.

[64] A. Lavrentieva, I. Majore, C. Kasper and R. Hass, “Effects of hypoxic culture conditions on umbilical cord-derived human mesenchymal stem cells,” *Cell Communication and Signalling,* vol. 8, no. 18, 2010.

[65] C.-T. Chen, Y.-R. V. Shih, T. K. Kuo, L. K. Oscar and Y.-H. Wei, “Coordinated changes of mitochondrial biogenesis and antioxidant enzymes during osteogenic differentiation of human mesenchymal stem cells,” *Stem Cells,* vol. 26, pp. 960-8, 2008.

[66] S. Palomäki, M. Pietilä, S. Laitinen, J. Pesälä, R. Sormunem, P. Lehenkari and P. Koivunen, “HIF-1α is upregulated in human mesenchymal stem cells,” *Stem Cells,* vol. 31, no. 9, pp. 1902-9, 2013.

[67] Y. Zhang, G. Marsboom, P. T. Toth and J. Rehman, “Mitochondrial respiration regulates adipogenic differentiation of human mesenchymal stem cells,” *PLoS ONE,* vol. 8, p. e77077, 2013.

[68] K. V. Tormos, E. Anso, R. B. Hamanaka, J. Eisenbart, J. Joseph, B. Kalyanaraman and N. S. Chandel, “Mitochondrial complex III ROS regulate adipocyte differentiation,” *Cell Metabolism,* vol. 14, no. 4, pp. 357-544, 2011.

[69] J. Estrada, C. Albo, A. Benguría, A. Dopazo, P. López-Romero, L. Carrera-Quintanar, E. Roche, E. Clemente, J. Enríquez, A. Bernard and E. Samper, “Culture of human mesenchymal stem cells at low oxygen tension improves growth and genetic stability by activating glycolysis,” *Cell Death and Differentiation,* vol. 19, pp. 743-55, 2012.

[70] S. Bahsoun, K. Coopman, N. R. Forsyth and E. C. Akam, “The Role of Dissolved Oxygen Levels on Human Mesenchymal Stem Cell Culture Success, Regulatory Compliance, and Therapeutic Potential,” *Stem Cells and Development,* vol. 27, no. 19, pp. 1303-21, 2018.

[71] D. Schop, *Growth and metabolism of mesenchymal stem cells cultivated on microcarriers (Doctoral Dissertation),* 2010.

[72] W. Widowati, L. Wijaya, I. Bachtiar, R. F. Gunanegara, S. U. Sugeng, Y. A. Irawan, S. B. Sumitro and M. A. Widowo, “Effect of oxygen tension on proliferation and characteristics of Wharton's jelly-derived mesenchymal stem cells,” *Biomarkers and Genomic Medicine,* vol. 6, no. 1, pp. 43-8, 2014.

[73] B. Annabi, Y.-T. Lee, S. Turcotte, E. Naude, R. R. Desrosiers, M. Champagne, N. Eliopoulos, J. Galipeau and R. Béliveau, “Hypoxia Promotes Murine Bone-Marrow-Derived Stromal Cell Migration and Tube Formation,” *Stem Cells,* vol. 21, no. 3, pp. 337-47, 2003.

[74] S.-C. Hung, R. R. Pochampally, S.-C. Hsu, C. Sanchez, S.-C. Chen, J. Spees and D. J. Prockop, “Short-Term Exposure of Multipotent Stromal Cells to Low Oxygen Increases Their Expression of CX3CR1 and CXCR4 and Their Engraftment In Vivo,” *PLoS ONE,* vol. 2, no. 5, p. e416, 2007.

[75] S.-P. Hung, J. H. Ho, Y.-R. V. Shih, T. Lo and O. K. Lee, “Hypoxia promotes proliferation and osteogenic differentiation potentials of human mesenchymal stem cells,” *Journal of Orthopaedic Research,* vol. 30, no. 2, pp. 260-6, 2012.

[76] M. Csete, “Oxygen in the Cultivation of Stem Cells,” *Annals of the New York Academy of Sciences,* vol. 1049, no. 1, pp. 1-8, 2005.

[77] D. Schop, R. van Dijkhuizen-Radersna, E. Bogart, F. Janssen, H. Rozemuller, H.-J. Prins and J. de Bruijn, “Expansion of human mesenchymal stromal cells on microcarriers: growth and metabolism,” *Journal of Tissue Engineering and Regenerative Medicine,* vol. 4, no. 2, pp. 131-40, 2010.

[78] P. Golstein and G. Kroemer, “Cell death by necrosis: Towards a molecular definition,” *Trends in Biochemical Sciences,* vol. 32, no. 1, pp. 37-43, 2007.

[79] C. Bertram and R. Hass, “Cellular responses to reactive oxygen species-induced DNA damage and aging,” *Biological Chemistry,* vol. 389, no. 3, pp. 211-20, 2008.

[80] A. Lavrentieva, T. Hatlapatka, R. Winkler, R. Hass and C. Kasper, “Strategies in umbilical cord-derived mesenchymal stem cells expansion: influence of oxygen, culture medium and cell separation,” *BMC Proceedings,* vol. Suppl 8, no. P88, p. 5, 2011.

[81] A. Krinner, M. Zscharnack, A. Bader, D. Drasdo and J. Galle, “Impact of oxygen environment on mesenchymal stem cell expansion and chondrogenic differentiation,” *Cell Proliferation,* vol. 42, no. 4, pp. 471-84, 2009.

[82] Y. Yamamoto, M. Fujita, Y. Tanaka, I. Kojima, Y. Kanatani, M. Ishihara and S. Tachibana, “Low Oxygen Tension Enhances Proliferation and Maintains Stemness of Adipose Tissue–Derived Stromal Cells,” *BioResearch Open Access,* vol. 2, no. 3, pp. 199-205, 2013.

[83] C.-C. Tsai, T.-L. Yew, D.-C. Yang, W.-H. Huang and S.-C. Hung, “Benefits of hypoxic culture on bone marrow multipotent stromal cells,” *American Journal of Blood Research,* vol. 2, no. 3, pp. 148-59, 2012.

[84] P. Malladi, Y. Xu, M. Chiou, A. J. Giaccia and M. T. Langaker, “Effect of reduced oxygen tension on chondrogenesis and osteogenesis in adipose-derived mesenchymal stem cells,” *American Journal of Physiology Cell Physiology,* vol. 290, no. 4, pp. C1139-49, 2006.

[85] C. Fehrer, R. Brunauer, G. Laschober, H. Unterluggauer, S. Reitinger, F. Kloss, C. Gülly, R. Gassner and G. Lepperdinger, “Reduced oxygen tension attenuates differentiation capacity of human mesenchymal stem cells and prolongs their lifespan,” *Aging Cell,* vol. 6, no. 6, pp. 745-57, 2007.

[86] J.-H. Lee and D. M. Kemp, “Human adipose-derived stem cells display myogenic potential and perturbed function in hypoxic conditions,” *Biochemical and Biophysical Research Communications,* vol. 341, no. 3, pp. 882-8, 2006.

[87] W. L. Grayson, F. Zhao, R. Izadpanah, B. Bunnell and T. Ma, “Effects of hypoxia on human mesenchymal stem cell expansion and plasticity in 3D constructs,” *Journal of Cellular Physiology,* vol. 207, no. 2, pp. 331-9, 2006.

[88] P. A. Sotiropoulo, S. A. Perez, M. Salagianni, C. N. Baxevanis and M. Papamichail, “Cell culture medium composition and translational adult bone marrow-derived stem cell research,” *Stem Cells,* vol. 24, no. 5, pp. 1409-10, 2006.

[89] C. Tekkatte, G. P. Gunasingh, K. M. Cherian and K. Sankaranarayanan, ““Humanized” stem cell culture techniques: the animal serum controversy,” *Stem Cells International,* vol. 2011.

[90] K. Bieback, “Platelet lysate as replacement for fetal bovine serum in mesenchymal stromal cell cultures,” *Transfusion Medicine and Hemotherapy,* vol. 40, pp. 326-35, 2013.

[91] C. Lange, F. Cakiroglu, A. Spiess, H. Cappallo-Obermann and A. R. Zander, “Platelet lysate for rapid expansion of human mesenchymal stromal cells,” *Cellular Therapy and Trnsplanation,* vol. 1, no. 2, pp. 49-53, 2008.

[92] K. Schallmoser, C. Bartmann, E. Rohde, A. Reinisch, K. Kashofer, E. Stadelmeyer, C. Drexler, G. Lanzer, W. Linkesch and D. Strunk, “Human platelet lysate can replace fetal bovine serum for clinical-scale expansion of functional mesenchymal stromal cells,” *Transplantation and Cellular Engineering,* vol. 47, no. 8, pp. 1436-46, 2007.

[93] G. Hassan, I. Kasem, C. Soukkarieh and M. Aljamali, “A simple method to isolate and expand human umbilical cord derived mesenchymal stem cells: Using explant method and umbilical cord blood serum,” *International Journal of Stem Cells,* vol. 10, no. 2, pp. 184-192, 2017.

[94] S. Jung, K. M. Panchalingam, L. Rosenberg and L. A. Behie, “Ex vivo expansion of human mesenchymal stem cells in defined serum-free media,” *Stem Cells International,* vol. 2012, 2012.

[95] A. C. Schnitzler, A. Verma, D. E. Kehoe, D. Jing, J. R. Murrell, K. A. Der, M. Aysola, P. J. Rapiejko, S. Punreddy and M. S. Rook, “Bioprocessing of human mesenchymal stem/stromal cells for theraputic use: Current technologies and challenges,” *Biochemical Engineering Journal,* vol. 108, pp. 3-13, 2015.

[96] R. M. Delaine-Smith and G. C. Reilly, “Mesenchymal stem cell responses to mechanical stimuli,” *Muscles, Ligaments and Tendons,* vol. 2, no. 3, pp. 169-80, 2012.

[97] P. Becquart, M. Cruel, L. Sudre, K. Pernelle, R. Bizios, D. Logeart-Avramoglou, H. Petite and M. Bensidhoum, “Human mesenchymal stem cell responses to hydrostatic pressure and shear stress,” *European Cells & Materials,* vol. 31, pp. 160-73, 2016.

[98] K. M. Kim, Y. J. Choi, J.-H. Hwang, A. R. Kim, H. J. Cho, E. S. Huang, J. Y. Park, S.-H. Lee and J.-H. Hong, “Shear Stress Induced by an Interstitial Level of Slow Flow Increases the Osteogenic Differentiation of Mesenchymal Stem Cells through TAZ Activation,” *PLoS One,* vol. 9, no. 3, p. e92427, 2014.

[99] R. J. McCoy and F. J. O'Brien, “Influence of Shear Stress in Perfusion Bioreactor Cultures for the Development of Three-Dimensional Bone Tissue Constructs: A Review,” *Tissue Engineering: Part B,* vol. 16, no. 6, pp. 587-601, 2010.

[100] D. Brindley, K. Moorthy, J.-H. Lee, C. Mason, H.-W. Kim and I. Wall, “Bioprocess Forces and Their Impact on Cell Behavior: Implications for Bone Regeneration Therapy,” *Journal of Tissue Engineering,* p. 620247, 2011.

[101] G. Yourek, S. M. McCormick, J. Mao and G. C. Reilly, “Shear stress induces osteogenic differentiation of human mesenchymal stem cells,” *Regenerative Medicine,* vol. 5, no. 5, pp. 713-24, 2010.

[102] F. Zhao, R. Chella and T. Ma, “Effects of Shear Stress on 3-D Human Mesenchymal Stem Cell Construct Development in a Perfusion Bioreactor System: Experiments and Hydrondynamic Modeling,” *Biotechnology and Bioengineering,* vol. 96, no. 3, pp. 584-95, 2007.

[103] V. Charwat, K. Schütze, W. Holnthoner, A. Lavrentieva, R. Gangnus, P. Hofbauer, C. Hoffmann, B. Angres and C. Kasper, “Potential and limitations of microscopy and Raman spectroscopy for live-cell analysis of 3D cell cultures,” *Journal of Biotechnology,* vol. 205, pp. 70-81, 2015.

[104] C. Canali, A. Heiskanen, H. B. Muhammad, P. Høyum, F.-J. Pettersen, M. Hemmingsen, A. Wolff, M. Dufva, Ø. G. Martinsen and J. Emnéus, “Bioimpedance monitoring of 3D cell culturing—Complementary electrode configurations for enhanced spatial sensitivity,” *Biosensors and Bioeletronics,* vol. 63, pp. 72-9, 2015.

[105] S.-M. Lee, N. Han, R. Lee, I.-H. Choi, Y.-B. Park, J.-S. Shin and K.-H. Yoo, “Real-time monitoring of 3D cell culture using a 3D capacitance biosensor,” *Biosensors and Bioelectronics,* vol. 77, pp. 56-61, 2015.

[106] J. H. Song, S.-M. Lee and K.-H. Yoo, “Label-free and real-time monitoring of human mesenchymal stem cell differentiation in 2D and 3D cell culture systems using impedance cell sensors,” *RSC Advances,* vol. 8, no. 54, pp. 31246-54, 2018.

[107] J. Melchor, E. L. Ruiz, J. M. Soto, G. Jiménez, C. Antich, M. Perán, J. M. Baena, J. A. Marchal and G. Rus, “In-bioreactor ultrasonic monitoring of 3D culture human engineered cartilage,” *Sensors and Actuators B: Chemical,* vol. 266, pp. 841-52, 2018.

[108] M. Mihailescu, I. A. Paun, M. Zamfirescu, C. R. Luculescu, A. M. Acasandrei and M. Dinescu, “Laser-assisted fabrication and non-invasive imaging of 3D cell-seeding constructs for bone tissue engineering,” *Journal of Material Sciences,* vol. 51, no. 9, pp. 4262-73, 2016.

[109] F. Rosa, K. C. Sales, J. G. Carmelo, A. Fernandes-Platzgummer, C. L. da Silva, M. B. Lopes and C. R. C. Calado, “Monitoring the ex-vivo expansion of human mesenchymal stem/stromal cells in xeno-free microcarrier-based reactor systems by MIR spectroscopy,” *Biotechnology Progress,* vol. 32, no. 2, 2015.

[110] D. Egger, *Concepts for the implementation of physiological conditions for the cultivation of human mesenchymal stem cells (Doctoral Dissertation),* 2017.

[111] A. C. Oliveira, *Optimization of three-dimensional cultivation conditions for the isolation and expansion of human mesenchymal stem cells (Master Thesis),* 2018.

[112] Z.-Z. Zhang, D. Jiang, S.-J. Wang, Y.-S. Qi, J.-Y. Zhang and J.-K. Yu, "Potential of Centrifugal Seeding Method in Improving Cells Distribution and Proliferation on Demineralized Cancellous Bone Scaffolds for Tissue-Engineered Meniscus," *ACS Applied Materials & Interfaces,* vol. 7, no. 28, pp. 15294-302, 2015.

[113] F. Zhao and T. Ma, "Perfusion Bioreactor System for Human Mesenchymal Stem Cell Tissue Engineering: Dynamic Cell Seeding and Construct Deelopment," *Biotechnology and Bioengineering,* vol. 91, no. 4, pp. 482-93, 2005.

[114] L. Bjerre, C. E. Bünger, M. Kassem and T. Mygrind, "Flow perfusion culture of human mesenchymal stem cells on silicate-substituted tricalcium phosphate scaffolds," *Biomaterials,* vol. 29, pp. 2616-27, 2008.

[115] J. F. Alvarez-Barreto, S. M. Linehan, R. L. Shambagh and V. I. Sikavitsas, "Flow Perfusion Improves Seeding of Tissue Engineering Scaffolds with Different Architectures," *Annals of Biomedical Engineering,* vol. 35, no. 3, pp. 429-442, 2007.

[116] D. Brindley, K. Moorthy, J.-H. Lee, C. Mason, H.-W. Kim and I. Wall, "Bioprocess Forces and Their Impact on Cell Behavior: Implications for Bone Regeneration Therapy," *Journal of Tissue Engineering,* vol. 1, p. 620247, 2011.

[117] S. Breslin and L. O'Driscoll, "Three-dimensional cell culture: the missing link in drug discovery," *Drug Discovery Today,* vol. 18, no. 5-6, pp. 240-9, 2013.

[118] C. Kallepitis, M. S. Bergholt, M. M. Mazo, V. Leonardo, S. C. Skaalure, S. A. Maynard and M. M. Stevens, "Quantitative volumetric Raman imaging of three dimensional cell cultures," *Nature Communications,* vol. 8, 2017.

Appendix

A.1 Materials and methods

Table A 1 Instruments and equipment used and respective manufacturer.

Product	Manufacturer
Arc punch, 6 mm	Turnus
Autoclave, Varioklav 500E	Thermo Scientific
Balance, AW-9202 and AW-224	Sartorius
Bioanalyser, YSI 2700 SELECT	YSI Incorporated
Cell counting chamber, Neubauer improved	Brand
Centrifuge, 5702	Eppendorf
Centrifuge, Heraeus™ Megafuge™ 16	Thermo Scientific
Fluorescence microscope DMIL LED	Leica
Fluorescence microscope camera DFC42C	Leica
Fluorescence microscope light EL6000	Leica
Freezing container, Mr. Frosty™	Thermo Scientific
Incubator, HERACELL 240i	Thermo Scientific
Incubator with integrated pumps	IncuReTERM GmbH
Liquid nitrogen tank, Cryotherm 55121	BiosafeMD
Magnetic stirrer	IKA-Labortechnik
Microscope (transmitted light), DMIL LED	Leica
Microscope camera, ICC50HD	Leica
Nitrogen generator	Parker
Pipettes Research® Plus	Eppendorf
Pipetting Pipetboy acu	IBS Integra Biosciences
Platereader, Infinite® M1000 Pro	Tecan
Screwdriver, PicoFinish 263 P	Wiha
Shaker, Skyline Orbital Shaker	Elmi
Sterile work bench, HERAsafe KS	Thermo Scientific
Vortexer, Vortexgenie 2	Scientific Industries
Water bath	GFL

Table A 2 Disposables used and respective manufacturer and order number.

Product	Manufacturer	Order number
6, 24, 96-well plates	Sarstedt	83.3920, 83.3922, 83.3924
12-well plate	TPP	92412
96-well, transparent bottom	Greiner bio-one	655906
Cell culture flask 25, 75, 175 cm^2	Sarstedt	83.3912, 83.3911, 83.3912
Cell strainer	Falcon®	352340
Centrifuge tube 15, 50 ml	Greiner bio-one	188271, 227261
Clear Resin	Formlabs	RS-F2-GPCL-04
Cryo tube, CRYO.S, 2 ml	Greiner bio-one	122278, 122279
High Temp Resin	Formlabs	RS-F2-HTAM-02
MatriDerm®	MedSkin Solutions Dr. Suwelack AG	83500-100

Table A 2 (Cont.) Disposables used and respective manufacturer and order number.

Product	Manufacturer	Order number
MatriStypt®	MedSkin Solutions Dr. Suwelack AG	83242-001
Parafilm® M	Bemis	PM996
Pasteur pipettes	Brand	747715, 747720
Petri dish	Greiner bio-one	664160
Pipette tip 0.5-50 µl	Roth	9260.1
Pipette tip 10-200; 50-1000 µl	Brand	732008, 732012
Reaction tube, 1.5 ml	Roth	7080.1
Safe-Lock Tubes 0.5 mL	Eppendorf	0030121120
Sterile filter, Filtropur S 0.2 µm	Sarstedt	83.1827
Sterile vaccum filter, Nalgene Rapid-Flow	Thermo Scientific	566-0020
Surgical scalpel blade no. 22	Swann Morton	0508
Syringe 5 ml	Braun	4617053
Syringe 10 ml	Terumo®	SS-10L
Serological pipettes (2, 5, 10, 15, 50 ml)	Greiner bio-one	710180, 606180, 607180, 760180, 768180

Table A 3 Chemicals used and respective manufacturer and order number.

Product	Manufacturer	Order
α-MEM basal medium	Gibco	1200-063
Accutase®	Sigma Aldrich	A6964-100ML
Alcian Blue 8GX	Sigma Aldrich	A3157-10G
Alizarin Red S	Carl Roth	0348.2
β-glycerol phosphate disodium salt pentahydrate	Sigma Aldrich	50020-100G
Calcein	Sigma Aldrich	C0875-5G
Calcein-AM	Invitrogen	C3099
Calcium chloride	Sigma Aldrich	C1016-100G
DAPI	Sigma Aldrich	D8417-1MG
Dexamethasone	Sigma Aldrich	D1756-25MG
D-Glucose	Sigma Aldrich	G7021-100G
DMSO	Sigma Aldrich	D8418-100ML
Dulbecco's MEM – high glucose	Sigma Aldrich	D7777-1L
EDTA sodium salt dihydrate	Sigma Aldrich	ED2SS-100G
Elo-Mel isotonic infusion solution	Fresenius Kabi	0760071/04A
Ethanol 96%	AustrAlco	
Fibronectin	Biochrom	L 7117
Formaldehyde solution (36.5-38%)	Sigma Aldrich	F8775
Gentamycin (10 mg/ml)	Lonza	BE02-012E
Heparin	PL Bioscience	PLHEP-001
Human platelet lysate	PL Bioscience	PL-S-100.01
ITS+	Gibco	41400-045
L-ascorbat-2-phosphate	Sigma Aldrich	49752-100G
L-Li-Lactate	Sigma Aldrich	L2250-5G
L-proline	Sigma Aldrich	P0380-10MG
NH AdipoDiff Media	Miltenyi Biotec GmbH	130-091-677
NH ChondroDiff Media	Miltenyi Biotec GmbH	130-091-679
NH OsteoDiff Media	Miltenyi Biotec GmbH	130-091-678
Oil Red O solution (0.5%)	Sigma Aldrich	O1516-250ML
Phosphate buffer saline (PBS)	Gibco	21600-044
Potassium chloride	Sigma Aldrich	P9333-1KG
Propidium iodide (PI)	Sigma Aldrich	81845-25MG
Silver nitrate solution (5%)	Carl Roth	N053.1
Sodium alginate	Sigma Aldrich	180947-100G
Sodium carbonate	Sigma Aldrich	S7795-1KG
Sodium benzoate	Sigma Aldrich	7130-250G
Sodium chloride	Sigma Aldrich	S9625-1KG

Table A 3 (Cont.) Chemicals used and respective manufacturer and order number.

Product	Manufacturer	Order
Sodium chloride	Sigma Aldrich	S9625-1KG
Sodium phosphate monobasic dihydrate	Sigma Aldrich	71500-250G
Sodium phosphate dibasic dihydrate	Sigma Aldrich	30435-500G
Tetrazolium bromide (MTT)	Sigma Aldrich	M5655-500MG
TGF-β	Sigma Aldrich	SRP3171-10UG
Trypan Blue solution (0.4%)	Sigma Aldrich	T8154

Table A 4 Buffers and solutions used and respective composition.

Solution	Composition
Alcian blue solution	1% (w/v) Alcian Blue 8 GX in 3% acetic acid
Alizarin red solution	0.5% (w/v) Alizarin Red S in ddH_2O
Alginate 1.2% (w/v) solution	12 mg/ml alginate in expansion medium
DAPI stock solution	20 mg/ml DAPI in ddH_2O
MTT stock solution	5 mg/ml in PBS
SDS solution	5% (w/v) in 0.01M HCl
YSI buffer	0.15 g/L EDTA disodium salt dihydrate, 0.7 ml/L gentamycin, 0.97 g/L sodium benzoate, 1.84 g/L sodium phosphate monobasic dihydrate, 9.14 g/L sodium phosphate dibasic dihydrate, 3.29 g/L sodium chloride, 0.027 g/L potassium chloride in ddH_2O
YSI calibration solution	0.53 g/L L-Li-lactate, 4 g/L D-glucose, 1.4 ml/L gentamycin in ddH_2O
Von Kossa decolourization solution	5% Na_2CO_3, 0.2% formaldehyde in ddH_2O

Table A 5 Kits used and respective manufacturer and order number.

Product	Manufacturer	Order
In vitro toxicology assay kit (TOX8)	Sigma Aldrich	TOX8-1KT

Table A 6 Media used and respective composition.

Media	Composition
Adipogenic medium	1% (v/v) gentamycin in NH AdipoDiff Media
Chondrogenic medium I (manufactured)	1% (v/v) gentamycin in NH ChondroDiff Media
Chondrogenic medium II (handmade)	1% (v/v) ITS+, 50 µg/ml L-ascorbate-2-phosphate, 100 nM dexamethasone, 40 µg/ml L-proline, 10 ng/ml TGF-β, 1% (v/v) gentamycin in DMEM-high glucose
Cryomedium	10% (v/v) hPL, 10% (v/v) DMSO in expansion medium
Expansion medium	2.5% (v/v) hPL, 0.5% (v/v) gentamycin, 1 U/ml heparin in α-MEM
Osteogenic medium I (manufactured)	1% (v/v) gentamycin in NH OsteoDiff Media
Osteogenic medium II (handmade)	5 mM β-glycerophosphate, 50 µg/ml L-ascorbate-2-phosphate, 100 nM dexamethasone in expansion medium

Table A 7 Bioreactor circuit components and respective manufacturer.

Component	Manufacturer
BPT tubing	PharMed
Catheter	Joanneum Research
Luer Lock connector female	Pieper Filter
Luer Lock connector male	Pieper Filter
Micro-perfusion pump, MPP 102 PC	Joanneum Research
Mini-perfusion bioreactor	Joanneum Research
Perfusion bag 10 mL, PEB001	Joanneum Research
Schott-flask (100 mL)	Simax

Table A 8 Software used and respective developer and version.

Product	Company	Version
Excel	Microsoft	Office 365
ImageJ-Fiji	Open source	
Leica Application Suite (LAS)	Leica	4.6.1

A.2 Results and discussion

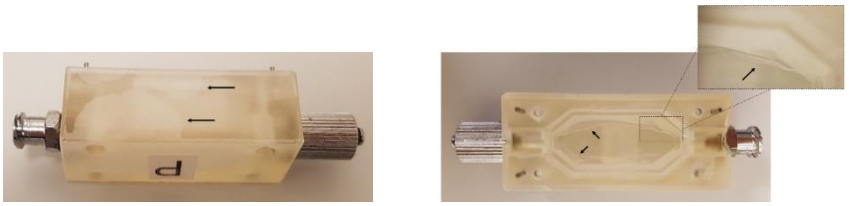

(a) (b)

Figure A 1 Decay of the parylene coating in the High Temp resin bioreactor after a series of autoclave steps: (a) outer view; (b) inner view with close up.

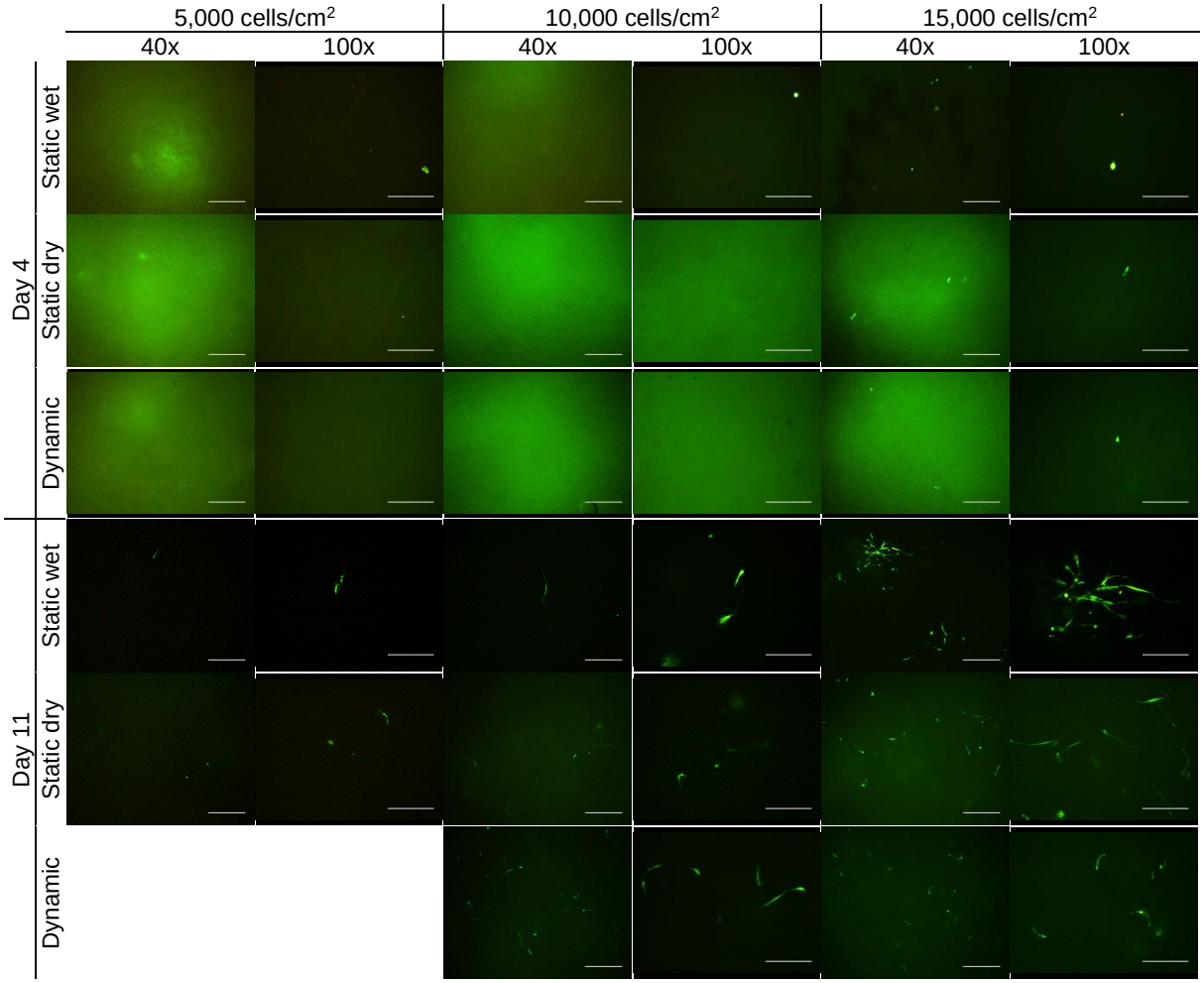

Figure A 2 Calcein-AM/PI staining of the top of Matristypt® membranes on days 4 and 11 of cell cultivation. Cells were seeded at a concentration of 5,000; 10,000 or 15,000 cells/cm^2 to dried (static and dynamic [centrifugation at 500 rpm; 5 min] seeding) or hydrated matrices (static seeding). Calcein-AM stains live cells in green; PI stains dead cells in red. Pictures were acquired by fluorescence microscopy; scale bar represents 500 and 250 µm in 40x and 100x magnification, respectively.

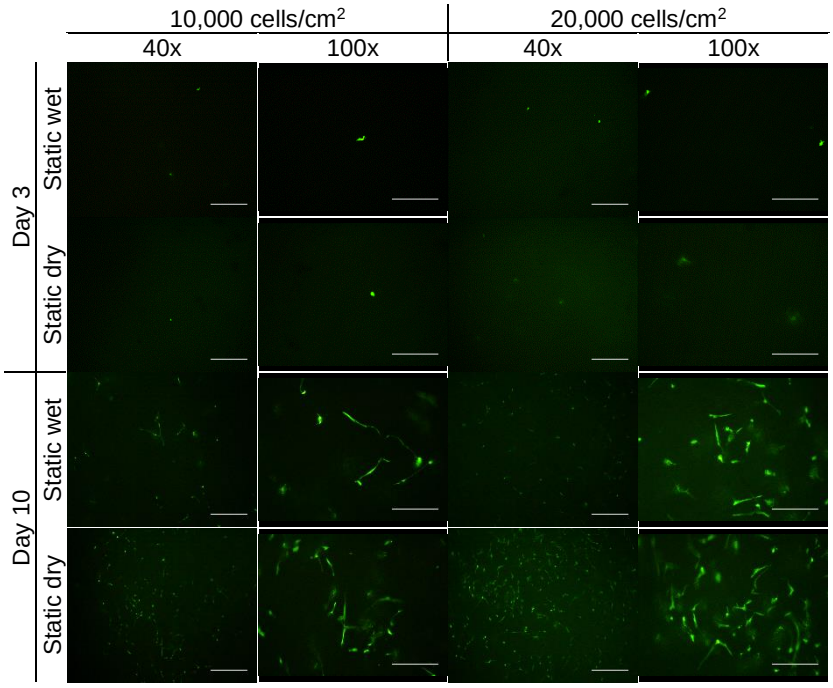

Figure A 3 Calcein-AM/PI staining of the top of Matristypt® membranes on days 3 and 10 of cell cultivation. Cells were seeded at a concentration of 10,000 or 20,000 cells/cm^2 to dried or hydrated (wet) matrices. Calcein-AM stains live cells in green; PI stains dead cells in red. Pictures were acquired by fluorescence microscopy; scale bar represents 500 and 250 µm in 40x and 100x magnification, respectively.

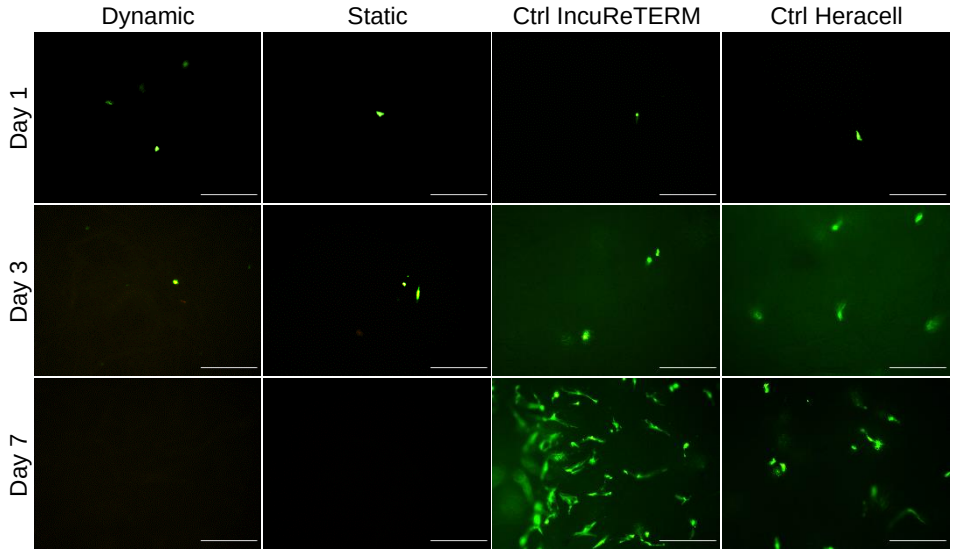

Figure A 4 Calcein-AM/PI staining of the top of Matristypt® membranes on days 1, 3 and 7 of cell cultivation inside parylene-coated High Temp resin reactors under dynamic (constant rate, 10 rpm) or static conditions, and in well-plates (Ctrl). Cells were seeded at a concentration of 15,000 cells/cm^2 to medium-soaked matrices; the reactors and one of the controls were incubated in IncuReTERM and a second control was incubated in Heracell. Calcein-AM stains live cells in green; PI stains dead cells in red. Pictures were acquired by fluorescence microscopy; scale bar represents 250 µm in 100x magnification.

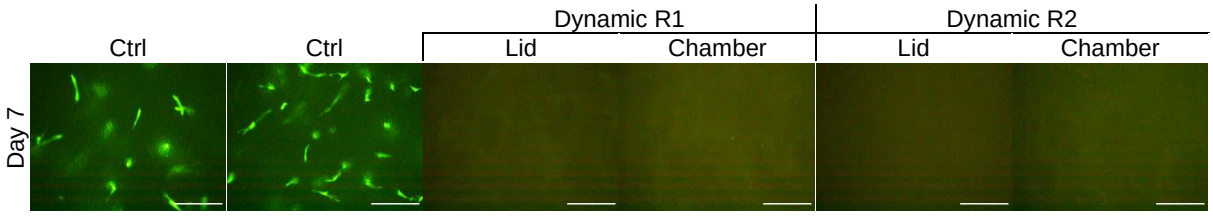

Figure A 5 Calcein-AM/PI staining of the top of MatriStypt® membranes on day 7 of cell cultivation inside two separate (R1 and R2) parylene-coated High Temp resin reactors under dynamic flow (constant rate, 5 rpm) or in well-plates (Ctrl). Cells were seeded at a concentration of 15,000 cells/cm^2 on hydrated matrices; the reactors were incubated in IncuReTERM and the controls were incubated in Heracell. Calcein-AM stains live cells in green; PI stains dead cells in red. Pictures were acquired by fluorescence microscopy; scale bar represents 250 µm in 100x magnification.

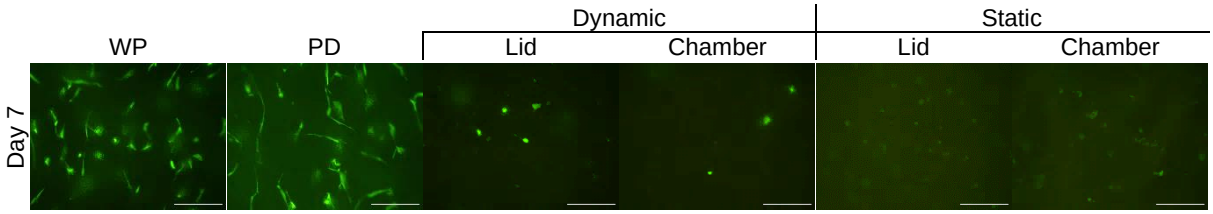

Figure A 6 Calcein-AM/PI staining of the bottom of MatriDerm® membranes on day 7 of cell cultivation inside parylene-coated High Temp resin reactors under dynamic (constant flow, 4 rpm) conditions or statically in a well-plate (WP) or in a petri-dish (PD). Cells were seeded at a concentration of 16,000 cells/cm^2 to hydrated matrices; the reactors were incubated in IncuReTERM and the controls were incubated in Heracell. Calcein-AM stains live cells in green; PI stains dead cells in red. Pictures were acquired by fluorescence microscopy; scale bar represents 250 µm in 100x magnification.

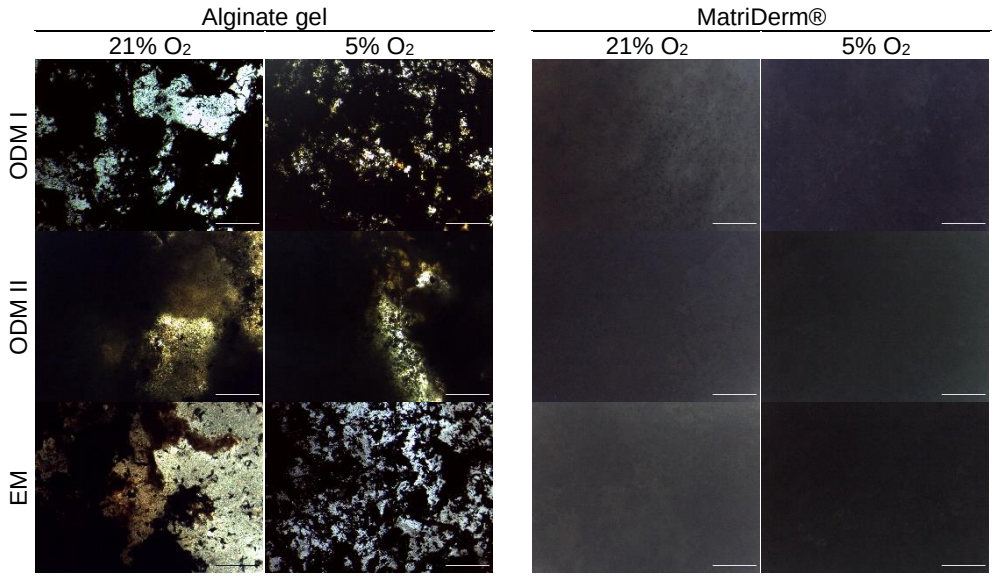

Figure A 7 von Kossa staining at day 21 on adMSC cultivated in alginate gel or MatriDerm® under normoxic (21% O_2) or hypoxic (5% O_2) conditions in manufactured osteogenic differentiation medium (ODM I), handmade osteogenic medium (ODM II) or expansion medium (EM). Von Kossa stains phosphate in dark grey. Pictures were acquired by phase contrast microscopy; scale bar represents 250 µm in 100x magnification.

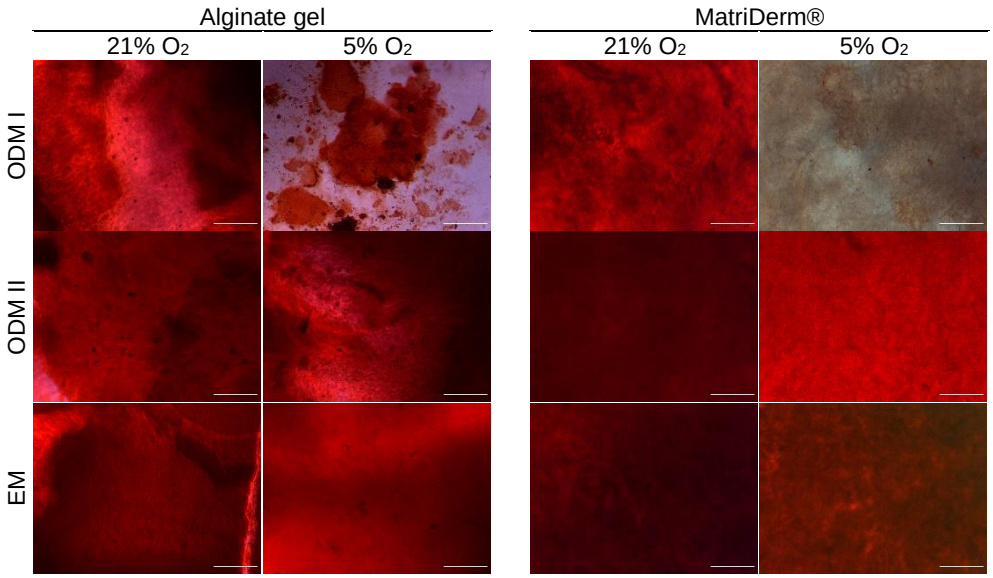

Figure A 8 Alizarin Red S staining at day 21 on adMSC cultivated in alginate gel or MatriDerm® under normoxic (21% O_2) or hypoxic (5% O_2) conditions in manufactured osteogenic differentiation medium (ODM I), handmade osteogenic medium (ODM II) or expansion medium (EM). Alizarin Red S stains calcium in red. Pictures were acquired by phase contrast microscopy; scale bar represents 250 µm in 100x magnification.

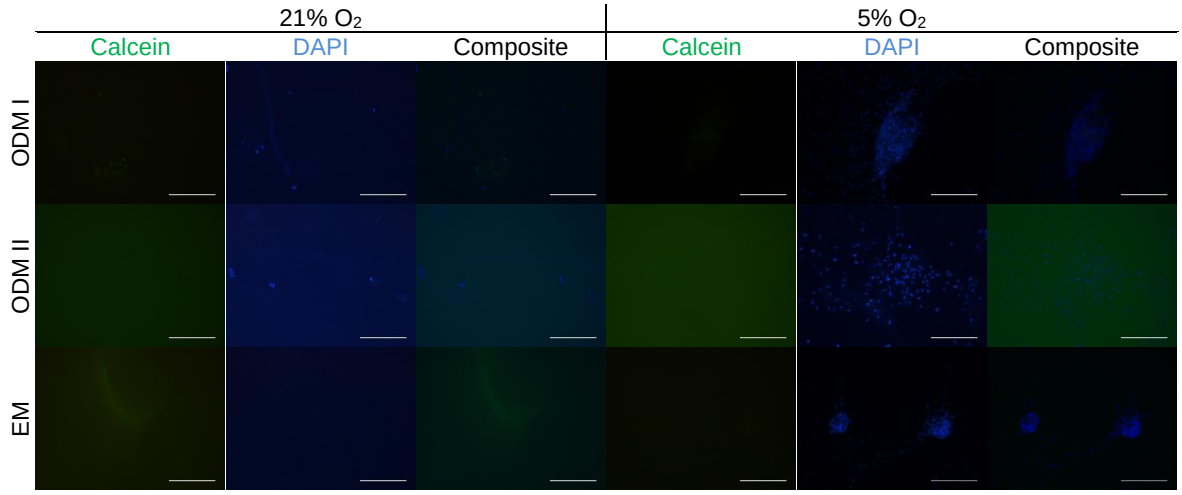

Figure A 9 Calcein and DAPI stainings at day 21 on adMSC cultivated in alginate gel under normoxic (21% O_2) or hypoxic (5% O_2) conditions in manufactured osteogenic differentiation medium (ODM I), handmade osteogenic medium (ODM II) or expansion medium (EM). Calcein stains calcium in green; DAPI stains the nuclei of live cells in blue. Pictures were acquired by fluorescence microscopy; scale bar represents 250 µm in 100x magnification.